On the variation of traits and tree range constraints

Leander D. Love-Anderegg

A dissertation

submitted in partial fulfillment of the

requirements for the degree of

Doctor of Philosophy

University of Washington

2017

Reading Committee:

Janneke Hille Ris Lambers, Chair

Abigail Swann

Thomas Hinckley

Program Authorized to Offer Degree:

Biology

University of Washington

Abstract

On the variation of traits and tree range constraints

Leander D. Love-Anderegg

Chair of the Supervisory Committee:
Professor Janneke Hille Ris Lambers
Department of Biology

Ecology in the 21st century faces the considerable challenge of predicting how ecosystem structure and function will respond to rapid global environmental change. In order to meet this challenge, ecology must transcend description through the development of broad ecological theory and ecological tools that can explain and predict ecological phenomena across multiple scales of spatial, temporal and taxonomic organization. This dissertation leverages within-species geographic variation in plant performance and functional traits to test the biogeographic predictive power of long-standing ecological theory, illuminate how tree drought resistance strategies will mediate geographic range shifts in a warming world, and explore the strengths and weaknesses of leaf functional traits as ecological tools.

Species geographic ranges are, in essence, the spatial manifestation of their ecological niche, yet the exact mechanisms that constrain species ranges remain elusive, limiting our ability to predict range shifts. In the first chapter of this dissertation, I collected tree cores from over 700 trees across the western U.S. to determine how climate and competition jointly constrain

elevation tree ranges. This work is based on the longstanding but rarely tested hypothesis that biotic and abiotic stress trade off, with species interactions (competition) being the main fitness constraint in benign environments and abiotic/climatic stress proving the main constraint in harsh environments. I found broad-scale evidence for this tradeoff in the tree core record. Across multiple species on multiple mountains, populations with the fastest tree growth (the most 'benign' sites) were most sensitive to competition while the slowest growing populations were the most sensitive to climate. However, this trade-off did not map cleanly onto range position. Of the nine species ranges examined, only two showed strong evidence for a trade-off between climatic and competitive growth constraints, although evidence for climatic constraints in harsh environments was more consistent. These findings highlight multiple processes that complicate local range dynamics, but suggest that the constraints on large-scale (e.g. latitudinal) tree distributions may still be predicted from ecological theory. Thus, existing correlational tools such as Climate Envelope Models may be appropriate for predicting shifts of large-scale plant range boundaries in climatically harsh environments.

Second, I used within-species variation in drought tolerance traits to elucidate the physiological mechanisms by which drought controls two specific tree range boundaries. I quantified elevational variation in the drought tolerance and drought avoidance traits of a widespread gymnosperm (ponderosa pine –*Pinus ponderosa*) and angiosperm (trembling aspen – *Populus tremuloides*) tree species in the southwestern USA. Although water stress increased and growth declined strongly at the lower range margins of both species, ponderosa pine and aspen showed contrasting patterns of clinal trait variation. Trembling aspen increased its drought tolerance at its dry range edge by growing stronger but more carbon dense branch and leaf tissues, implying an increased cost of growth. By contrast, ponderosa pine showed little

elevational trait variation but avoided drought stress at low elevations through stomatal closure, such that its dry range boundary experienced limited carbon assimilation even in good years. Thus, the same climatic factor (drought) may drive range boundaries through different physiological mechanisms – a result that has important implications for process-based modeling approaches to tree biogeography. Further, I show that comparing intraspecific patterns of trait variation across ranges, something rarely done in a range-limit context, helps elucidate a mechanistic understanding of range constraints.

Finally, I collected and compiled an extensive dataset on leaf functional trait variation within and between species in order to test some of the foundational assumptions of trait-based ecology. Functional traits have great potential to stimulate a predictive ecology, providing scale-free tools for understanding ecological interactions, community dynamics and ecosystem function. Yet their utility relies in part on four key assumptions: 1) that most trait variation lies between rather than within species, 2) that global patterns of trait covariation are the result of universal evolutionary or physiological trade-offs that are independent of taxonomic scale, and 3) that traits respond predictably to environmental gradients. I examined three traits central to the leaf economics spectrum, leaf mass per area (LMA), leaf lifespan, and leaf nitrogen content, and quantified patterns of leaf trait variation, particularly within-species. Although I found that some foliar traits do vary primarily between species (as predicted), others – particularly area-based leaf nitrogen content – vary enormously within-species. I also found that some of the global trait relationships central to the leaf economics spectrum hold true across taxonomic scales. However, other patterns of trait covariation show surprisingly different patterns within- versus between-species, calling into question some of the putative evolutionary and physiological mechanisms linking these leaf traits. Finally, in a subset of well sampled conifers in the northwestern U.S.A.,

I found that leaf lifespan was reasonably responsive to environmental gradients but other foliar traits had very weak links to environmental variation. Taken together, my results challenge the 'scale-free' nature of the currently proposed mechanisms driving leaf trait covariation. However, my results demonstrate the potential power of intra-specific trait variation to deepen our understanding of the causes and consequences of functional trait variation.

Acknowledgements

This dissertation would not exist without the help of many people, most proximally my advisor Janneke Hille Ris Lambers and my various scientific counselors, mentors and collaborators. Thank you to Janneke for years of support and good advice, to my graduate committee, to Joe Berry and Margie Mayfield (whose labs I crashed for various lengths of time, and sorry Joe, there seems no end in sight for you). Thank you also to Bev Law for collecting and Logan Berner for compiling the trait data I drew upon in Chapter 3. Thank you to the small army of undergraduates, post-bachs, honors students, friends and family who helped me in the lab and the field. And thank you to the members of the Hille Ris Lambers Lab, who made the lab both fun and intellectually stimulating. More distally, this dissertation would not be were it not for the unfailing support of my wife, Ericka Sohlberg, my parents Maggie Love and Mike Anderegg, and of course my brother Bill Anderegg (who was at once an emotional support, a scientific consultant, and the major lender of much of my field equipment). Thank you also to Terry Root, who took me under her wing when I was an undergraduate and convinced me to be a global change ecologist.

Table of Contents

Introduction

Ecology in the 21st century will be the ecology of change. Anthropogenic influences on the climate system, global land cover, nutrient cycling and regional species pools (i.e. species extirpations and species introductions) guarantee that the magnitude and rate of 21st century environmental change will exceed anything experienced over the timespan of human civilization (Assessment, 2005). For instance, even the most optimistic projected rates of human-caused climate change over the coming century likely exceed by orders of magnitude the fastest potential rates of animal evolution (Quintero & Wiens, 2013). By the end of the century global temperatures may exceed anything the earth has experienced since the Eemian (125,000 yr ago) or even since the early Eocene (50 million yr ago) (Lunt *et al.*, 2012; Masson-Delmotte *et al.*, 2013; Kidwell, 2015). Thus, ecologists are tasked with understanding complex natural systems that are probably changing faster than we can describe their initial conditions. Given this context, physiological ecology, community ecology, and ecosystem studies must do more than detail the who and the how of ecological systems. They must guide practitioners, land stewards, policy makers and the general public in efforts to mitigate and adapt to rapidly unfolding local and global environmental changes.

To this end, this dissertation aims to help develop the theory and tools needed to predict ecosystem responses to global change. An increasing literature has focused on quantitative modeling of community or ecosystem properties for prediction (Clark *et al.*, 2001; Evans *et al.*, 2013; Dakos *et al.*, 2017). However, perhaps a more basic imperative in ecologic research is to develop and refine the robust, generalizable theory necessary to structure such models. Climate change-induced species range shifts are an excellent example of the need for such theory. Multiple quantitative modeling approaches exist, ranging from empirical (e.g. Climate Envelope

Models or CEMs), to semi-mechanistic (e.g. physiologically based CEMs or dispersal-constrained CEMs) to fully mechanistic vegetation models (stand development models, land surface models). These many modeling approaches each have strengths and weaknesses, trading off the processes they capture, the assumptions on which they rely, and the data necessary to parameterize them. However, their resulting predictions of future range dynamics can differ quite dramatically (Morin & Thuiller, 2009; Buckley *et al.*, 2011).

The lack of robust predictions across modeling methods suggests a grave need for additional ecological theory to spur further model development and guide model implementation. Emerging biogeographic patterns such as the tendency for terrestrial ectotherms to extend beyond their physiological poleward boundary but not reach their physiological tropical boundary based on their thermal performance curves (Sunday *et al.*, 2012) suggest that the ecological mechanisms of species range constraints may exhibit generalizable patterns. The Stress Tradeoff Hypothesis (STH) is one potentially powerful theory that provides general predictions of where species ranges are constrained directly by climate versus where they are constrained by species interactions. The STH posits that climate is the primary constraint on organismal fitness in harsh environments, and species interactions are the key constraint on fitness in benign environments (MacArthur, 1972; Brown, 1995). The biogeographic corollary of this theory is that species tend to be climatically constrained at their environmentally 'harsh' range boundary, and constrained by species interactions such as competition at their 'benign' range boundary (Loehle, 1998; Koehler *et al.*, 2012; Savage & Cavender-Bares, 2013). Chapter one of this dissertation uses evidence from tree cores and forest surveys to test this theory across the elevation ranges of many tree species in many climates. The goal of this chapter is to test and

refine biogeographic theory to differentiate the potential mechanisms of range constraint using empirical observations of actual range constraints.

The impetus for this chapter was a prevailing emphasis on the abiotic controls on species presence and performance in both the range shift modeling literature and the dendroecological literature. In the range shift literature, essentially all prediction-focused work has been based in some way on Climate Envelope Models, which explicitly attribute all range boundaries to abiotic factors (Lawler *et al.*, 2009; Iverson *et al.*, 2011; Higgins *et al.*, 2012; Schloss *et al.*, 2012; Lawler *et al.*, 2013). Meanwhile, dendroecologists have been amassing large datasets of tree growth through space and time, datasets that can provide powerful inferences about spatial variation of the constraints on tree growth (Peterson & Peterson, 2002; Case & Peterson, 2005; Nakawatase & Peterson, 2006; Littell *et al.*, 2008; Griesbauer & Green, 2010; D'Orangeville *et al.*, 2016; Girardin *et al.*, 2016; Restaino *et al.*, 2016). However, possibly due to dendrochronology's roots in dendroclimatology, this vast literature has focused almost entirely on climatic factors that control tree growth. Biotic interactions, particularly competition, have been explored extensively using tree rings in the forestry literature, but almost never with an explicit biogeographic focus (e.g. Contreras *et al.*, 2011; Das *et al.*, 2011). However, a growing body of evidence suggests that biotic interactions can prove the primary drivers of plant range boundaries (Ettinger *et al.*, 2011; Ettinger & Hillerislambers, 2013; Brown & Vellend, 2014, reviewed in Hillerislambers *et al.*, 2013). More-over, the few studies that have explicitly attempted to determine spatial patterns in the effects of competition on tree growth have revealed considerable variation along climate gradients (Kunstler *et al.*, 2011; Copenhaver-Parry & Cannon, 2016). Thus, a multi-system, biogeographically explicit treatment of climatic versus biotic constraints on tree growth leveraging the power of tree rings seemed a high-yield approach

to push both the range constraint and tree ring literature and seek synthetic insight about how biotic and abiotic factors trade off in importance through climate space.

The results of this analysis revealed complexity at essentially every level, the complexity of downscaling from large to local patterns of range constraint, the complexity of biotic interactions as the foil to purely abiotic range constraints, even the complexity of statistically modeling and detecting relatively straight-forward abiotic constraints on tree growth. This last complexity, in particular, shed light on the difficulty of translating abiotic harshness into plant physiological stress. I initially expected climatic range constraints to be relatively straightforward to detect using tree rings and then decompose into their particular climatic components (e.g. cold stress versus growing season length limitations versus drought stress). However, this proved surprisingly difficult due to the hidden microclimatic complexity along even the most simple real-world climate gradients, the temporal lags in climatic effects on tree growth that complicated statistical analyses, and complex interactions between climate and tree physiology that defied a priori attempts to define climatic 'harshness'. Thus, even where abiotic factors appeared to constrain tree growth, complexity emerged. In an attempt to unpack this complexity, in the second chapter of this dissertation I focus specifically on 'simple', climatically controlled range boundaries to explore how climate stress (in this case water limitation) physiologically enforces elevational range boundaries.

In addition to guiding theory, ecological prediction also requires tools for quantifying, synthesizing, and simplifying the biosphere's ecological, evolutionary, and physiological complexity. Chapter two focuses in on two of the climatic range boundaries identified from the tree ring record in Chapter one for a case study of the power of within-species physiological variation as a tool for ecological inference. Chapter two quantifies the drought avoidance and

drought tolerance strategies of two tree species based on the physiological trait and rate changes each species manifests approaching its dry range boundary. Drought resistance is a complex attribute to quantify, as it can be achieved via multiple strategies, through multiple physiological and morphological adjustments (Larcher *et al.*, 1973; Levitt, 1980; Ludlow, 1989; Chaves *et al.*, 2003; Barbeta *et al.*, 2016). For example, plants can survive drought stress by limiting water loss, transpirational area, hydraulic resistance, etc. to avoid experiencing negative water potentials. Alternatively, they could grow stress tolerant roots, leaves and shoots to tolerate drought stress without suffering physiological damage. Finally, they could instead depend on a speedy recovery following drought to recover physiological function as soon as water is available again. Or they could employ some combination of the above. This diversity of drought resistance strategies, each of which involves a complex suite of physiological traits, pose a considerable challenge for physiologists seeking to predict, for example, tree mortality during drought (McDowell *et al.*, 2011; Anderegg *et al.*, 2012; 2013). As Chapter 1 revealed, this diversity of drought physiological strategies also challenge biogeographers seeking to predict the range dynamics of even obvious drought controlled plant distributions. Chapter two explores how within-species geographic variation in a suite of morphological and physiological traits can reveal the drought tolerance and avoidance strategies employed by two widespread tree species. By quantifying and simplifying each species' complex drought physiology into their predominant drought resistance strategy, Chapter two seeks insight into the mechanisms that govern the dry range margin of each species. Knowledge of these mechanisms can then yield at least qualitative inferences about potential range dynamics in a changing climate.

As shown in Chapter two, plant functional traits can be a powerful tool for understanding complex plant physiologies and life histories, potentially allowing ecologists to scale across time,

space and levels of taxonomic organization. Spurred by the utility of within-species trait variation to provide ecological inference not possible from between-species analyses shown in Chapter two, Chapter three of this dissertation explores within-species trait variation at much larger geographic scales in many more species. The results of Chapter Two suggested that within-species trait-by-environment relationships could provide fertile ground for understanding species geographic ranges. However, what I discovered instead is that our understanding of many plant functional traits themselves is imperfect. Before employing traits as an ecological tool, we need to better understand what exactly we have in our ecological toolbox. This chapter explores the functionality of one of the most widely acknowledge trait associations in the plant functional literature, the leaf economics spectrum. The leaf economics spectrum simplifies up to >75% of the world-wide variation in leaf morphology and physiological function into a single axis related to the rate of resource use and acquisition (Wright *et al.*, 2004). Leaves from all parts of the tree of life tend to converge on a resource use strategy that ranges from 'fast' (with high physiological rates, low leaf mass per area, and short leaf lifespan) to 'slow' (with low physiological rates, high leaf mass per area, and long leaf lifespan). This dominant axis of leaf trait covariation is startling in its ubiquity, and is much stronger than trait variation across environmental gradients (Wright *et al.*, 2004; 2005; Lamanna *et al.*, 2014; Maire *et al.*, 2015). There is more 'fast' to 'slow' leaf trait variation within most communities than there is stress tolerant to intolerant variation across biomes (Wright *et al.*, 2004), suggesting that many of these leaf traits may be powerful proxies for general plant life history strategies (Reich, 2014). Chapter three tests whether the global trait associations of the LES hold true at various levels of taxonomic aggregation. If the putative physiological and evolutionary mechanisms that drive the LES are truly universal, we would expect patterns of LES trait covariation to be independent of

taxonomic scale. Chapter three compiles a global dataset of within-species and between-species trait variation to test whether most foliar trait variation is truly between species (as is often assumed), whether the LES trait correlations are consistent within- as well as between-species, and whether the LES traits respond to environmental gradients within a species. This chapter scrutinizes some of foundational assumptions about the utility of leaf functional traits, in order to further refine our understanding of what functional traits can and cannot do. By furthering our understanding of the causes and consequences of functional trait variation, Chapter three of this dissertation seeks to improve the tools with which many ecologists try to understand species interactions, community structure, and ecosystem function.

Chapter four of this dissertation is composed of supplementary materials, including appendices for the first three chapters. Chapter five synthesizes the results of the previous chapters, and draws conclusions about what this dissertation accomplishes and fruitful paths forward.

Works Cited

Anderegg LDL, Anderegg WRL, Berry JA (2013) Not all droughts are created equal: translating meteorological drought into woody plant mortality. *Tree Physiology*, **33**, 672–683.

Anderegg WRL, Berry JA, Field CB (2012) Linking definitions, mechanisms, and modeling of drought-induced tree death. *Trends in Plant Science*, **17**, 693–700.

Assessment ME (2005) *Ecosystems and Human Well-being: Synthesis*. Island Press, Washington, DC.

Barbeta A, Peñuelas J, Barbeta A, Peñuelas J (2016) Sequence of plant responses to droughts of different timescales: lessons from holm oak (Quercus ilex) forests. *Plant Ecology & Diversity*, **00**, 1–18.

Brown CD, Vellend M (2014) Non-climatic constraints on upper elevational plant range expansion under climate change. *Proceedings of the Royal Society B: Biological Sciences*, **281**, 20141779–20141779.

Brown JH (1995) *Macroecology*. The University of Chicago Press.

Buckley LB, Waaser SA, MacLean HJ, Fox R (2011) Does including physiology improve species distribution model predictions of responses to recent climate change? *Ecology*, **92**, 2214–2221.

Case MJ, Peterson DL (2005) Fine-scale variability in growth climate relationships of Douglas-fir, North Cascade Range, Washington. *Canadian Journal of Forest Research*.

Chaves MM, Maroco JP, Pereira JS (2003) Understanding plant responses to drought — from genes to the whole plant. *Functional Plant Biology*, **30**, 239–264.

Clark JS, Carpenter SR, Barber M, Collins S (2001) Ecological forecasts: an emerging imperative. ....

Contreras MA, Affleck D, Chung W (2011) Evaluating tree competition indices as predictors of basal area increment in western Montana forests. *Forest Ecology and Management*, **262**, 1939–1949.

Copenhaver-Parry PE, Cannon E (2016) The relative influences of climate and competition on tree growth along montane ecotones in the Rocky Mountains. *Oecologia*, **182**, 13–25.

D'Orangeville L, Duchesne L, Kneeshaw D, Côté B, Pederson N (2016) Northeastern North America as a potential refugium for boreal forests in a warming climate. *Science*, **352**, 1452–1455.

Dakos V, Glaser SM, Hsieh C-H, Sugihara G (2017) Elevated nonlinearity as an indicator of shifts in the dynamics of populations under stress. *Journal of The Royal Society Interface*, **14**, 20160845.

Das A, Battles J, Stephenson NL, van Mantgem PJ (2011) The contribution of competition to tree mortality in old-growth coniferous forests. *Forest Ecology and Management*, **261**, 1203–1213.

Ettinger AK, Hillerislambers J (2013) Climate isn't everything: competitive interactions and variation by life stage will also affect range shifts in a warming world. *American Journal of Botany*, **100**, 1344–1355.

Ettinger AK, Ford KR, HilleRisLambers J (2011) Climate determines upper, but not lower, altitudinal range limits of Pacific Northwest conifers. *Ecology*.

Evans MR, Bithell M, Cornell SJ et al. (2013) Predictive systems ecology. *Proceedings of the Royal Society B: Biological Sciences*, **280**, 20131452–20131452.

Girardin MP, Bouriaud O, Hogg EH et al. (2016) No growth stimulation of Canada's boreal

forest under half-century of combined warming and CO 2fertilization. *Proceedings of the National Academy of Sciences of the United States of America*, **113**, E8406–E8414.
Griesbauer HP, Green DS (2010) Assessing the climatic sensitivity of Douglas-fir at its northern range margins in British Columbia, Canada. *Trees-Structure and Function*.
Higgins SI, O'Hara RB, Bykova O et al. (2012) A physiological analogy of the niche for projecting the potential distribution of plants. *Journal of Biogeography*, **39**, 2132–2145.
Hillerislambers J, Harsch MA, Ettinger AK, Ford KR, Theobald EJ (2013) How will biotic interactions influence climate change-induced range shifts? *Annals of the New York Academy of Sciences*.
Iverson LR, Prasad AM, Matthews SN, Peters MP (2011) Lessons Learned While Integrating Habitat, Dispersal, Disturbance, and Life-History Traits into Species Habitat Models Under Climate Change. *Ecosystems*, **14**, 1005–1020.
Kidwell SM (2015) Biology in the Anthropocene: Challenges and insights from young fossil records. *Proceedings of the National Academy of Sciences of the United States of America*, **112**, 4922–4929.
Koehler K, Center A, Cavender-Bares J (2012) Evidence for a freezing tolerance-growth rate trade-off in the live oaks (Quercus series Virentes) across the tropical-temperate divide. *New Phytologist*, **193**, 730–744.
Kunstler G, Albert CH, Courbaud B (2011) Effects of competition on tree radial-growth vary in importance but not in intensity along climatic gradients. *Journal of ….*
Lamanna C, Blonder B, Violle C et al. (2014) Functional trait space and the latitudinal diversity gradient. *Proceedings of the National Academy of Sciences of the United States of America*, **111**, 13745–13750.
Larcher W, Heber U, Santarius KA (1973) Limiting Temperatures for Life Functions. In: *link.springer.com* (eds Precht H, Christopherson J, Hensel H, Larcher W), pp. 195–263. Temperature and Life, Berlin, Heidelberg.
Lawler JJ, Ruesch AS, Olden JD, McRae BH (2013) Projected climate-driven faunal movement routes (ed Haddad N). *Ecology letters*, **16**, 1014–1022.
Lawler JJ, Shafer SL, White D, Kareiva P, Maurer EP, Blaustein AR, Bartlein PJ (2009) Projected climate-induced faunal change in the Western Hemisphere. *Ecology*, **90**, 588–597.
Levitt J (1980) *Responses of plants to environmental stresses, Volume 2: Water, radiation, salt and other stresses*, 2nd edn. Springer, Berlin.
Littell JS, Peterson DL, Tjoelker M (2008) Douglas-fir growth in mountain ecosystems: water limits tree growth from stand to region. *Ecological Monographs*.
Loehle C (1998) Height growth rate tradeoffs determine northern and southern range limits for trees. *Journal of Biogeography*, **25**, 735–742.
Ludlow MM (1989) Strategies of response to water stress. In: *Structural and functional responses to environmental stresses: Water shortage*. International Botanical Congress.
Lunt DJ, Dunkley Jones T, Heinemann M et al. (2012) A model–data comparison for a multi-model ensemble of early Eocene atmosphere–ocean simulations: EoMIP. *Climate of the Past*, **8**, 1717–1736.
MacArthur D (1972) *Geographical Ecology: Patterns in the Distribution of Species*. Harper & Row, New York.
Maire V, Wright IJ, Prentice IC et al. (2015) Global effects of soil and climate on leaf photosynthetic traits and rates. *Global ecology and biogeography*, **24**.
Masson-Delmotte V, Schulz M, Abe-Ouchi A, Beer J (2013) Information from paleoclimate

archives. *Climate Change*.
McDowell NG, Beerling DJ, Breshears DD, Fisher RA, Raffa KF, Stitt M (2011) The interdependence of mechanisms underlying climate-driven vegetation mortality. *Trends in Ecology & Evolution*, **26**, 523–532.
Morin X, Thuiller W (2009) Comparing niche-and process-based models to reduce prediction uncertainty in species range shifts under climate change. *Ecology*.
Nakawatase JM, Peterson DL (2006) Spatial variability in forest growth – climate relationships in the Olympic Mountains, Washington. *Canadian Journal of Forest Research*, **36**, 77–91.
Peterson DW, Peterson DL (2002) Growth responses of subalpine fir to climatic variability in the Pacific Northwest. *Canadian Journal of Forest Research.*
Quintero I, Wiens JJ (2013) Rates of projected climate change dramatically exceed past rates of climatic niche evolution among vertebrate species (eds Quintero I, Wiens JJ). *Ecology letters*, **16**, 1095–1103.
Reich PB (2014) The world‐wide "fast–slow"plant economics spectrum: a traits manifesto. *Journal of Ecology*.
Restaino CM, Peterson DL, Littell J (2016) Increased water deficit decreases Douglas fir growth throughout western US forests. *Proceedings of the National Academy of Sciences of the United States of America*, 201602384.
Savage JA, Cavender-Bares J (2013) Phenological cues drive an apparent trade-off between freezing tolerance and growth in the family Salicaceae. *Ecology*, **94**, 1708–1717.
Schloss CA, Nuñez TA, Lawler JJ (2012) Dispersal will limit ability of mammals to track climate change in the Western Hemisphere. *Proceedings of the National Academy of Sciences*, **109**, 8606–8611.
Sunday JM, Bates AE, Dulvy NK (2012) Thermal tolerance and the global redistribution of animals. *Nature Climate Change*.
Wright IJ, Reich PB, Cornelissen JHC et al. (2005) Assessing the generality of global leaf trait relationships. *New Phytologist*, **166**, 485–496.
Wright IJ, Reich PB, Westoby M et al. (2004) The worldwide leaf economics spectrum. *Nature*, **428**, 821–827.

Chapter 1: Climate and competitive tree growth constraints trade off at large scales but not local scales

Leander DL Anderegg[1*], Janneke Hille Ris Lambers[1]

[1] Department of Biology, University of Washington, Seattle, WA
[*]corresponding author: ldla@uw.edu, +1 541.790.1096

Short title:
Climate and competition trade off at large but not local scales

Keywords:
Range margins, tree rings, elevation ranges, Stress Tradeoff Hypothesis, range constraint mechanisms

Supplemental Material referenced in text can be found in Appendix A-C

Abstract:

Knowledge of the mechanisms that constrain species geographic ranges is critical for anticipating and managing climate change-induced range shifts. Long-standing ecological theory suggests a tradeoff between climatic range constraints in harsh environments and biotic constraints in benign environments, but this theory has rarely been tested. We measured competitive and climatic constraints on tree growth in multiple species across their elevational ranges in three distinct climatic regions to test whether a climate-competition tradeoff can explain elevation distributions. We show that for most species, tree growth at environmentally harsh range boundaries is climatically constrained, but that tree growth at environmentally benign range boundaries was not often constrained by competition. As a result, a climate-competition tradeoff explained few local ranges. Additionally, it was difficult to predict a-priori which range boundaries (low or high) were climatically vs. competitively constrained. However, across all species and study sites, climatic growth constraints increased and competitive constraints decreased in harsh environments consistent with a broad-scale climate-competition tradeoff. Our findings highlight multiple processes that complicate local range dynamics, but suggest that the constraints on large-scale (e.g. latitudinal) tree distributions may still be predicted from ecological theory. Thus, existing correlational tools such as Climate Envelope Models may be appropriate for predicting shifts of large scale plant range boundaries in climatically harsh environments.

Significance statement:

Species will respond and have already responded to human-caused climate change by shifting where they occur on the landscape. To anticipate these shifts, we need to understand the forces

that determine where species currently occur. We test whether a tradeoff between climate and competitive constraints explains where tree species grow on mountain slopes. We find that climate often controls environmentally harsh elevation range boundaries and that climate and competition trade off at large spatial scales. However, we find that climate-competition tradeoffs are rare at local scales (e.g. across one mountain slope). Our work underscores the difficulty of predicting local-scale range dynamics, but suggests that current tools for predicting range shifts may be appropriate for forecasting large-scale range limits, especially in harsh environments.

Introduction:

Species geographic ranges are, in essence, the spatial manifestation of their ecological niche, and have thus fascinated ecologists for over two centuries (Humboldt & Bonpland, 1805; MacArthur, 1972; Gaston, 2009a). One long-standing ecological hypothesis posits that biotic interactions are the dominant constraint on organismal fitness in benign environments, while abiotic stress is the dominant fitness constraint in harsh environments (henceforth the Stress Tradeoff Hypothesis, or STH - (Dobzhansky, 1950; MacArthur, 1972; Brown, 1995). This Stress Tradeoff Hypothesis implies that species inhabiting a gradient of climatic harshness (e.g. elevation or latitude) should be constrained by species interactions (e.g. competition) at their benign range boundary and by climatic stress (e.g. limits to their physiological tolerance) at their harsh range boundary (Loehle, 1998; Koehler *et al.*, 2012; Lusk *et al.*, 2013; Savage & Cavender-Bares, 2013). If so, the STH could broadly explain the mechanisms of geographic range constraints, helping scientists understand climate change-induced range shift dynamics for unstudied or poorly studied species.

With unprecedented rates of anthropogenic climate change expected during the next century (Quintero & Wiens, 2013), our need to understand geographic ranges has elevated from theoretical to practical. Yet few useful generalizations have emerged from the growing range constraint and range shift literature (Gaston, 2009b; Angert *et al.*, 2011; Buckley & Kingsolver, 2012; Sunday *et al.*, 2012; Talluto *et al.*, 2015). Broad concordance between species ranges and climate isoclines (e.g. (Woodward & Williams, 1987; Root, 1988; Buckley *et al.*, 2010), records of paleo-range shifts with climate during the Quaternary (e.g. (Williams *et al.*, 2004; Jackson & Blois, 2015), and ongoing range shifts coinciding with recent anthropogenic warming (Parmesan & Yohe, 2003; Root *et al.*, 2003; Lenoir *et al.*, 2008; Tingley *et al.*, 2012) suggest that climate plays a large role in constraining species ranges. However, these recent range shifts have been extremely variable, ranging from unexpectedly large shifts to no shifts to shifts in the opposite of the predicted direction, suggesting climate is not the sole, uniform driver of range limits. Moreover, species interactions are known to greatly complicate the relationship between climate and species ranges, limiting robust predictions (Araújo & Luoto, 2007; Ettinger & Hillerislambers, 2013; Hillerislambers *et al.*, 2013). The Stress Tradeoff Hypothesis provides testable predictions about where climate or competition is more likely to constrain a species geographic range. If true, the STH could provide critical guidance regarding the kinds of models and information needed to accurately forecast range shifts.

Unfortunately, the Stress Tradeoff Hypothesis has rarely been tested empirically, due to the paucity of detailed information on range constraint mechanisms. The STH has been posited to explain the distributions of North American tree species (Loehle, 1998), but has received mixed support from small-scale investigations of tree elevation range boundaries (Ettinger et al. 2011, Ettinger et al, in press) and a glasshouse experiment (Savage & Cavender-Bares, 2013). To

our knowledge, no study has tested the predictions of the STH in multiple species at a large geographic scale using actual observations of range constraint mechanisms.

A robust test of the STH requires measurements of both climatic and biotic/competitive constraints on at least one component of organismal fitness across multiple geographic ranges, ideally in a variety of climatic settings. Tree rings offer a useful tool for testing the Stress Tradeoff Hypothesis because they can be used to reconstruct tree growth sensitivity to both inter-annual climate fluctuations and competitive environment and can easily be collected across large geographic space. Within species, growth of adult trees is often correlated with both survival and fecundity (Wyckoff & Clark, 2000; 2002; Clark *et al.*, 2004), making inferences on growth reasonable proxies for other fitness components that are harder to quantify. A burgeoning tree ring literature has documented increased growth sensitivity to climate near high latitude or elevation boundaries (Case & Peterson, 2005; Ettinger *et al.*, 2011; Griesbauer & Green, 2012), or increasing competitive constraints approaching low elevation boundaries ((Callaway, 1998; Coomes & Allen, 2007; Copenhaver-Parry & Cannon, 2016) but see (Ettinger & Hillerislambers, 2013)). However, collectively these studies cover a small number of species, sites, climates and range margins. More importantly, studies that quantify only one constraint type across space (e.g. growth sensitivity to climate across climate gradients (D'Orangeville *et al.*, 2016; Restaino *et al.*, 2016)), or both climatic and biotic growth constraints in small study areas (Sanchez-Salguero *et al.*, 2015; Copenhaver-Parry & Cannon, 2016) do not provide complete tests of the generality of the STH.

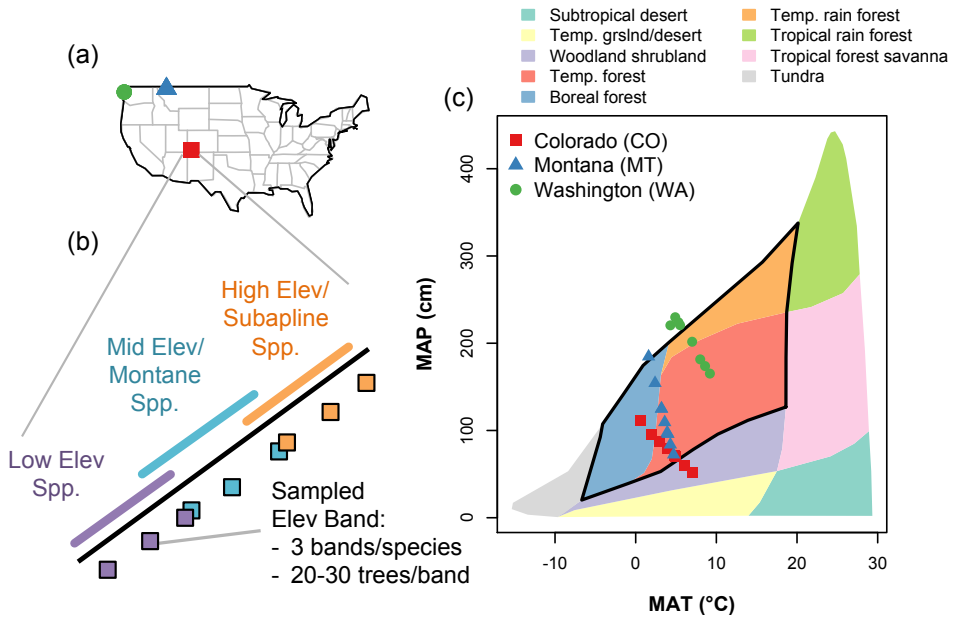

Figure 1: *(a) Three sampled mountain transects in the western U.S.A. (b) Diagram of sampling scheme at each transect. We cored 20-30 trees each in elevation bands at the high range margin, low range margin and range center of the dominant low elevation, montane and subalpine tree species on each transect. (c) Transects in Mean Annual Temperature (MAT) – Mean Annual Precipitation (MAP) space, plotted over Whittaker's biome map* (Whittaker, 1975) *– the transects cover much of temperate forest biome climate space (outlined in black). Climate normals were calculated for each elevation band using the ClimateWNA downscaling algorithm of the gridded PRISM 1970-2000 climate normals* (Wang *et al.*, 2012).

We present a multi-species, multi-site analysis of both climatic and competitive constraints on tree growth across the elevation ranges of tree species throughout a large range of climates in the western U.S.A. (Figure 1). We collected tree cores along elevation transects of approximately 1200m at three western U.S. sites in Colorado (CO), Montana (MT), and Washington (WA) encompassing 17 species elevation range boundaries (Figure S1). We used tree rings to quantify environmental harshness, climatic growth constraints and competitive growth constraints at the high and low range margins and range center of three dominant tree species per transect (Table 1). Some species were sampled on multiple transects, so we refer to each species cored at each mountain as one species-replicate (i.e. we sampled three species-replicates per transect, see

Table S1 for transect descriptions). These three transects span much of the temperate climate space containing woody biomes (Figure 1c).

Table 1: *The three metrics calculated from tree ring records in order to test the Stress Tradeoff Hypotheses, including details and rational for their calculation.*

	Environmental Harshness	**Climatic Constraint**	**Competitive Constraint**
Metric	Mean Growth Rate	Population Growth Synchrony	Growth Sensitivity to Competition
Details	*Size- and competition-standardized mean Basal Area Increment (2003-2012) calculated using linear mixed effects models*	*Mean correlation of growth anomalies between trees in an population (synchrony of growth through time)*	*Growth suppression from +1 sd increase in neighborhood density (based on tree-to-tree variation in mean growth)*
Rational	*Mean growth rates will reflect general environmental harshness, with slower growth rates indicating a harsher environment*	*Synchronous growth anomalies between widespread trees indicate a broad-scale driver (i.e. climate), while asynchronous growth indicates that local factors (competition, pets/pathogens) drive growth anomalies*	*Large growth differences between trees growing in low and high neighborhood densities indicate that competition greatly constrains tree growth.*

We tested whether the Stress Tradeoff Hypothesis explains elevational patterns of climate and competition sensitivity within species. At the scale of elevation ranges, the STH predicts that populations near environmentally harsh range boundaries should show high climatic growth constraints compared to the rest of the species' range, while populations at 'benign' range boundaries should show increased competitive constraints (i.e. increasingly negative effect of neighbor density on annual growth). We adopted a tree-centric definition of harshness based on a population's mean radial growth rate (size and competition standardized), rather than a-priori definitions based upon elevation or climate (Table 1). Populations with the highest radial growth

rates were assumed to inhabit benign environments and populations with low growth rates harsh environments.

We quantified climatic constraints based on how synchronous growth fluctuations were between trees in a population (Table 1). We consider synchronized annual growth a simple and intuitive proxy for climatic constraints, because climate is the most likely driver of synchronous growth fluctuations at the scale of an entire population (Ettinger *et al.*, 2011; Shimatani & Kubota, 2011; Shestakova *et al.*, 2016). We also calculated climate sensitivity based on multiple metrics from various statistical growth-climate models, but found growth synchrony to be the most parsimonious, assumption free and easily interpretable metric (see Supplemental Methods: Alternative metrics of climate sensitivity). We assessed the strength of competitive constraints based on how much increased stand density suppressed average tree growth rates in a population (See Table 1, Methods).

We first evaluated the evidence for climatic and competitive range constraints for each elevation range boundary. We then examined climate and growth constraints more broadly across all species and sites, as it is also possible that the STH could manifest as a general tradeoff between climatic and competitive growth constraints at broad scales regardless of range position, even if local factors such as disturbance history, microclimate and small-scale edaphic variation obscure local-scale signals of the STH. Specifically, we differentiated harsh and benign range boundaries and calculate climatic and competitive growth constraint metrics from the tree ring record to ask:

1) Do harsh elevation range boundaries exhibit increased growth sensitivity to climate and benign boundaries increased sensitivity to competitive environment?

2) Do species typically show a tradeoff between one climatically and one competitively constrained range boundary, suggesting that the STH applies at the scale of local elevation ranges?
3) At a broader scale, do competitive growth constraints increase and climatic growth constraints decrease in populations with faster growth rates across all species and sites regardless of population range position?

Results and Discussion:

At the local level, we found that trees growing at harsh range boundaries did typically have greater sensitivity to climate, but trees were not more constrained by competition at benign boundaries. As a result, few species-replicates showed evidence of the climate-competition tradeoff hypothesized by the STH at the local scale. However, across all species and all mountains, we found broad evidence that climatic constraints on adult tree growth increase in harsh environments and competitive constraints increase in benign environments, consistent with the STH. We discuss our findings in more detail below.

STH and local elevation range boundaries

Surprisingly, we found only a few examples of elevational range boundaries that supported a tradeoff between climatic and competitive constraints on growth, as proposed by the STH. One such species was *Pinus ponderosa* in Colorado, which showed a large increase in basal area growth moving from the low elevation (hot-dry) range margin to the high elevation (cool-wet) range margin, suggesting that low elevations are more environmentally harsh and high elevations benign (Figure 2). Growth synchrony (interpreted as in index of climatic

constraint, See Table 1 and Methods) also increased from the range center to the lower range margin (beta regression $p<0.0001$, Table S2), and decreased from the range center to the high range margin ($p<0.0001$) consistent with a decreasing climatic growth constraint with increasing elevation and a climatically controlled low elevation range boundary. Meanwhile, the strength of competitive suppression was relatively small at mid and low elevation, but became much larger at the high elevation range margin (Figure 2f, linear mixed effects model $p=0.0041$), consistent with an increased competitive growth constraint at *P. ponderosa's* high elevation, benign range boundary.

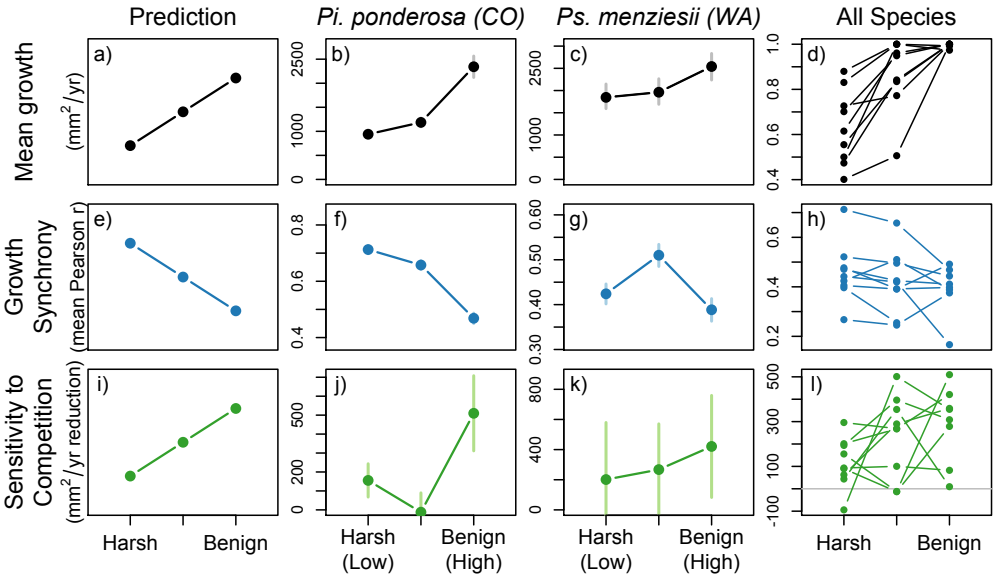

Figure 2: *Predicted and observed patterns of mean basal area growth (proxy for climatic harshness, a-d), growth synchrony (indicator of climatic growth constraint, e-h), and growth sensitivity to competition (competitive growth constraint, i-l). Pinus ponderosa in Colorado (b,f,d) shows the hypothesized tradeoff between a climatic growth constraint at its harsh (low elevation) range boundary and a competitive constraint at its benign (high elevation) range boundary. Pseudotsuga menziesii in Washington (c,g,k) showed no such tradeoff. Patterns for all species-replicates are shown in panels d,h and i. Error bars show ±SE (see Table S2 for full statistics). Note, the y axis for panel d is proportion of species-replicate maximum basal area growth, rather than mm^2/yr as in a-c.*

However, growth of most species-replicates (seven of nine) did not show a clean tradeoff between climatic and competitive range constraints. For example, growth of *Pseudotsuga menziesii* from Washington changed little from low to mid and mid to high elevations,

suggesting only a slight environmental harshness gradient at most (Figure 2c, Table S2). Contrary to expectations, growth synchrony peaked at its mid-elevation range center (Fig 2g), and growth of trees at all elevations were relatively insensitive to competition (large error bars nearly overlapping zero on Fig. 2k). In short, we found a climate-competition tradeoff for only two of nine species-replicates (Fig. 3). Thus, the predictive power of the STH for determining the mechanisms driving local elevation range boundaries appears limited, at least in our data set.

Despite the inability of the STH to map onto local elevation boundaries, useful patterns did emerge. First, all but one species-replicate reached its maximum growth rate at one range boundary and minimum growth rate at the other (Figure 2d, Fig. S2, Table S2). Thus, most species-replicates did appear to have one 'harsh' and one 'benign' range boundary. Second, the majority of harsh range boundaries (seven of nine) did show evidence of climatic growth limitation (Figure 3). However, only three of eight benign boundaries (one species-replicate did not have a benign range boundary, see Methods) showed evidence of competitive constraints – perhaps because competitive constraints are either less prevalent or more difficult to detect in the tree ring record, or because other biotic interactions constrain growth at these range boundaries. However, the preponderance of climatic range constraints at harsh boundaries supports the findings of various single species or single site dendroecological studies (Nakawatase & Peterson, 2006; Case & Peterson, 2007; Griesbauer, 2010; Griesbauer *et al.*, 2011; Lévesque *et al.*, 2014). Together, the emerging evidence indicates that identifiably harsh range boundaries tend to be under climatic control (but see (Urli *et al.*, 2016)). This result emerged across a wide range of climatic conditions (Figure 1), providing a useful rule of thumb for predicting where correlative distribution models may be used to forecast changes in suitable habitat under climate change.

However, our results also highlight the difficulty of predicting a-priori what range boundaries are actually 'harsh', and which tree populations are likely to be most sensitive to climate change. Our growth-rate related metric of environmental suitability identified both harsh upper margins (4/9 species-replicates) and harsh lower range margins (5/9 species-replicates). Patterns were neither consistent for the same species on different transects nor for different species on the same mountain (Figure 3, Figure S4). In fact, had we assumed either winter harshness or summer dryness to be the dominant climatic stress structuring all sampled ranges, we would have mis-identified four range margins as harsh that were actually the fastest growing populations for that species-replicate. Thus, the importance of both macroclimatic context (difference across mountains) and microclimatic context (difference between species on a mountain) appear paramount in determining how climatic harshness actually maps on to an elevational range.

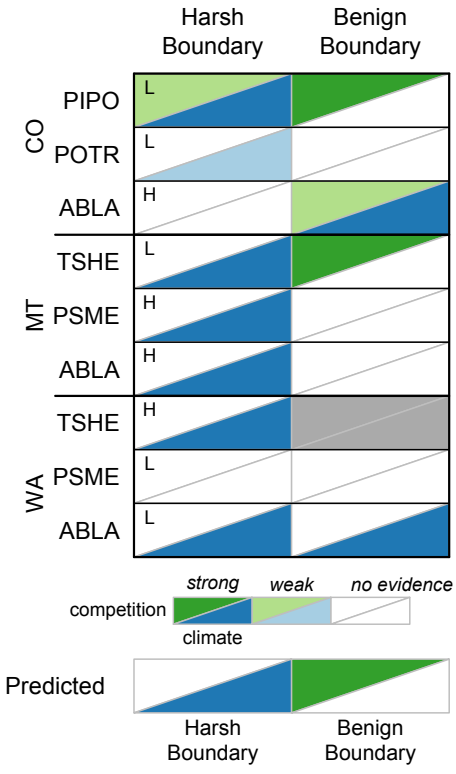

Figure 3: *Summary of evidence for climatic and competitive constraints for 17 tree elevation range margins across the western U.S. (see also Table S2). The Stress Tradeoff Hypothesis predicts a climatic constrain (blue) at harsh boundaries and a competitive constraint (green) at benign boundaries. 'Harsh' and 'benign' were designated based on mean size- and competition-standardized growth rate, with the margin showing the slowest growth designated as 'harsh' (as in Fig. 2). Letter in the Harsh column indicates whether the harsh boundary was low ('L') or high ('H') elevation. Gray cell indicates that the range margin was not samples (T. heterophylla extends to sea level in Washington and has now lower margin). Strong evidence: $p<0.01$ difference between growth constraint at range margin and range center, weak evidence: $0.1 > p > 0.01$ (or that competitive constraint was much stronger at the other range margin for Pi. Ponderosa in CO). PIPO: Pinus ponderos, POTR: Populus tremuloides, ABLA: Abies lasiocarpa, TSHE: Tsuga heterophylla, PSME: Pseudotsuga menziesii.*

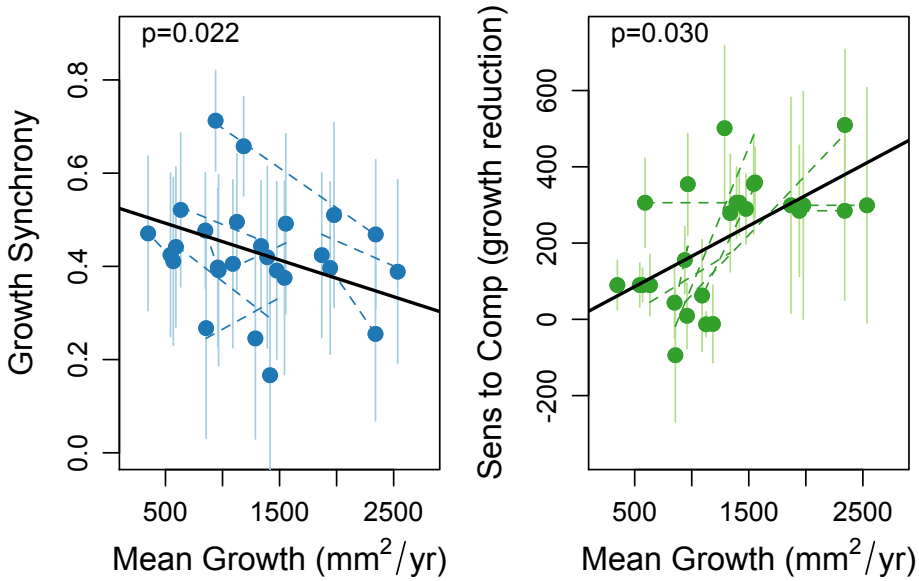

Figure 4: *Across all species-replicates, population growth synchrony decreased with increasing mean size- and competition-standardized growth rate (panel a) while growth sensitivity to competitive environment increased with population mean growth rate (panel b). Points indicate population means, error bars indicate the standard deviation of growth synchrony (a) or the standard error of mean parameter estimates (b), dotted lines show trends for each species-replicate, and the solid line shows the global trend line estimated from the site trends using hierarchical linear mixed effects models. P values indicate the significance of the global trend calculated from population means weighted by the inverse of the population SE.*

Broad scale evidence of STH

Although the STH did not consistently predict growth constraints at individual range boundaries, we did find broad evidence for the Stress Tradeoff Hypothesis at large scales. Specifically, we found that tree populations (across all species and sites) that grew more slowly on average had more tree-to-tree synchronized annual growth, suggesting greater climatic growth constraints in harsh environments (Figure 4a, SE-weighted linear mixed effects model p= 0.028). Across all populations, we also found that the fastest growing populations of trees (we assume experiencing the most benign environments) showed the largest growth suppression due to

competition (Figure 4b, p=0.001). This trend of increasing competitive growth suppression with increasing growth rates was qualitatively similar if growth suppression was expressed as a proportion of population growth rather than raw Basal Area Increment reduction (Figure S4), though the global relationship was no longer statistically significant (p=0.35). Thus, even though the relationships between mean growth and the climatic and competitive constraints on growth do not map cleanly onto individual range margins according to the STH, tree populations in the optimal conditions are generally most constrained by competition, while those in the least optimal conditions are more constrained by climate.

However, despite this broad scale evidence of the STH, mean growth, synchrony or competitive sensitivity did not vary consistently across any climate gradient we examined, highlighting the complexity of climate-growth relationships (Figure S5). Mean growth showed patterns somewhat indicative of a transition between radiation limitation and drought limitation with increasing aridity. Species-replicates in wet locations showed increased growth at higher Climatic Moisture Deficits (CMD or potential evapotranspiration – precipitation) while species-replicates in dry locations showed decreased growth at higher CMDs (Fig S5c). But species at intermediate aridities (e.g. CMD between 150mm and 350mm) showed a mix of both positive and negative mean growth relationships with CMD, rather than a common inflection point. The only significant large-scale relationship across all species-replicates was between growth synchrony and Climatic Moisture Deficit, though this was driven primarily by the strong responses of the two driest species-replicates (*Pinus ponderosa* and *Populus tremuloides* in Colorado, Figure S2, p=XXX).

Factors that complicate the STH at local scales

One reason growth constraints (regardless of whether they are competitive or climatic) may not have mapped onto elevational range boundaries is because growth is only one aspect of fitness. We found mixed evidence for lower performance at range limits for fitness components besides adult growth, implying this may partly but not entirely explain the complex results we observed with adult growth. For example, we found that recruitment (to seedling or sapling stages) and adult survival for roughly half of species-replicates was highest at 'benign' range boundaries, as predicted if recruitment and survival are correlated with growth (Fig. 5). However, these vital rates followed the opposite pattern at range boundaries of several species. In the case of the two species that show unexpected mortality trends (i.e. highest benign mortality and lowest harsh mortality), we suspect that these patterns reflect the importance of biotic agents of mortality (Fig. 5a, Fig. S3, Table S3). Both these species-replicates had benign range boundaries unexplained by adult growth, which could suggest a biotic range constraint driven by mortality from biotic agents rather than competition. In this case, one additional species-replicate (*A. lasiocarpa* in Montana) would conform to the STH.

For recruitment density, we generally found unexpected elevational patterns in the closed canopy forests of WA and MT (Figure 5b, S3, S7). Specifically, regeneration densities were actually highest at the harsh range boundary if all three Montana species-replicates and hump or trough-shaped for species-replicates in Washington. For *A. lasiocarpa* in Montana, we believe this inverse relationship between regeneration and adult growth is likely a function of increased residency time at sapling stage at tree line and/or a switch from competitive suppression to facilitation near treeline (Fig. S7, (Callaway, 1998)). For the remaining species-replicates, however, these patterns could indicate that competition or pest/pathogen load controls the benign range boundary by limiting recruitment, despite an absence of evidence of competitive

constraints for adults. Regardless of the reasons, these demographic measurements suggest climatic / competitive constraints are likely to operate with different strengths at different life history stages – but that this alone is unlikely to explain the complexity of our results.

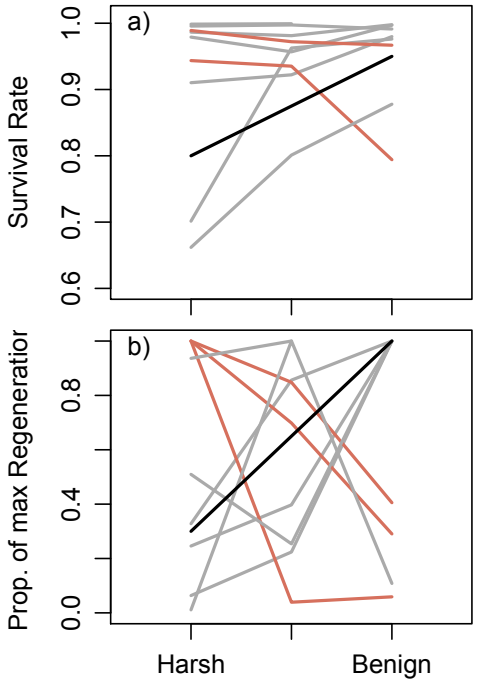

Figure 5*: Survival and recruitment near study trees at the harsh and benign range margins and range center of nine species-replicates. (a) Recent (approx. 5 year) survival rates as a function of range position and (b) sapling/seedling density at mean stand density as a proportion of species-replicate maximum recruitment density. Black lines show expected patterns if survival*

The strong effects of disturbance on the establishment of tree populations may additionally complicate the interpretation of elevation range boundaries and range constraints for some species. For example, in the closed canopy, old growth forests of Montana and Washington, altitudinal ranges of shade intolerant species such as *Pseudotsuga menziesii* and *Abies lasiocarpa* may be the legacy of stand replacing fires, such that elevation range margins actually represent the distribution of historic fires rather than edges of the fundamental niche. Given large scale evidence for climatic growth constraints across the entire continental range of *Pseudotsuga menziesii* (Littell *et al.*, 2008; Restaino *et al.*, 2016), this could well explain at least a portion of the unexplained range boundaries in this study (Fig. 4). While our dispersed

sampling strategy attempted to sample across variation in edaphic environment and stand history in each range margin population (see Methods), there was some evidence for elevational differences in tree size that did not mirror mean growth trends (see MT-TSHE and WA-PSME in Table S1), suggesting the possibility of large disturbance events that homogenized stand age across a range margin or range center population and established contrasting stand ages between populations. This may be consistent with long-term disturbance history mediating some elevational distributions.

Finally, our results highlight the complexity of real world climate gradients, where disconnects between micro- and macroclimate challenge the assumption that an elevation gradient represents a monotonic stress gradient. Specifically, while almost all species replicates showed monotonic growth increases from one range margin to the other, it was difficult to predict a-priori which (upper or lower) range margin is 'harsh' for any species. One tree-line species-replicate (*Abies lasiocarpa* in WA), for example, actually reached its highest growth rates at the apparent tree line, likely due to the intricacy of local microclimates across even small topographic and aspect variation that swamped the assumed elevation climate gradient. However, we suspect complex and unexpected results would have emerged even if we had had perfect information on the microclimate experienced at all sampling locations. This is because the complexity of plant physiology and phenology means the relationship between plant stress and climate is often complicated and unpredictable (Anderegg & HilleRisLambers, 2015), see Supplementary Methods: Alternative metrics of climate sensitivity).

Conclusions:

In all, our findings suggest that the Stress Tradeoff Hypothesis operates at broad spatial scales and may be useful for inferring climate change responses at these scales (e.g. latitudinal range boundaries); especially in environmentally 'harsh' regions where range constraint mechanisms seem most predictable. One major implication of our work is that high latitude range boundaries or subcontinental scale dry range boundaries (e.g. across maritime to continental climate gradients) are likely climatically constrained for many trees. Correlative models such as Climate Envelope Models may provide useful predictions of future dynamics of these particular range boundaries (assuming the short-term mechanisms of range contraction or expansion are understood). At the same time, our findings also highlight complexities that might prevent the STH from being useful for climate change forecasts at finer spatial scales (e.g. altitudinal range limits). However, these are also fruitful areas of future study. For example, the location of the climatically harsh range boundary (upper or lower?) and the life history stages at which population growth is constrained are major unknowns, as is the role of non-competitive biotic interactions at benign range limits. The importance of historical contingency (e.g. disturbance history) and complex microclimate in determining current local ranges (which may not appear in equilibrium with assumed climate gradients) may also be important for predicting local-scale range dynamics. Despite these complexities, we are cautiously optimistic that future work on large scale range boundaries will continue to reveal generalizations about range constraint mechanisms that can guide the development and application of range shift modeling tools. We also hope that explicitly biogeographic studies of tree regeneration and survival constraints will continue to improve our ability to understand local range dynamics and yield land-management relevant knowledge.

Methods:

Study Locations

We collected tree cores from a total of 740 trees along elevation transects climbing three mountains: Shark's Tooth in the San Juan National Forest, Colorado (henceforth 'CO'); Mt. Brown in Glacier National Park, Montana ('MT'); and Hurricane Hill in Olympic National Park, Washington ('WA') (Figure 1a, Figure S1). We cored 20-30 trees each from populations at the high and low elevation range margins and range center of three species per transect (Figure 1b). Each transect contains a strong climate gradient across elevation, principally defined for all three mountains by decreasing summer aridity and decreasing growing season temperature with increasing elevation (Figure S2a). However, the three transects differ considerably in terms of winter/dormant season (Nov-April) precipitation, and seasonal temperature variation (continentality) (Figure S2b). At each of three study mountain slopes, we identified a transect running from the mountain base (or in Colorado the lower elevation boundary of closed forest) to high elevation tree line while maintaining a roughly western aspect. To identify the dominant low elevation, montane and subalpine species at each mountain and determine their elevation range boundaries, we quantified species relative abundance and turnover across elevation at each mountain via 3-6 strip transects (5m wide by 50m long counting every stem >10cm DBH) at every ~50m of elevation gain. In CO, our study species going from low to high elevation were *Pinus ponderosa, Populus tremuloides,* and *Abies lasiocarpa*. In MT and WA, our study species (low to high elevation) were *Tsuga heterophylla, Psuedotsuga menziesii,* and *Abies lasiocarpa* (Figure S1). In total, we examined nine species-replicates and 17 elevation range boundaries (in Washington, *Tsuga heterophylla*'s range extends essentially to sea level, so we were only able to

sample its upper and not its lower range margin). We determined climate normals for each sampled population based on the 1961-1990 PRISM climate normals (Daly et al. 2008) using the scale-free interpolation technique of ClimateWNA (ClimateWNA version 5.21, Wang et al. 2012).

Sampling Design

At each site we collected tree cores from dispersed trees in ~100m elevation bands along the high and low elevation range margins and the range center of each of the three focal species. The purpose of this dispersed sampling strategy was to accurately capture population radial growth rates and growth sensitivies while sampling across variation in microtopography and stand history. In each population, we cored 10-15 pairs of mature canopy trees (total of 20-30 trees per elevation) selected to include a range of diameters representative of the forest structure. Trees in a pair were <30m apart and of a similar diameter, one tree growing in a high competitive environment and one in a low competitive environment (typically a tree-fall gap) in order to capture as much variation in competition as possible. Pairs of trees were >40m apart, and all were located away from visible drainages. We quantified competitive environment using multiple metrics including stand basal area (assessed using a variable radius wedge prism), number of trees within 5m of the focal tree, number of canopies touching the focal tree and the focal tree's active crown fraction (percent of tree height supporting foliage). We also quantified the number of recent dead conspecific trees (i.e. still maintaining either needles or all bark and fine twigs) in the variable radius wedge prism plot around each tree to estimate mortality within the last ~5 years (Hicke *et al.*, 2012). Finally, we counted all conspecific saplings and seedlings within 5m of the focal tree with a height >5cm but a diameter at breast height <5cm.

We collected two tree cores at 1.35m height from opposite sides of each tree perpendicular to the aspect. Cores were mounted on wooden blocks, sanded and scanned with a high resolution scanner, and annual growth rings were measured to 0.001 mm using WinDENDRO (Version 2008e; Regent Instruments, Quebec City, Quebec, Canada). All cores were visually crossdated using WinDENDRO and then statistically crossdated with the Dendrochronology Program Library (dplR) package (Bunn 2010, version 1.6.4) in the R statistical environment (R Core Team 2016, version 3.2.4). One tree was excluded from further analysis because it could not be reliably crossdated. Annual ring widths from the two cores per individual tree were then averaged.

Ring width data were analyzed in two forms. First, to assess the effect of competitive environment and elevation on mean growth, we used the annual ring widths, the tree diameter at breast height, and bark depth measured on each tree in the field to calculate annual Basal Area Increment (BAI) from the outside of the tree inward. We then calculated the mean annual BAI for each tree for the 2003-2012 decade, a time over which the competitive environment assessed in 2013 was likely accurate. Second, to determine the correlation between annual growth anomalies between trees in a population we created unitless ring index (RWI) time series for the analysis of climate sensitivity by detrending each tree's ring width chronology using a spline (with 50% rigidity at 0.67*series length, Bunn 2010) and then pre-whitening this detrended timeseries using an AR1 autoregressive model. This removes low frequency growth variation due to both tree size/age and alterations in stand structure (Cook and Peters 1981).

Mean growth and competition

We quantified mean annual basal area growth (averaged for each tree from the 2003-2012 period) for each population by constructing linear models or linear mixed-effects models for each species-replicate relating tree mean basal area increment (BAI) to range position, tree size, and competitive environment. In short, we used an iterative model selection technique (Zuur et al. 2009) to determine whether tree pair was necessary as a random effect, and then determine the optimal variance structure and fixed structure (relating mean BAI to range position, tree DBH, and one or more non-colinear competitive metrics) using the *nlme* and *stats* packages in R (Pinheiro et al. 2016). Significant differences in mean growth at species-replicate mean tree size and competitive environment between range margins and the range center were determined by centering predictors and comparing range margin intercepts to the range center intercept with t-tests. Significant changes in competitive sensitivity (specific significant range position-by-competition interactions) were also assessed via t-tests. See Table S2 for a description of the final model selected for each species-replicate, and Supplemental Materials: Example code for example R code showing the model selection technique.

Broadly speaking, we interpreted size- and competition- standardized mean growth as an indication of environmental suitability of a population. Populations with low growth were interpreted as being environmentally 'harsh' and high growth as environmentally 'benign'. We present population mean growth both in raw form (mean BAI, Figure 4) and standardized as a proportion of the fastest growing elevation band for each species-replicate (Figure 2). We quantified the detrimental effect of competition on mean BAI as the raw growth suppression at each elevation band resulting from a one standard deviation increase in competitive environment, or standardized as the proportion of that elevation's mean growth suppressed by a one standard deviation increase in competition.

Climatic growth constraints

We estimated the general importance of climate for constraining growth by assessing the growth synchrony between trees in each population. Synchronous growth fluctuations across all trees in a population suggest that broad scale factors, namely climate, drive growth fluctuations. Conversely, asynchronous growth suggests that local factors (pathogen attack, mechanical damage, changes in competitive environment) drive growth fluctuations (Ettinger *et al.*, 2011; Shimatani & Kubota, 2011; Housset *et al.*, 2016). We quantified growth synchrony using the distribution of pair-wise correlations (Pearson's *r*) between the RWI of all trees in an elevation band. All RWI timeseries for a species-site were trimmed to the length of the shortest time-series across the species' three elevations to avoid artifacts due to differing chronology lengths across elevation. For each species-replicate, we then assessed significant differences in growth synchrony between range margins and the range center using beta-regressions (correlation coefficients were first transformed to be bounded 0 to 1 rather than -1 to 1) using the *betareg* function in the R package *betareg* (Cribari-Neto & Achim Zeileis, 2010, version 3.0-5) with logit link and elevationally varying precision.

We explored several additional metrics of growth sensitivity to climate from linear mixed-effects models designed to identify specific climate drivers of growth anomalies (size of standardized climate coefficients, ΔAIC of best model from null model, marginal or conditional R^2 of best model, mean R^2 of individual tree growth-climate models, etc). However, specific inferences proved highly dependent on which model selection technique, climate dataset, and method for selecting potential climate covariates (i.e. choices for dealing with multi-colinearity) we employed (See Supplemental Methods: Alternative metrics of climate sensitivity). This was,

at least in part, due to the complexity of memory effects (lagged effects of climate on growth from years prior to the growth year, Figures S9-S16) and the difficulty of defining appropriate climate variables over such a wide range of climates (e.g. growing season length differed by up to three months across the study sites, making universal definitions of seasonal variables difficult). Moreover, the statistical properties of goodness-of-fit metrics on mixed-effects models based on standardized, unitless Ring Width Indices (whose variance properties depend on the standardization technique) and the difficulties of establishing a best model-selection technique limited the robustness of these metrics. Results from these analyses are presented in the Supplemental Material, and qualitatively agree with the growth synchrony results presented here. So we present only the results of growth synchrony, as this is the most assumption-free and easily interpreted metric of climatic constraint.

Recruitment and Survival

Survival probabilities were calculated for each population based on the proportion of live versus recent dead conspecific trees measured in the variable radius plots around each cored tree. We turned count data into binary survival data and used generalized linear mixed models with a binomial error distribution, a logit link function, and a random plot effect to model recent survival as a function of range position. Models were fit in R using the *glmer* function in the *lme4* package (Bates et al. 2015, version 1.1-12). Trees were considered 'recent dead' in the model if the maintained dead foliage in their canopy or if they retained all bark and fine branches (see Table S3 for full details).

Sapling and seedling density was statistically modeled for each species-replicate as a function of elevation band, competitive density (either total stand basal area, stand basal area of

conspecifics, or number of stems >10cm DBH within 5m) using generalized linear models with a poisson distribution and log link. Model structure (and best competitive environment predictor) was selected based on model AIC (model results are shown in Table S4 and Figure S7), and used to predict regeneration densities at species-replicate mean competitive densities for each elevation band. Models were fit in R using the *glm* function in the *stats* package (R Core Team 2016). Significant differences between seedling/sapling densities at range margins and the range center (at species-replicate mean competitive density) were assessed by mean centering competitive predictor variables and using a Wald z test on the intercept parameters. Recruitment of *Pinus ponderosa* in Colorado could not be modeled in this way because sapling/seedling densities were extremely low. Instead, we present the median sapling/seedling densities from 10 additional 10m by 50m seedling transects.

Broad scale test of STH

Broad scale relationships between mean growth and growth synchrony/sensitivity to competition were assessed using hierarchical linear mixed effects models with mean growth as a fixed effect and species-replicate as random slope and random intercept effects. Models were constructed with both unweighted data and data weighted by the inverse of the standard error, but results were qualitatively similar and only SE-weighted p-values are presented in the text. Models were fit using the *lmer* function in the *lme4* and *lmerTest* R packages (Bates et al. 2015, Kuznetsova et al. 2016). Reported p-values are t-tests for the significance of the fixed effect of mean growth based on Satterthwaite's estimated degrees of freedom. All statistical analyses were performed in the R statistical environment (R Core Team 2016, version 3.2.4).

Acknowledgements:
We thank G Seigmund and J Landenburger for assistance with fieldwork, many lab assistants with the HilleRisLambers Lab for assistance measuring tree cores, and the staff of Glacier National Park and Olympic National Park for the opportunity to perform this research. We thank G Badgley, WRL Anderegg, I Breckheimer, … for insightful comments on the manuscript. This research was supported by the National Science Foundation (NSF DGE-1256082 and NSF DDIG-1500837 to LDLA and NSF Career DEB-1054012 to JHRL), a UW Biology Wingfield/Ramenofsky Research Award (to LDLA), a WRF Hall Research Fellowship (to LDLA).

Works Cited:

Anderegg LD, HilleRisLambers J (2015) Drought stress limits the geographic ranges of two tree species via different physiological mechanisms. *Global Change Biology*, **22**, 1029–1045.
Angert AL, Crozier LG, Rissler LJ, Gilman SE, Tewksbury JJ, Chunco AJ (2011) Do species' traits predict recent shifts at expanding range edges? *Ecology letters*, **14**, 677–689.
Araújo MB, Luoto M (2007) The importance of biotic interactions for modelling species distributions under climate change. *Global ecology and biogeography*, **16**, 743–753.
Bates D, Maechler M, Bolker B, Walker S (2015). Fitting Linear Mixed-Effects Models Using lme4. *Journal of Statistical Software*, 67(1), 1-48. doi:10.18637/jss.v067.i01.
Brown JH (1995) *Macroecology*. The University of Chicago Press.
Buckley LB, Kingsolver JG (2012) Functional and Phylogenetic Approaches to Forecasting Species' Responses to Climate Change. *Annu Rev Ecol Evol Syst*, **43**, 205–226.
Buckley LB, Urban MC, Angilletta MJ, Crozier LG, Rissler LJ, Sears MW (2010) Can mechanism inform species' distribution models? *Ecology letters*, **13**, 1041–1054.
Callaway RM (1998) Competition and facilitation on elevation gradients in subalpine forests of the northern Rocky Mountains, USA. *Oikos*.
Case MJ, Peterson DL (2005) Fine-scale variability in growth climate relationships of Douglas-fir, North Cascade Range, Washington. *Canadian Journal of Forest Research*.
Case MJ, Peterson DL (2007) Growth-climate relations of lodgepole pine in the North Cascades National Park, Washington. *Northwest Science*.
Clark JS, LaDeau S, Ibáñez I (2004) Fecundity of trees and the colonization–competition hypothesis. *Ecological Monographs*.
Coomes DA, Allen RB (2007) Effects of size, competition and altitude on tree growth. *Journal of Ecology*, **95**, 1084–1097.
Copenhaver-Parry PE, Cannon E (2016) The relative influences of climate and competition on tree growth along montane ecotones in the Rocky Mountains. *Oecologia*, **182**, 13–25.
Cribari-Neto R, Zeileis A (2010). Beta Regression in R. *Journal of Statistical Software* 34(2), 1-24. URL http://www.jstatsoft.org/v34/i02/.
D'Orangeville L, Duchesne L, Kneeshaw D, Côté B, Pederson N (2016) Northeastern North America as a potential refugium for boreal forests in a warming climate. *Science*, **352**, 1452–1455.
Dobzhansky T (1950) Evolution in the tropics. *American Scientist*.
Ettinger AK, Hillerislambers J (2013) Climate isn't everything: competitive interactions and variation by life stage will also affect range shifts in a warming world. *American Journal of*

Botany, **100**, 1344–1355.
Ettinger AK, Ford KR, HilleRisLambers J (2011) Climate determines upper, but not lower, altitudinal range limits of Pacific Northwest conifers. *Ecology*.
Gaston KJ (2009a) Geographic range limits of species. *Proceedings of the Royal Society B: Biological Sciences*, **276**, 1391–1393.
Gaston KJ (2009b) Geographic range limits: achieving synthesis. *Proceedings of the Royal Society B*
Griesbauer H (2010) Regional and ecological patterns in interior Douglas-fir climate-growth relationships in British Columbia, Canada. *Canadian Journal of ….*
Griesbauer HP, Green DS (2012) Geographic and temporal patterns in white spruce climate–growth relationships in Yukon, Canada. *Forest Ecology and Management*.
Griesbauer HP, Green DS, O'Neill GA (2011) Using a spatiotemporal climate model to assess population-level Douglas-fir growth sensitivity to climate change across large climatic gradients in British Columbia, …. *Forest Ecology and Management*.
Hicke JA, Johnson MC, Hayes JL, Preisler HK (2012) Effects of bark beetle-caused tree mortality on wildfire. *Forest Ecology and Management*, **271**, 81–90.
Hillerislambers J, Harsch MA, Ettinger AK, Ford KR, Theobald EJ (2013) How will biotic interactions influence climate change-induced range shifts? *Annals of the New York Academy of Sciences*.
Housset JM, Carcaillet C, Girardin MP, Xu H, Tremblay F, Bergeron Y (2016) In situ Comparison of Tree-Ring Responses to Climate and Population Genetics: The Need to Control for Local Climate and Site Variables. *Frontiers in Ecology and Evolution*, **4**, 95.
Humboldt Von A, Bonpland A (1805) Essay on the Geography of Plants.
Jackson ST, Blois JL (2015) Community ecology in a changing environment: Perspectives from the Quaternary. *Proceedings of the National Academy of Sciences of the United States of America*, **112**, 4915–4921.
Koehler K, Center A, Cavender-Bares J (2012) Evidence for a freezing tolerance-growth rate trade-off in the live oaks (Quercus series Virentes) across the tropical-temperate divide. *New Phytologist*, **193**, 730–744.
Kuznetsova A, Brockhoff PB, Bojesen Christensen RH (2016). lmerTest: Tests in Linear Mixed Effects Models. R package version 2.0-30. https://CRAN.R-project.org/package=lmerTest
Lenoir J, Gégout JC, Marquet PA, de Ruffray P, Brisse H (2008) A significant upward shift in plant species optimum elevation during the 20th century. *Science*, **320**, 1768–1771.
Lévesque M, Rigling A, Bugmann H, Weber P, Brang P (2014) Agricultural and Forest Meteorology. *Agricultural and Forest Meteorology*, **197**, 1–12.
Littell JS, Peterson DL, Tjoelker M (2008) Douglas-fir growth in mountain ecosystems: water limits tree growth from stand to region. *Ecological Monographs*.
Livneh B., Pierce D.S., Bohn T.J., Munoz-Ariola F., Nijssen B., Cayan D., Vose R., and Brekki L.D., 2015: Development of a spatially comprehensive, daily hydrometeorological data set for Mexico, the conterminous U.S., and southern Canada: 1950-2013, *Nature Scientific Data*, 2, 150042, doi:10.1038/sdata.2015.42
Loehle C (1998) Height growth rate tradeoffs determine northern and southern range limits for trees. *Journal of Biogeography*, **25**, 735–742.
Lusk CH, Kaneko T, Grierson E (2013) Correlates of tree species sorting along a temperature gradient in New Zealand rain forests: seedling functional traits, growth and shade tolerance. *Journal of Ecology,* **101**, 1531-1541.

MacArthur D (1972) *Geographical Ecology: Patterns in the Distribution of Species*. Harper & Row, New York.
Nakawatase JM, Peterson DL (2006) Spatial variability in forest growth – climate relationships in the Olympic Mountains, Washington. *Canadian Journal of Forest Research*, **36**, 77–91.
Parmesan C, Yohe G (2003) A globally coherent fingerprint of climate change impacts across natural systems. *Nature*, **421**, 37–42.
Pinheiro J, Bates D, DebRoy S, Sarkar D and R Core Team (2016). _nlme: Linear and Nonlinear Mixed Effects Models_. R package version 3.1-128, <URL: http://CRAN.R-project.org/package=nlme>.
Quintero I, Wiens JJ (2013) Rates of projected climate change dramatically exceed past rates of climatic niche evolution among vertebrate species (eds Quintero I, Wiens JJ). *Ecology letters*, **16**, 1095–1103.
R Core Team (2016). R: A language and environment for statistical computing. R Foundation for Statistical Computing, Vienna, Austria. URL https://www.R-project.org/.
Restaino CM, Peterson DL, Littell J (2016) Increased water deficit decreases Douglas fir growth throughout western US forests. *Proceedings of the National Academy of Sciences of the United States of America*.
Root T (1988) Energy constraints on avian distributions and abundances. *Ecology*, **69**, 330–339.
Root TL, Price JT, Hall KR, Schneider SH, Rosenzweig C, Pounds JA (2003) Fingerprints of global warming on wild animals and plants. *Nature*, **421**, 57–60.
Sanchez-Salguero R, Linares JC, Camarero JJ et al. (2015) Forest Ecology and Management. *Forest Ecology and Management*, **358**, 12–25.
Savage JA, Cavender-Bares J (2013) Phenological cues drive an apparent trade-off between freezing tolerance and growth in the family Salicaceae. *Ecology*, **94**, 1708–1717.
Shestakova TA, Gutiérrez E, Kirdyanov AV et al. (2016) Forests synchronize their growth in contrasting Eurasian regions in response to climate warming. *Proceedings of the National Academy of Sciences of the United States of America*, **113**, 662–667.
Shimatani IK, Kubota Y (2011) The spatio-temporal forest patch dynamics inferred from the fine-scale synchronicity in growth chronology. *Journal of Vegetation Science*, **22**, 334–345.
Sunday JM, Bates AE, Dulvy NK (2012) Thermal tolerance and the global redistribution of animals. *Nature Climate Change*.
Talluto MV, Boulangeat I, Ameztegui A et al. (2015) Cross-scale integration of knowledge for predicting species ranges: a metamodelling framework. *Global ecology and biogeography*, **25**, 238–249.
Tingley MW, Koo MS, Moritz C, Rush AC (2012) The push and pull of climate change causes heterogeneous shifts in avian elevational ranges - Tingley - 2012 - Global Change Biology - Wiley Online Library. *Global Change …*.
Urli M, Brown CD, Narváez Perez R, Chagnon P-L, Vellend M (2016) Increased seedling establishment via enemy release at the upper elevational range limit of sugar maple. *Ecology*, **97**, 3058–3069.
Wang T, Hamann A, Spittlehouse DL, Murdock TQ (2012) ClimateWNA—High-Resolution Spatial Climate Data for Western North America. *Journal of Applied Meterology and Climatolgoy*, **51**, 16–29.
Whittaker RH (1975) *Communities and Ecosystems. Macmil*. Collier Macmillan, New York, NY.
Williams JW, Shuman BN, Webb T III, Bartlein PJ, Leduc PL (2004) Late-Quaternary vegetation dynamics in North America: Scaling from taxa to biomes. *Ecological*

Monographs, **74**, 309–334.
Woodward FI, Williams BG (1987) Climate and plant distribution at global and local scales. 189–197.
Wyckoff PH, Clark JS (2000) Predicting tree mortality from diameter growth: a comparison of maximum likelihood and Bayesian approaches. *Canadian Journal of Forest Research*.
Wyckoff PH, Clark JS (2002) The relationship between growth and mortality for seven co-occurring tree species in the southern Appalachian Mountains. *Journal of Ecology*, **90**, 604–615.

Chapter 2: Drought stress limits the geographic ranges of two tree species via different physiological mechanisms

Leander D.L. Anderegg & Janneke HilleRisLambers

Citation:
Anderegg LD, HilleRisLambers J (2015) Drought stress limits the geographic ranges of two tree species via different physiological mechanisms. Global Change Biology, 22, 1029–1045.

Supplemental Material referenced in text can be found in Appendix D

Global Change Biology (2015), doi: 10.1111/gcb.13148

Drought stress limits the geographic ranges of two tree species via different physiological mechanisms

LEANDER D. L. ANDEREGG and JANNEKE HILLERISLAMBERS
Department of Biology, University of Washington, Box 351800, Seattle, WA 98195, USA

Abstract

Range shifts are among the most ubiquitous ecological responses to anthropogenic climate change and have large consequences for ecosystems. Unfortunately, the ecophysiological forces that constrain range boundaries are poorly understood, making it difficult to mechanistically project range shifts. To explore the physiological mechanisms by which drought stress controls dry range boundaries in trees, we quantified elevational variation in drought tolerance and in drought avoidance-related functional traits of a widespread gymnosperm (ponderosa pine – *Pinus ponderosa*) and angiosperm (trembling aspen – *Populus tremuloides*) tree species in the southwestern USA. Specifically, we quantified tree-to-tree variation in growth, water stress (predawn and midday xylem tension), drought avoidance traits (branch conductivity, leaf/needle size, tree height, leaf area-to-sapwood area ratio), and drought tolerance traits (xylem resistance to embolism, hydraulic safety margin, wood density) at the range margins and range center of each species. Although water stress increased and growth declined strongly at lower range margins of both species, ponderosa pine and aspen showed contrasting patterns of clinal trait variation. Trembling aspen increased its drought tolerance at its dry range edge by growing stronger but more carbon dense branch and leaf tissues, implying an increased cost of growth at its range boundary. By contrast, ponderosa pine showed little elevational variation in drought-related traits but avoided drought stress at low elevations by limiting transpiration through stomatal closure, such that its dry range boundary is associated with limited carbon assimilation even in average climatic conditions. Thus, the same climatic factor (drought) may drive range boundaries through different physiological mechanisms – a result that has important implications for process-based modeling approaches to tree biogeography. Further, we show that comparing intraspecific patterns of trait variation across ranges, something rarely done in a range-limit context, helps elucidate a mechanistic understanding of range constraints.

Keywords: drought avoidance, drought tolerance, ecophysiology, functional trait, intraspecific trait variation, *Pinus ponderosa*, ponderosa pine, *Populus tremuloides*, trembling aspen

Received 10 July 2015; revised version received 11 October 2015 and accepted 15 October 2015

Introduction

Species geographic ranges are ideal ecological study systems because they are a highly visible outcome of the fundamental forces shaping the abundance and distribution of organisms. It is therefore surprising that despite two centuries of study on geographic distributions, the processes controlling range boundaries are still poorly understood (Von Humboldt & Bonpland, 1805; MacArthur, 1972; Gaston, 2009; Sexton *et al*., 2009). Because evolutionary responses are likely to be too slow to allow species to adapt to rapid anthropogenic climate change in place (especially long-lived species) – (Aitken *et al*., 2008; Dullinger *et al*., 2012; Quintero & Wiens, 2013), range shifts are projected to be a major ecological response to climate change over the next century (Parmesan & Yohe, 2003; Root *et al*., 2003). Unfortunately, ecologists and conservation biologists lack a strong understanding of the fundamental physiological mechanisms that limit species ranges, and therefore have little ability to predict and manage for the 'emergent risk' (i.e., complex, multisystem risk that spans local and national boundaries) of climate change-induced range shifts and the resulting potential for species extinction (IPCC, 2014). Indeed, current approaches to predicting range boundary movement are by necessity largely correlational and mechanistic approaches are rare (Handa *et al*., 2005; Morin, 2009; Sexton *et al*., 2009; Buckley *et al*., 2011). Within-species patterns of functional trait variation may provide an underexplored tool for identifying the physiological mechanisms underpinning climate-controlled range boundaries.

Plant functional traits are a fundamental link between the environment and organismal fitness, thus providing a powerful tool for ecological inquiry at multiple spatial, temporal, and taxonomic scales (Violle

Correspondence: Leander D. L. Anderegg, tel. +1 541 790 1096, fax +1 206 543 3041, e-mail: ldla@uw.edu

et al., 2014). Functional traits have therefore become a pillar of many ecological subdisciplines. They serve as a tool for understanding plant community assembly (McGill *et al*., 2006), drive next-generation vegetation dynamics in land-surface models (Moorcroft *et al*., 2001; Medvigy *et al*., 2009; Pavlick *et al*., 2013; Scheiter *et al*., 2013) and provide a generalized understanding of plant responses to environmental change (Angert *et al*., 2011; Buckley & Kingsolver, 2012; Díaz *et al*., 2013; Mouillot *et al*., 2013; Soudzilovskaia *et al*., 2013). In particular, recent global between-species trait comparisons have revealed fundamental constraints on plant physiology (Reich *et al*., 2003; Reich, 2014) that translate into powerful life history trade-offs (Adler *et al*., 2014). In addition, intraspecific trait variation, which can be a substantial fraction of between-species trait variation (Albert *et al*., 2010; Messier *et al*., 2010), can influence species coexistence (Clark, 2010), predict climate change impacts on plant physiology (Anderegg, 2014), or project future range shifts (Benito-Garzón *et al*., 2011). However, intraspecific functional trait variation across species ranges is still poorly understood (Martinez-Vilalta *et al*., 2009; Violle *et al*., 2014), but could greatly improve our mechanistic understanding of range constraints by suggesting limits to physiological adjustment.

We explore within-species variation in a suite of plant drought stress resistance traits to explore the physiological basis underlying tree range limits along an aridity gradient. Moisture availability controls plant biogeography and productivity across much of the globe (Boisvenue & Running, 2006), and water stress is thought to control the lower elevation range boundaries of many plant species in semi-arid environments (Kelly & Goulden, 2008; Fellows & Goulden, 2012). Moreover, drought is likely to change in spatial and temporal extent and magnitude over the coming century (Dai, 2011; Hartmann, 2011), driving plant range shifts. Thus, we focus on drought resistance traits near the dry range margins of two widely distributed tree species. These traits have classically been divided into 'avoidance traits', 'tolerance traits', and 'recovery traits' (see parallel terms in Larcher *et al*., 1973 and Levitt, 1980): traits that relate to the ability to avoid experiencing drought stress, the ability to tolerate stress without injury when stress occurs, and the ability to recover when stress injures performance. We explore within-species variation in key plant hydraulic traits (Maherali *et al*., 2004) and morphological traits (Reich *et al*., 2003) that together represent multiple aspects of drought avoidance and tolerance (Table 1). We do not focus on recovery traits, belowground traits, or phenological traits (all of which may vary within a species and influence plant drought resistance),

Table 1 Physiological and morphological variables measured on study trees, categorized by whether traits are thought to help trees avoid or tolerate drought stress

Drought avoidance traits	Physiological implication
Tree height (m)	Decreased height lowers xylem tensions by reducing gravity potential and hydraulic resistance due to path length (Koch & Fredeen, 2005)
Sapwood area-to-leaf area ratio (A_s:A_L – m^2 per cm^2)	Decreased leaf area to sapwood area increases hydraulic efficiency and reduces the xylem tensions required to supply evaporative area with water (Martinez-Vilalta *et al*., 2009)
Median Leaf Size (cm^2)	Decreased leaf size reduces distances from major leaf veins, decreasing hydraulic resistance from xylem to the leaf evaporative site (Zwieniecki & Boyce, 2004)
Maximum xylem area-specific hydraulic conductivity (K_{max})	Increased K_{max} indicates greater potential xylem hydraulic efficiency (in the absence of embolism), which reduces hydraulic resistance and decreases the xylem tensions needed to move water from root to leaf (Maherali *et al*., 2004)
Leaf area-specific native hydraulic conductivity (K_{nat_Leaf})	Increased K_{nat_Leaf} (conductivity with native embolism present) increases hydraulic efficiency and indicates greater hydraulic support of each unit leaf area
Decreased stomatal conductance (g_s)	Stomatal closure prevents the development of large xylem tensions by limiting water loss
Drought Tolerance Traits	**Physiological Implication**
Specific leaf area (SLA)	Decreased SLA (leaf area per unit dry mass) can increase tolerance of leaves to large xylem tensions (Mitchell *et al*., 2008)
Xylem vulnerability to cavitation (in branches)	Decreased xylem vulnerability to embolism increases the xylem tensions possible before conductivity is curtailed by drought-induced xylem embolism (Maherali *et al*., 2004)
Hydraulic safety margin	Difference between most extreme xylem tension experienced in the field and xylem tension required to cause 50% embolism (Choat *et al*. 2012)

because these are either poorly understood or difficult to quantify. In general, tree species may avoid increasing water stress at their dry range edge via adjustments to tree height, leaf area-to-sapwood area ratio, leaf size, hydraulic efficiency, and stomatal regulation of water loss. By contrast, species may become more tolerant to water stress at their range edge via changes to specific leaf area, hydraulic vulnerability to cavitation, or hydraulic safety margin (see Table 1).

In this study, we build on successful across-species trait analyses (e.g., Carnicer *et al*., 2013; Reich, 2014) to explore the strategies by which individual species deal with water limitation across their ranges. We compare two woody species, a dominant gymnosperm (ponderosa pine – *Pinus ponderosa* Dougl. ex Laws) and a clonal angiosperm (trembling aspen – *Populus tremuloides* Michx.) in the southwestern USA. Annual growth is increasingly sensitive to previous year moisture availability at the low-elevation range boundaries of both species (L.D.L. Anderegg & J. HilleRisLambers in prep.), suggesting that ponderosa pine and aspen's low/dry range boundaries are both constrained by moisture stress at the study site. First, we confirm that performance is constrained at range limits by examining rangewide variations in radial growth and water stress. Second, we quantify trait variation in multiple functional traits to assess the physiological strategies by which each species copes with increasing water stress. Finally, we synthesize growth and trait variation patterns to speculate how and whether the study species differ in the physiological drivers of their dry range limits.

We find that radial growth of both tree species decreased dramatically at the dry range margins, but the species showed contrasting patterns of trait variation. Ponderosa avoided water stress at low elevations by curtailing water loss, whereas aspen maintained transpirational losses but built more drought-tolerant – yet carbon dense – tissues at its dry range boundary. Thus, ponderosa pine may be limited at its dry range boundary by lack of carbon assimilation, whereas aspen faces the increasing carbon cost of growing drought-tolerant organs.

Materials and methods

Study design

The study was conducted on the west slope of the La Plata Mountains in the San Juan National Forest (37.4825°N, 108.1970°W), Southwest Colorado (USA) in the summer of 2014. Plant communities transition from lowland piñon–juniper woodland to ponderosa pine forest to montane aspen forest to subalpine spruce–fir forest with elevation (Fig. S1), crossing a large temperature and precipitation gradient while maintaining a relatively consistent southwest aspect. Our study sites (Table 2) start at the lower transition from closed canopy forest to scrub/open woodland (at ~2250 m) and nearly reach upper tree line (at ~3550 m). Mean annual temperature ranges from 7.3 °C to 2.6 °C, and mean annual precipitation ranges from 480 mm to 760 mm (Fig. 1). Because precipitation is bimodally distributed throughout the year (~50% falls during the winter and the rest falls as summer monsoons beginning mid- to late-July), these forests usually experience peak water stress in early- to mid-July (Anderegg *et al*., 2013a).

We investigated the gymnosperm ponderosa pine (*Pinus ponderosa* Dougl. ex Laws) and the clonal angiosperm trembling aspen (*Populus tremuloides* Michx.), both widespread throughout North America and forming monodominant stands across most of the study site. Focal species differ in xylem anatomy (ponderosa have only tracheids, aspen have tracheids and xylem vessels) and leaf lifespan (evergreen vs. winter deciduous). Because aridity strongly increases with decreasing elevation in semi-arid, midlatitude mountains (e.g., Fig. 1), drought stress likely controls the low-elevation limit of most tree species at the study site (Adams & Kolb, 2005; Fellows & Goulden, 2012), including the two study species.

Table 2 Characteristics (mean ± SD) of study stands (5 stands per elevation). DBH is the mean diameter at breast height (1.3 m) of focal trees (3 per stand), while density and basal area are the mean number of trees per hectare and stand basal area per hectare across stands based on the stand average density and basal area assessed for each focal tree using 15-m (ponderosa pine) or 10-m-diameter (trembling aspen) plots

	Elevation (m)	DBH (cm)	Density (trees ha^{-1})	Basal area (m^2 ha^{-1})	Age (years)
Ponderosa					
Low	2320 ± 10	44 ± 11	248 ± 70	23 ± 11	100 ± 8
Mid	2480 ± 27	47 ± 7	356 ± 107	38 ± 8	102 ± 8
High	2676 ± 14	51 ± 4	281 ± 84	29 ± 10	101 ± 9
Aspen					
Low	2665 ± 9	25 ± 4	588 ± 202	27 ± 8	101 ± 5
Mid	2889 ± 38	40 ± 9	949 ± 175	55 ± 16	98 ± 26
High	3081 ± 8	36 ± 7	1082 ± 431	57 ± 11	97 ± 24

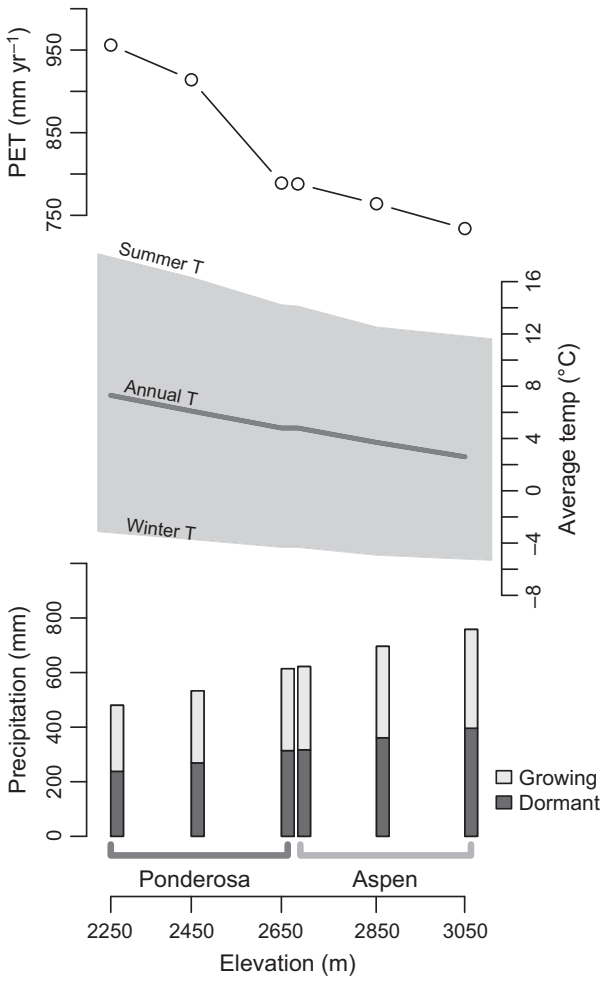

Fig. 1 Climate variation across the study elevation gradient in SW Colorado, USA. Elevation ranges of ponderosa pine and trembling aspen are shown at the bottom of the figure. Mean annual growing season precipitation (light gray bars) and dormant season precipitation (dark gray bars) at the three ponderosa study elevations and three aspen study elevations increase with increasing elevation. Mean annual temperature (solid line), as well as mean summer temperature (upper edge of gray shading) and mean winter temperature (lower edge of shading) decrease with elevation. Annual potential evapotranspiration (PET, points with lines) also decreases with elevation. Data are from 30 years PRISM climate normals (Daly *et al.*, 2002) interpolated using the ClimateWNA algorithm (Wang *et al.*, 2012).

We located five mature stands each at the lower elevation range margin, at the range center, and at the upper range margin of each species (total of 15 stands per species). Stands were >100 m apart on gentle (<8% slope) southwest to west facing aspects and were >30 m from any major topographic or hydrological features such as drainages or hill tops (see Table 2 for stand characteristics). In each stand, we randomly selected three mature, dominant, visually healthy trees for growth and trait measurements (below, see Table 1).

Trait measurements

Growth. To quantify growth, we collected two tree cores from each focal tree at 1.3 m height on opposite sides of the bole perpendicular to the aspect. Cores were sanded and scanned with a high-resolution scanner, and annual growth rings were measured to 0.001 mm using the WINDENDRO software (Version 2008e. Regent Instruments, Quebec City, Quebec, Canada). Cores were visually and statistically cross-dated using the dplR package in R (Bunn, 2010, R Development Core Team 2014), and ring widths averaged per tree. We used diameter at breast height (DBH) and bark depth to calculate annual basal area increment (BAI) from annual ring widths, and then calculated mean annual BAI (2003–2012) for each tree. To assess how stand density affects growth, we performed stand surveys and calculated Hegyi's distance-dependent competitive index (Hegyi, 1974) for each tree. Hegyi's index sums the neighbor DBH divided by the focal tree DBH and the distance to the neighbor for all neighboring trees within 15 m (for ponderosa pine) or 10 m (for aspen) of the focal tree. This competition index correlates with BAI in ponderosa forests (Contreras *et al.*, 2011), and was therefore included as a covariate in all statistical tests involving BAI. Because our response variable (BAI) and density covariate (Hegyi's competitive index) were highly variable, we included growth data from 12 to 25 closely co-located trees per elevation (cored in 2013 for a separate project) to increase sample size and statistical power (L.D.L. Anderegg & J. HilleRisLambers, in prep.). Unlike other focal individuals in this study, 2013 trees were selected for high-vs.-low competitive environments; however, other selection criteria were identical to this study (see description with Fig. S2). Competitive environment was estimated for 2013 trees via multiple techniques, which we converted into Hegyi's competitive index (see Fig. S2). When excluding these additional trees, results were qualitatively similar, albeit non-significant for trembling aspen (Fig. S3). The combined dataset resulted in a final sample size of 27–40 trees per elevation (mean = 35 trees) for growth estimates.

Xylem tension measurements. We estimated ψ_{min} (the largest xylem tension, i.e., most negative plant water potential) for focal trees by measuring branch xylem tension between June 29th and July 9th of 2014. This period captured the driest portion of the growing season (monsoonal rains began on July 10th) and largest xylem tensions of the year. Although 2014 was an average year climatologically (the water year precipitation was 4.7 cm or 6% below the 20-year average, and mean annual temperature was 1.3 °C hotter than the 20-year average at a SNOTEL station ~5 km away), single growing season ψ_{min} is often used to approximate interannual ψ_{min} (Sperry, 2000; Choat *et al.*, 2012). Furthermore, our measured xylem tensions were quite similar to previous maximum tensions measured in low-elevation aspen stands in this region (~0.2 MPa less than most extreme tensions measured since 2010; Anderegg *et al.*, 2012, 2013a, 2014).

Xylem tensions were measured twice daily on distal twigs of focal trees: once predawn (03:00–05:30 local time,

generally considered lowest daily tensions) and again at midday (13:00–15:00). Assuming no nighttime transpiration, predawn xylem tensions reflect soil water potential across the rooting depth of the tree and are an indication of soil moisture limitation, whereas midday xylem tensions represent the maximum tensions experienced by the tree (Ritchie & Hinckley, 1975). The assumption of limited nighttime transpiration was supported for both species by preliminary experiments comparing predawn water potentials of juveniles bagged in plastic overnight vs. unbagged juveniles (data not shown). Branches of ~5 cm diameter were collected from the mid-to-upper, sun-exposed, south-facing canopy via shotgun and immediately placed in humid plastic bags. Xylem tension of 1–3 intact twigs from these branches (recut >30 cm from the initial branch break) was measured using a Scholander-type pressure bomb (PMS Instruments, Corvalis, OR) within three minutes of sample collection. Weather was sunny and cloud free when xylem tensions were measured.

Morphological traits. Morphological traits can allow trees to avoid water stress when soil moisture is limiting (Table 1). Large reductions in tree height can limit maximum xylem tensions by reducing gravitational potential and lowering the hydraulic path length between soil and leaf (McDowell *et al*., 2002; Koch & Fredeen, 2005), while decreased branch leaf area-to-sapwood area ratio (A_L: A_S) can increase hydraulic efficiency, thereby decreasing the xylem tensions necessary to deliver water to the leaf (Martinez-Vilalta *et al*., 2009). In addition, decreased leaf size can increase leaf hydraulic efficiency (decrease hydraulic resistance) by decreasing the distance between leaf evaporative sites and large (low resistance) veins (Zwieniecki & Boyce, 2004; Sack & Holbrook, 2006). We also quantified elevational variation in specific leaf area (SLA = leaf area/leaf dry mass), because decreasing SLA is associated with increased drought tolerance as more structural carbon increases a leaf's ability to withstand high xylem tensions without losing turgor (Mitchell *et al*., 2008). In addition, water storage and capacitance can increase as SLA decreases (Ishii *et al*., 2014).

We used various field and laboratory techniques to measure these traits. Tree heights were measured with a digital inclinometer. We used digital photographs and ImageJ image processing software (US National Institute of Health; http://www.nih.gov/) to quantify total one-sided leaf area (A_L) and median leaf size (Pérez-Harguindeguy *et al*., 2013) of one sun-exposed branch 3–15 mm in diameter from the south-facing mid-to-upper canopy of each tree (collected for hydraulic measurements discussed below). We calculated SLA (A_L/leaf dry mass) and calculated A_L:A_S using the sapwood diameter at the basal end of the branch segment. When branch leaf area was very large, leaf area was estimated by calculating the SLA of a subset of leaves/needles and multiplying by the total leaf/needle dry mass of the branch. Following measurement of branch hydraulic conductivity, we measured branch wood density on a 3- to 5-cm section by dividing the green volume (assessed via water displacement on an analytical balance) by sample dry mass.

Hydraulic traits. We measured branch hydraulic efficiency across elevation in both species to quantify drought avoidance-related hydraulic adjustment. We used a shotgun to collect one large (diameter >10 cm), sun-exposed, mid-to-upper canopy branch from the south side of each focal tree at midday during maximum summer water stress (June 29th – July 9th). Because branch severing under tension can cause artificial embolism (Wheeler *et al*., 2013), an unbranched segment (>12 cm long, bearing no foliage and typically 5–9 mm diameter) was immediately cut from the original branch under water as far away from the initial break as possible (typically >10 cm) to relax xylem tension. This segment was sprayed with water, sealed in a moist plastic bag, and placed in a cooler for transport back to the laboratory. In the laboratory, branch segments were recut underwater using a sharp razor (final length >8 cm). Aspen stems were cut as long as possible (typically >10 cm in length) to accommodate long maximum vessel lengths (between 8 cm and 15 cm, mean vessel length is 1.9 cm; Sperry & Sullivan, 1992; Sperry *et al*., 1994; Zimmermann & Jeje, 1981). Native or maximum conductivity and branch length were uncorrelated, suggesting no open vessels in shorter aspen branch segments (data not shown). Branch native conductance (k_{nat}) was measured using the standard pressure-flow method (Sperry *et al*., 1988), stems were flushed of embolisms via vacuum infiltration, and then maximum conductance (k_{max}) was measured. Native conductance values were standardized by the leaf area of the branch and stem segment length to give leaf area-specific conductivity (K_{nat_Leaf}), reflecting how well hydraulically supported each unit of leaf area is. Maximum conductance values were standardized by stem sapwood area and stem length to give maximum sapwood specific conductivity (K_{max}), representing maximum hydraulic efficiency allowed by the branch xylem anatomy. The degree of embolism present in these branches was also quantified as the percentage loss of conductance:

$$\mathrm{PLC} = \frac{(k_{max} - k_{nat})}{k_{max}} \times 100. \quad (1)$$

On a second set of branch segments (collected as above but following the onset of the summer monsoons), we quantified xylem vulnerability to cavitation via a standard vulnerability curve technique. Artificial xylem tensions were induced via air injection, following the protocols of Anderegg *et al.* (2013b) for aspen stems and Maherali & DeLucia (2000) for ponderosa pine stems. Native conductance and maximum conductance were measured for each branch, and then, conductance was measured following air injection-induced xylem tensions of 1, 2, 3, and 4 MPa. This method has previously produced reliable vulnerability curves for both of these species, and results for trembling aspen have been verified against the centrifuge method (Anderegg *et al*., 2013b). For ponderosa pine, we had difficulty maintaining the slight positive pressure recommended by Maherali & DeLucia (2000) in the six-chamber pressure manifold used to induce xylem tensions. Because of this, we removed data from some branches that appeared to refill considerable cavitation at higher xylem tensions (final n = 25 branches). Xylem P50, the xylem tension at which branches reach 50% loss of conductivity, was calculated for

each elevation by fitting an exponential sigmoidal function of the form:

$$\mathrm{PLC} = \frac{100}{1 + \exp(a(\psi - b))}, \quad (2)$$

where PLC is the percentage loss of conductance, ψ is the induced xylem tension, a is the shape parameter, and b is the P50 value (i.e., the ψ that causes 50% loss of conductivity) (Pammenter & Vander Willigen, 1998). Parameters a and b and their 95% confidence intervals were estimated for each elevation by nonlinear least squares using the R statistical software (R Core Team 2014) combining data from all branches from that elevation. Vulnerability curve results are reported in terms of percentage loss of conductivity from maximum conductance, but vulnerability curves were also constructed using raw conductance values with qualitatively similar results (see Fig. S4). The hydraulic safety margins (the difference between the xylem tension required to induce 50% embolism – P50 – and the strongest xylem tensions experience in the field—$\psi_{\min}$) for each elevation were calculated using the P50 estimated from xylem vulnerability curves (above) and the actual midday xylem tensions measured at that elevation.

Finally, we integrated the xylem tension, A_L:A_S and stem conductivity measurements to model stomatal conductance, using the model proposed by Whitehead & Jarvis (1981) to estimate water movement through a plant at steady state. Specifically, canopy gas exchange is modeled as:

$$g_s = c\frac{1}{A_L : A_S}K_s\left(\frac{\Delta\psi}{h}\right)\frac{1}{\mathrm{VPD}}, \quad (3)$$

where g_s is stomatal conductance; c is a coefficient representing the specific heat and density of air, the latent heat of vaporization, and the viscosity of water; A_L:A_S is the leaf area-to-sapwood area ratio; K_s is the sapwood area-specific conductivity; $\Delta\psi$/h is the pressure drop across the plant (midday xylem tension – predawn xylem tension) divided by the total path length (typically approximated by tree height); and VPD is the vapor pressure deficit (Whitehead & Jarvis, 1981). We estimated mean midday VPD (average of measurements at 13:00 hours and 15:00 hours) for each elevation between June 1st and June 18th 2014 using four temperature and relative humidity sensors (Maxim iButtons, DS1923) shielded by white funnels and placed in the canopy of focal trees or nearby conifers (Lundquist & Huggett, 2008), two at ponderosa's low-elevation range margin, one at the ponderosa/aspen transition zone (high ponderosa margin, low aspen margin), and one at aspen's high-elevation margin, and then linearly interpolating VPD at the range center of each species. Using the individual values of branch A_L:A_S, branch $K_{\max}$, $\Delta\psi$ (midday xylem tension minus predawn xylem tension), and h (tree height as a proxy for total path length), we calculated relative g_s for each focal tree. We assume whole tree K and A_L:A_S values to be proportional to branch values and report stomatal conductance values calculated via Eqn (3) as the percentage of mean mid-elevation g_s for each species. Ponderosa A_L:A_S and $K_{\max}$ were corrected for branch diameter based on the branch diameter or log(branch diameter) coefficients from the mixed-effects models for each trait discussed below. As is heuristically evident by Eqn (3), stomatal conductance (g_s) is intimately tied to whole-plant hydraulics and multiple feedback and feedforward processes relate g_s to leaf xylem tension. Stomatal behavior is often discussed as falling on a spectrum between 'isohydric' (plants that limit conductance to maintain a stable maximum xylem tension) and 'anisohydric' (plants that regulate stomata less strongly in response to either xylem tension or evaporative demand and thus have larger variations in xylem tension)(Klein, 2014), and stomatal behavior is tightly coupled with hydraulic parameters and a plant's general water use strategy (Sperry *et al.*, 2002).

Statistics

To assess the effect of elevation on individual traits, we constructed mixed-effects models for each species relating raw trait values, or in some cases, power transformed-trait values (see Tables S1 and S2), to elevation, with a random effect of stand to account for the nested data structure. We coded elevation categorically (low, mid, and high), and tested for a significant effect of elevation via a likelihood ratio test (LRT) against a null model (model with only random effects and an intercept). Where elevation proved significant via likelihood ratio testing, we also used the Satterthwaite approximation of marginal fixed effect significance implemented in the 'lmerTest' R package (Kuznetsova *et al.*, 2014) to test post hoc whether trait values at either range margin differed significantly from the range center. We report these significant differences with an asterisk (*) over significantly differing range margins in figures. A subset of ponderosa pine traits showed a relationship with branch diameter, so we also included branch diameter (wood density, A_L:A_S) or log(branch diameter) (SLA, $K_{\text{nat\_Leaf}}$, $K_{\max}$) as a covariate in these models (Table S1). For mean annual BAI, we performed the same likelihood ratio test to assess the effect of elevation on growth, but included Hegyi's competitive index and diameter at breast height as covariates.

Competitive index was never included in the best model as determined by AIC for any trait other than growth, so we did not include it in analyses of morphological and physiological traits variation. Although tree age did not differ significantly across elevation, we also built trait models including tree age as a covariate to test for maturation-related effects on tree traits. However, with the exception of tree height in ponderosa pine, tree age was never included in the best-fit models and was therefore excluded from the final analysis.

We also fit mixed-effects models with elevation as a continuous linear predictor and a quadratic predictor to assess whether these continuous models better described our results, using AIC to compare categorical vs. continuous models. However, continuous models never showed a ΔAIC of >2 from the null or best categorical models, and results were qualitatively very similar to categorical elevation models, so we report only results from the categorical models.

For xylem tension measurements, we performed model selection on mixed-effects models (with stand and tree as random effects to account for nested data structure) including a null model, elevation as a continuous linear predictor, time of

day, and an elevation*time of day interaction (quadratic elevation was not included due to the difficulty of interpreting elevation*time of day interactions). We then selected the best-fit model based on AIC and performed a likelihood ratio test against the null model and the next best model. A best-fit model including an interaction effect suggests that predawn and midday xylem tensions of a species did not change similarly across elevation. All models were constructed using the 'lme4' package (Bates *et al.*, 2014) and 'lmerTest' package (Kuznetsova *et al.*, 2014) in the R statistical environment version 3.1.0 (R Core Team 2014). For xylem tension measurements, significance of individual fixed effects was determined using the Satterthwaite approximation implemented in the 'lmerTest' package (Kuznetsova *et al.*, 2014). We verified the normality of all model residuals visually, and either log transformed or power transformed the trait data where necessary (see Tables S1 and S2 for details). Where necessary, extreme outliers were removed (see Tables S1 and S2 for final samples sizes excluding missing data and extreme outliers). Data files and R code for all analyses are provided in the Appendix S1–S6.

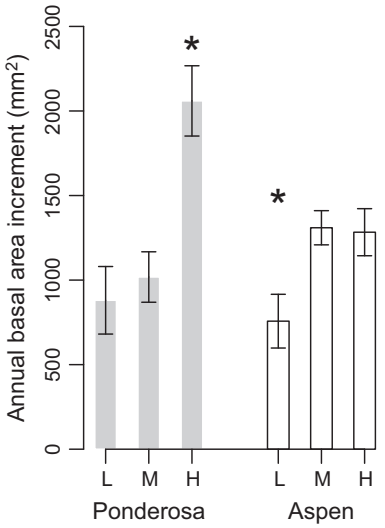

Fig. 2 Mean annual basal area increment (BAI) increased with elevation across the range of ponderosa pine and aspen. Bars show the mean (±SE) annual growth (averaged from 2003 to 2012) for a tree of mean DBH and mean competitive environment. Asterisks (*) indicate margins significantly different (alpha = 0.05) from the range center based on mixed-effects models.

Results

Growth analysis

Mean annual basal area increment (BAI) increased with elevation, almost tripling from the low to the high-elevation range margin in ponderosa (from 762 ± 75 to 2179 ± 186 mm^2 yr^{-1}, mean ± SE) and almost doubling in aspen (from 696 ± 58 to 1245 ± 97 mm^2 yr^{-1} – Fig. 2). After accounting for the effects of DBH and competitive index, BAI of ponderosa pine remained low at the lower range margin and the mid-elevation range center, and significantly increased only at high elevations ($P < 0.0001$, Table S1). Meanwhile, aspen BAI also increased nonlinearly with elevation, increasing from low- to mid-elevation ($P < 0.0001$, Table S2), but then remaining stable from mid- to high elevation.

Xylem tensions across elevation

Predawn measurements of branch xylem tension (a proxy for soil water potential) of both species showed increasingly limited midsummer soil moisture (higher tensions) descending across the elevational range (Fig. 3, effect of elevation on predawn tension from mixed-effects model: ponderosa $P < 0.00001$, aspen $P = 0.008$, see Table S3). For both species, the elev * time of day interaction model was the best mixed-effects model as determined by AIC (likelihood ratio test, ponderosa: $P =< 0.00001$; aspen: $P = 0.005$). Interestingly, predawn xylem tensions varied considerably more across the range of ponderosa pine (1.44–0.89 MPa from low- to high elevation) than across that of aspen (0.58–0.47 MPa). This variation is more similar to the nonlinear decrease in PET with increasing elevation than the linear increase in precipitation across the study gradient (Fig. 1). Also, even though high-elevation ponderosa stands and low-elevation aspen stands were closely co-located in the ponderosa-aspen transition zone (plot centers of aspen and ponderosa stands sometimes differed by <100 m), aspens showed lower predawn xylem tensions by on average 0.3 MPa. This difference is not explained by their ~5 m height difference at this elevation, which accounts for only 0.05 MPa of added gravitational potential.

Midday xylem tensions also were greater at low elevation in both species (Fig. 3). However, in ponderosa pine the increase in midday xylem tensions was significantly less than the increase in predawn xylem tensions (Fig. 3, elev*midday interaction $P = 0.001$), resulting in an average daily change in xylem tension due to daily transpiration ($\Delta\psi$) of 0.73 ± 0.08 MPa (mean ± SE) at high elevation and only 0.31 ± 0.06 MPa at low elevation. This suggests either a very large increase in hydraulic efficiency or considerable stomatal closure at low elevations. In contrast, approaching the low-elevation margin of aspen midday xylem tensions increased slightly more than did predawn xylem tensions, resulting in a predawn to midday tension difference of 0.94 ± 0.05 MPa at high elevations and 1.12 ±0.04 MPa at low elevations (Fig. 3, Table S4, elev*midday interaction $P = 0.006$).

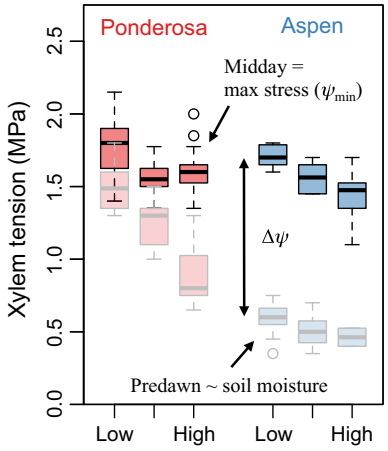

Fig. 3 Predawn (light) and midday (dark) xylem tensions across the elevation range of ponderosa pine (red) and aspen (blue). Xylem tensions were assessed at the peak of growing season water stress. Midday xylem tensions represent the maximum water stress experienced by the sampled trees, while predawn xylem tensions are indicative of soil water potential. The difference between them is the potential drop ($\Delta\psi$) used in Eqn 3.

Morphological traits

The study species showed clinal variation in very different morphological traits. Median leaf size decreased strongly with decreasing elevation in ponderosa (Fig. 4a, Table S1, LRT $P = 0.0018$) but not in aspen (Table S2, LRT $P = 0.14$). The height of adult canopy trees was similar for both tree species, and remained stable across all elevations except at aspen's low elevational range edge (Fig. 4b, ponderosa LRT $P = 0.29$; aspen LRT $P = 0.00003$). In contrast, the ratio of leaf area to sapwood area (A_L:A_S) showed no pattern in aspen ($P = 0.73$) but increased significantly at the upper range margin of ponderosa pine (Fig. 4c, LRT $P = 0.025$).

Finally, SLA and wood density showed an increase in the carbon cost of tissues at aspen's low-elevation range boundary, but showed no elevational trends for ponderosa pine. SLA of low-elevation aspen trees was significantly lower (i.e., more carbon per unit leaf area) than SLA at the range center or upper range margin (Fig. 5a, LRT $P = 0.012$, low elevation differed from mid $P = 0.016$) whereas ponderosa pine showed no significant change in SLA. Branch wood density also showed no significant relationship with elevation in ponderosa pine (Fig. 5b), while wood density decreased strongly across the elevational range of aspen (LRT $P = 0.0008$).

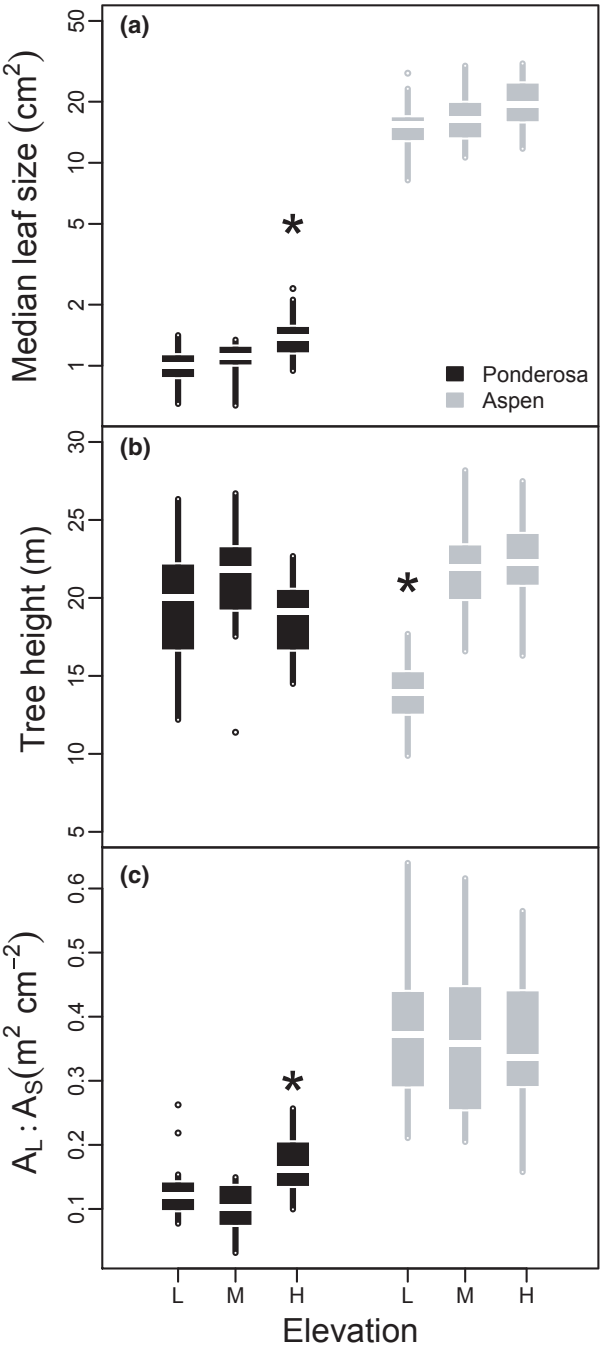

Fig. 4 Morphological adjustments across the elevation range of ponderosa pine (black) and trembling aspen (gray). (a) Median leaf/needle size (note log y axis), (b) tree height, (c) leaf area-to-sapwood area ratio (A_L:A_S). Asterisks (*) denote a significant difference (alpha = 0.05) of the range margin from the range center. Boxplots show the median (bar), interquartile range (box), range (lines), and outliers (points).

Hydraulic traits

At the height of midsummer water stress, neither native leaf area-specific hydraulic conductivity (K_{nat_Leaf}: a measure of how well hydraulically supported a unit leaf area is) nor sapwood area-specific maximum conductivity (K_{max}: conductivity with embolism removed,

a measure of maximum xylem hydraulic efficiency) showed any trend with elevation in aspen (Fig. 6). In ponderosa, once log(stem diameter) was included as a covariate in the mixed-effects models, K_{nat_Leaf} also showed no relationship with elevation (Fig. 6a). Meanwhile, ponderosa K_{max} decreased significantly from mid- to low elevation (Fig. 6b, LRT $P = 0.001$, low differs from mid-elevation $P = 0.02$).

Xylem vulnerability to cavitation increased significantly with elevation in aspen, but showed no significant clinal variation in ponderosa (Fig. 7). The vulnerability curve of low-elevation aspen was considerably more resistant than that of mid- and high-elevation aspen (Fig. 7b), resulting in a higher P50 value (xylem tension required to cause 50% cavitation) at low elevation (Fig. 7b, 95% confidence interval 2.4–2.8 MPa at low elevation vs. 1.6–1.9 MPa at mid-elevation and 1.4–1.9 MPa at high elevation). We found a slight but nonsignificant decrease in the P50 with increasing elevation in ponderosa (Fig. 7a, all 95% confidence intervals overlap), although there was considerably more uncertainty in our estimates of ponderosa P50 than aspen P50.

By subtracting the midday xylem tensions measured in the field from P50 values estimated for each elevation from the xylem vulnerability curves above, we calculated the 'hydraulic safety margin' for each elevation. Even though aspen midday xylem tensions were elevated at lower elevations, the hydraulic safety margin was much larger in low-elevation trees than mid- or high-elevation trees (e.g., low-elevation safety margin of 0.96 ± 0.02 MPa compared to mid-elevation margin of 0.21 ± 0.03 MPa, LRT $P \ll 0.001$ Fig. 8a). This suggests that aspen do not just grow stronger xylem at low elevations, but are actually more conservative in their xylem anatomy at low elevations. Hydraulic safety margin also decreased significantly with elevation in ponderosa ($P < 0.001$, Fig. 8a, Table S2). However, these calculations do not incorporate the relatively large uncertainty in ponderosa P50 values (Fig. 7a) because safety margins for each tree were calculated using the elevation mean P50 value. Because the documented change in safety margin is small (0.25 MPa from low- to mid-elevation) compared both to the uncertainty in P50 value (mean P50 confidence interval range was 1.1 MPa) as well as to the safety margin differences observed in aspen (0.75 MPa from low- to mid-elevation), the observed differences in hydraulic safety margin for ponderosa pine are not necessarily biologically significant.

Further corroborating a biologically relevant increase in hydraulic safety margin in low-elevation aspens, native embolism (measured as percentage loss of conductivity or PLC) *increased* with increasing elevation in this species (Fig. 8b, LRT $P = 0.001$, low differs from mid $P = 0.004$), despite decreasing midday xylem tensions. Meanwhile, ponderosa pine branch PLC at midsummer was consistently quite low at all elevations (Fig. 8b), suggesting that the significant decrease in hydraulic safety margin in this species may be either a statistical artifact or not biologically significant.

Finally, estimates of steady state, midsummer stomatal conductance (g_s) appeared stable across the elevational range of aspen (Fig. 8c), but decreased precipitously across the elevation range of ponderosa pine (Fig. 8c, LRT $P = 0.002$). In ponderosa, large differences in g_s despite relatively small differences in

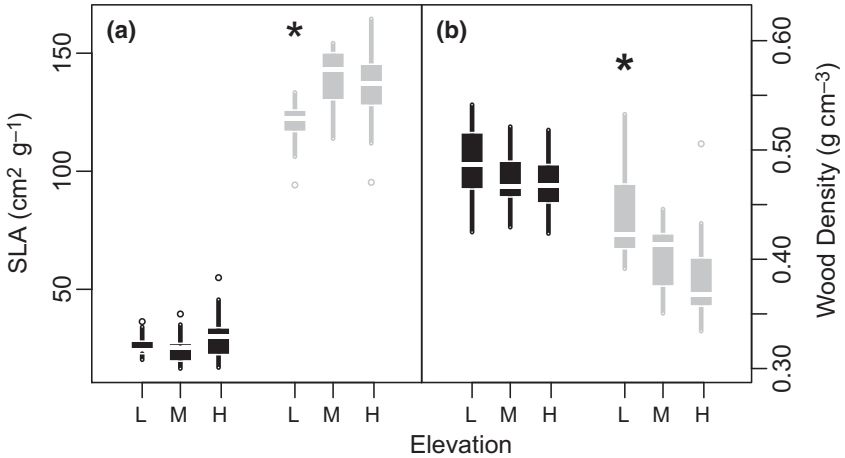

Fig. 5 Variation in specific leaf area (a) and branch wood density (b) with elevation in ponderosa pine (black) and aspen (gray). Specific leaf area (SLA = leaf area/dry mass) decreased and branch wood density increased near the lower (dry) range boundary of trembling aspen but showed no significant variation with elevation in ponderosa pine. Asterisks (*) denote a significant difference (alpha = 0.05) of the range margin from the range center. Boxplots show the median (bar), interquartile range (box), range (lines), and outliers (points).

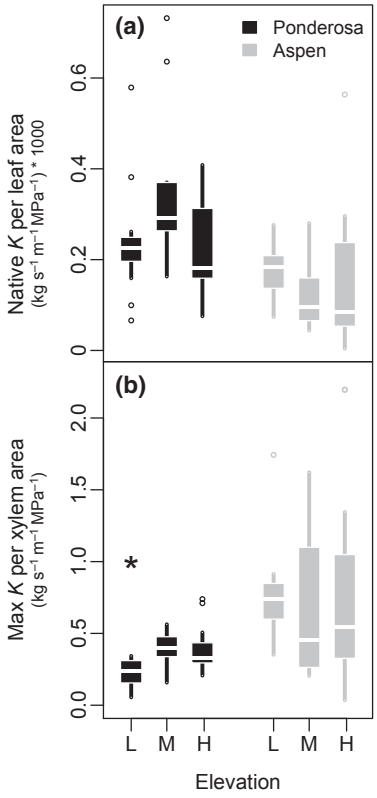

Fig. 6 Ponderosa show decreased hydraulic efficiency at low elevation while aspen show no clinal hydraulic trait variation. (a) Branch native conductivity per unit leaf area (K_{nat_Leaf}) shows no elevational variation in either species (b) maximum hydraulic conductivity (post embolism removal) per unit xylem area (K_{max}) is higher at mid- and high elevations than at low elevation for ponderosa pine (*Pinus ponderosa*). Boxplots show the median (bar), interquartile range (box), range (lines) and outliers (circles). Asterisks (*) indicate a margin significantly different (alpha = 0.05) from the range center based on mixed-effects models.

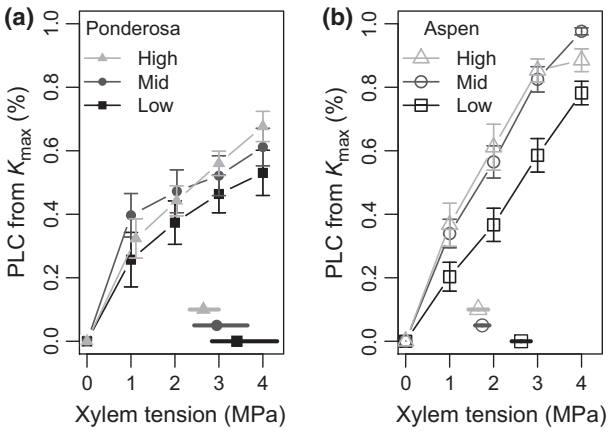

Fig. 7 Xylem vulnerability curves for low-, mid-, and high-elevation trees of (a) ponderosa pine, and (b) trembling aspen. Points in curve show means ± SE of PLC values (percentage loss of conductivity from K_{max}) at xylem tensions induced via air seeding. P50 values, or the xylem tension at which 50% PLC is reached, are displayed as points along the bottom of the figure (solid horizontal lines indicate 95% confidence intervals for P50 estimates). Xylem vulnerability to cavitation did not differ significantly across elevation in ponderosa, while low-elevation aspen showed significantly more resistant xylem than mid- and high-elevation aspen.

maximum xylem tensions (Fig. 3) suggest a relatively isohydric strategy compared to aspens, which experience larger geographic variation in xylem tensions with no decrease in g_s (although such a delineation can be somewhat difficult, Klein, 2014; Franks *et al.* 2007). By integrating values of morphological (Fig. 4c) and hydraulic traits (Fig. 6b) with xylem tensions measured in the field (Fig. 3) and changes in evaporative demand (VPD, not shown), our model estimates suggest that mid- and low-elevation ponderosas have 41% and 22% (respectively) of the stomatal conductance of ponderosa at the high-elevation range margin, implying drastically curtailed transpiration near the dry range boundary of this species. Meanwhile, the model suggests that, decreases in height in low-elevation aspen sufficiently offset increases in VPD to maintain g_s equal to or greater than mid-elevation g_s.

Discussion

Our results suggest that two major North American tree species occurring along different portions of an aridity gradient employ drastically different strategies for coping with increased water limitation at their dry range boundary. Ponderosa pine showed little variation in key morphological and hydraulic traits influencing drought avoidance and drought tolerance, and thus appeared to minimize water stress primarily by strongly limiting transpiration in drier habitats. In contrast, trembling aspen showed a considerable decrease in the vulnerability of its hydraulic system to drought-induced cavitation at its dry range edge, suggesting a strategy of increased drought tolerance in response to aridity. Despite these adjustments, growth of both species was constrained at their low-elevation range boundary, potentially indicative of a limit to ponderosa's drought avoidance capacity and aspen's drought tolerance capacity at higher levels of aridity. Below we discuss each species in turn.

Trembling aspen

Aspen trees tolerate water limitation near their dry range edge by protecting their hydraulic system against xylem cavitation during chronic stress, rather

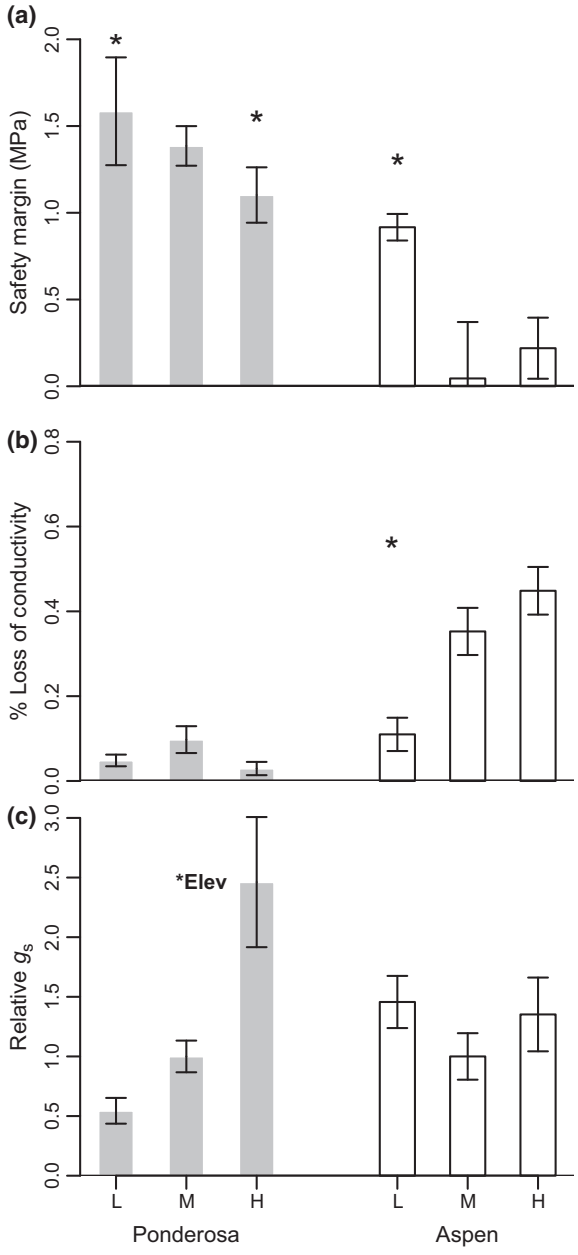

Fig. 8 At low elevations, aspen increase hydraulic safety while ponderosa pine curtail stomatal conductance. (a) Hydraulic safety margin (±SE) calculated from xylem vulnerability curves and midday water potentials, (b) percentage loss of conductivity (PLC) due to extant embolism in branches, and (c) modeled stomatal conductance (g_s) of ponderosa pine (gray) and trembling aspen (white). g_s is standardized so that mid-elevation g_s equals one for each species. Trembling aspen exhibits an increased hydraulic safety margin and decreased PLC at low elevation, while ponderosa shows greatly decreased g_s at mid- and low elevations. Asterisks (*) show range margins that significantly differ (alpha = 0.05) from the range center based on linear mixed-effects models, and '*Elev' indicates a significant effect of elevation but no post hoc significant differences between range margins and range center.

than by avoiding water stress through increased hydraulic efficiency or decreased water use. Predawn xylem tension measurements suggested that soil moisture becomes only slightly more limited approaching aspen's low-elevation boundary. However, maximum water stress (i.e., midday xylem tensions) increased significantly approaching aspen's low-elevation margin (Fig. 3) presumably due to increased evaporative demand. Aspens respond by growing shorter trees with denser wood, bearing smaller, lower SLA (i.e., more carbon dense) leaves, and by growing stronger xylem. Previous research suggests that the main mechanism of drought-induced mortality in aspen is the deterioration of hydraulic function caused by cavitation during drought and subsequent xylem 'cavitation fatigue' (Anderegg *et al.*, 2012, 2013b). Given the possibly fatal consequences of cavitation, evolutionary forces may drive aspen to become increasingly hydraulically conservative where drought is most prevalent (Fig. 8). This intraspecific pattern contrasts with the findings of Choat *et al.* (2012), who found little relationship between climate dryness and angiosperm hydraulic safety margins across species.

Basal area growth decreased strongly in low-elevation aspen, even as leaf and stem tissue showed increased carbon investment. Although wood density arises through many aspects of xylem anatomy, reduced xylem vulnerability to cavitation via increased vessel wall thickness likely plays some role in increasing branch wood density in low-elevation aspens (Lens *et al.*, 2010) while making each unit of conducting area more energy intensive to grow. Likewise, SLA varies in response to multiple environmental cues and anatomical differences, but low SLA aspen leaves likely increase leaf drought tolerance, possibly by decreasing leaf turgor loss point, (Merchant *et al.*, 2007; Bartlett *et al.*, 2012) and/or increasing leaf capacitance (Ishii *et al.*, 2014). This increased drought tolerance appears to come at the cost of more structural carbon for every unit of leaf area. We lack data on whole-plant carbon balance, but a significant positive relationship between SLA and mean BAI (LRT = 0.046) and a negative but non-significant relationship between wood density and BAI (LRT = 0.289) at the individual level supports this idea (Fig. S5). Even though available photosynthate and nonstructural carbon stores do not directly regulate growth (Körner, 2015), this coordination between increased cost of growth and decreased amount of growth may indicate a limit to aspen's drought tolerance with increasing aridity mediated by the carbon cost of tolerance traits.

Ponderosa pine

Low-elevation ponderosa pines considerably curtail their transpiration, and most likely carbon uptake, during some if not most of the growing season. This reduction in water use is associated with vastly reduced growth at the low-elevation range margin and range center compared to the high-elevation margin (Fig. 2). In contrast to aspen, ponderosa pine showed remarkably few trait adjustments toward either increased drought tolerance or drought avoidance at the lower range margin, despite increasing soil moisture limitation and evaporative demand (Figs 1 and 3). For example, ponderosa pine exhibited no elevational variation in height and wood density, and only slight clinal variation in leaf morphology (Fig. 4). Surprisingly, we found only subtle, although statistically significant, variation in branch-level leaf area:sapwood area ratio – A_L:A_S (Fig. 4, 0.151 ± 0.027 m^2 cm^{-2} at low elevation vs. 0.199 ± 0.023 m^2 cm^{-2} at high elevation), a trait that has been implicated as a main mediator for hydraulic adjustment across space in other pine species (e.g., branch level: Martinez-Vilalta *et al*., 2009; whole tree level: Mencuccini & Bonosi, 2001) and in previous studies of montane vs. desert ponderosa pine populations (Maherali & DeLucia, 2000; Maherali *et al*., 2002). Variation in A_L:A_S appeared to be primarily driven by changes in leaf area, rather than branch scale adjustments – as changes in leaf size and A_L:A_S were similar in magnitude from high to low elevation (median leaf area −28.2% and A_L:A_S −23.7% decrease). Indeed, when trees were relativized to percentage change from the high-elevation average, the slope of the total least squares regression between $\%\Delta A_L$:A_S and %Δmedian leaf area was near one (Fig. S5). A different study of water relations in ponderosa pine in a contiguous riparian and hill-slope population did not find ecotypic variation in branch A_L:A_S (Stout & Sala, 2002), which suggests that intraspecific variation in A_L:A_S may only be detectable across larger geographic gradients, possibly because specific hydraulic adjustments are tailored to the moisture release curves of the soils on which the trees grow (Barnard *et al*., 2011). In addition, our study trees had limited variation in age, density, and tree size (Table 2), which further constrains potential variation compared to previous studies. Future study is required to determine how changes in branch A_L:A_S relate to whole tree A_L:A_S, as whole tree characteristics can be modified by canopy structure (Berninger *et al*., 1995) and stand development/tree size (Mencuccini & Bonosi, 2001; McDowell *et al*., 2002; Martinez-Vilalta *et al*., 2009) and represent an additional scale of hydraulic adjustment not measured here.

Ponderosa pine also exhibited little hydraulic adjustments to tolerate or avoid high xylem tensions in drier habitats in our study. Specifically, we found no clinal variation in branch vulnerability to cavitation, consistent with previous work on ponderosa populations (Maherali & DeLucia, 2000; Stout & Sala, 2002) and more geographically extensive work in other pine species (Martinez-Vilalta *et al*., 2009; Lamy *et al*., 2013; Sáenz-Romero *et al*., 2013). We found a small increase in hydraulic safety margins in low-elevation ponderosa; however, this did not translate into increased cavitation in trees with smaller margins. We also found slight elevational differences in xylem area-specific maximum conductivity (K_{max}), suggesting *less* hydraulic efficiency at low elevation (Fig. 6) contrary to expectations and to some previous findings in ponderosa pine (Maherali *et al*., 2002; Barnard *et al*., 2011 but see Stout & Sala, 2002). Xylem capacitance (the amount of water stored in xylem) is a final mechanism that ponderosa may use to buffer their hydraulic system against extreme xylem tensions without curtailing transpiration (Domec & Gartner, 2003; Barnard *et al*., 2011). However, capacitance has previously been found to correlate strongly with xylem P50 and less strongly with K_{max} in trunk xylem of ponderosa pine (Domec & Gartner, 2003; Barnard *et al*., 2011), suggesting minimal elevational differences in xylem capacitance in our system.

Our estimates of relative stomatal conductance (g_s) suggest that study ponderosa pines strongly regulate water loss via stomatal closure at low elevations (Fig. 8c), rather than avoiding or tolerating drought through hydraulic or morphological adjustment. This 78% decrease in g_s is likely associated with a smaller but considerable decrease in assimilation. Maintaining assimilation at such reduced conductance rates would require water use efficiency (WUE) to more than double, which is considerably beyond the ~40% increase in WUE to be expected at low values of g_s based on ponderosa assimilation curves (e.g., Cregg, 1994). Nor is such a large WUE decrease consistent with plastic or genetic differences in WUE documented in ponderosa pine provenance trials (e.g., Cregg & Olivas-García, 2000), drought experiments (e.g., Cregg, 1994; Zhang *et al*., 1997), or observations across elevation (McDowell *et al*., 2010). Thus, the greatly reduced g_s per leaf area suggested by our measurements and decreased branch A_L:A_S likely results in decreased whole-tree carbon assimilation.

Alternatively, high transpiration and assimilation could theoretically be maintained at low elevation despite small potential differences between predawn and midday xylem tensions ($\Delta\psi$) (Fig. 3) via drastic increases in hydraulic efficiency or capacitance. How-

ever, our hydraulic results show decreasing efficiency (K_{max}) at low elevations (Fig. 6). While mid- and low-elevation branch A_L:A_S did show on average a ~25% and ~27% decrease (respectively) from high elevation A_L:A_S (Fig. 4), the Whitehead & Jarvis (1981) model suggests that a decrease of 76% and 86% would be necessary to offset the decreased $\Delta\psi$ and increased VPD at mid- and low elevation and maintain transpiration. Martinez-Vilalta *et al.* (2009) found A_L:A_S changes approaching this magnitude across the entire geographic range of Scots pine (*Pinus sylvestris* L.) in Europe, but this trait appears more constrained either in ponderosa pine as a species, in the study population in the absence of local adaptation, or in stands of very similar structure.

Other factors influencing drought responses

Although this study suggests that trembling aspen is drought tolerating and ponderosa pine is drought avoiding at their dry range edges, additional drought avoidance and tolerance mechanisms may also be important. In particular, belowground traits related to rooting depth, morphology, hydraulics, and allometry (not measured in this study) could influence the elevational trends in xylem tensions that we documented. Lower predawn xylem tensions of low-elevation aspen compared to co-occuring high-elevation ponderosa pine (some aspen and ponderosa stands were located <50 m apart) suggests that rooting depth may play a role in the two species' drought resistance strategies (Fig. 3). However, aspens at the study site have extremely shallow functional rooting depths even when the shallow soil is dry (i.e., during natural or experimental drought, Anderegg *et al.*, 2013a). This suggests that lower predawn xylem tensions in aspen result from either slightly wetter micro-sites or a more extensive rooting area with less local soil-dry down, not from a deeper rooting depth than ponderosa. In addition, elevational differences in recovery potential following drought stress (a third class of drought resistance strategy) could be important. Assessment of recovery potential in the field is difficult because easily measured functional traits have rarely been linked to recovery ability, although some evidence suggests that embolism refilling may be correlated with wood density and P50 in angiosperms (Ogasa *et al.*, 2013). This relationship suggests that low-elevation aspens may be both more drought tolerant and better at postdrought recovery if it holds within species as well as between species. Finally, phenology of leaf/needle expansion and senescence compared to xylem growth may vary across elevation, and could alter plant hydraulics over the growing season by shifting leaf area:sapwood area ratios on relatively short time scales. Our study provides only a midsummer (peak water stress) snapshot of these traits, and additional temporally resolved studies are warranted.

We also note that the clinal trait variation we observed in trembling aspen may be somewhat larger than that observed elsewhere in aspen's range, owing to a massive drought-induced mortality event in the early 2000s (affecting ~20% of the aspen in the study area – Huang & Anderegg, 2011), principally at low elevations. This mortality event may have selected for ramets with extreme trait values at low elevations, although some of the traits showing clinal variation have previously shown considerable temporal plasticity in the study area (e.g., P50: Anderegg *et al.*, 2013b; leaf size: Anderegg *et al.*, 2014). However, the P50 differences within aspen documented herein are in the opposite direction of the xylem fatigue documented by Anderegg *et al.* (2013b) in low-elevation aspen following the mortality inducing drought, suggesting this trait may actually show *larger* clinal trait variation in other parts of aspen's geographic range.

In addition, the morphological and physiological adjustments to geographic variations in water availability documented here are distinct from but still relevant to the short-term physiological responses of plants to acute drought, including those leading to mortality. Drought-induced tree mortality is an area of active research (Hartmann *et al.*, 2015), centering around the interlinked roles of the hydraulic and carbon economies in trees (McDowell *et al.*, 2011; Anderegg *et al.*, 2012). It has become clear that mortality is a complex set of many interacting processes and mechanisms, many of which will be strongly influenced by the traits explored here. In particular, widespread mortality of aspen in the region has been linked to the gradual deterioration of plant hydraulic transport (Anderegg *et al.*, 2014, 2015), fitting our observation of increased drought tolerance with apparently little stomatal closure in chronically dry, low-elevation aspens (suggesting a relatively anisohydric stomatal strategy).This may maximize tree performance in dry habitats during most years but make them susceptible to hydraulic damage during drought. In addition, drought-induced mortality in ponderosa pine has been associated with increased growth sensitivity to climate and chronically constrained gas exchange (McDowell *et al.*, 2010), which aligns well with the responses to chronic water limitation documented here.

Determining whether the functional trait variation documented in this study is driven by phenotypic plasticity or local genetic adaptation is critical for understanding future range boundary dynamics of these two species. We believe phenotypic plasticity

likely plays a predominant role in this system. For ponderosa pine, gene flow is large and population differentiation is low across much larger geographic distances than studied here (Maherali *et al*., 2002), suggesting that elevational trait differences in this species are principally plastic. For aspen, much trait variation likely resulted from phenotypic plasticity as well. We were able to partially examine plasticity for this clonal species by comparing trait variation within stand (representing within-individual variation) and between stands (representing variation between individuals) for all traits except P50 (not measured per individual). Within-stand (likely plastic) variation was considerably larger than between-stand variation for leaf size, SLA, A_L:A_S, PLC, and wood density (Table S3), Meanwhile, height, $K_{\text{nat\_Leaf}}$, and g_s showed equal or greater between-stand variation than within-stand variation, which may possibly indicate a genetic or micro-site signal.

Implications for range shifts

Both focal species showed very large decreases in basal area growth at their low-elevation range boundary likely related to general fitness decreases – implying that the differences in the physiological strategies employed by the two species to cope with drought stress will matter during climate change-induced range shifts. It is also possible that these growth decreases may represent adaptive responses to water stress (particularly if carbon is invested below ground instead). More study is clearly warranted, but we think fitness differences are more likely. For one, reproductive output is typically a function of tree size that then compounds over a tree's life time (such that growth and fecundity are correlated if mortality rates are constant). In addition, at least within a stand, growth and mortality rate tend to be inversely correlated (slow growing trees die more often, Wyckoff & Clark, 2000, 2002). While a trade-off between growth and survival (i.e. a positive correlation between growth and mortality or 'demographic compensation') has been documented across the range of alpine perennials (Doak & Morris, 2010), we found no evidence for such a trade-off, at least in aspen (tree age did not differ between high and low elevation in aspen, see Fig. S7).

The diametrically opposite drought tolerance and drought avoidance strategies and (therefore) contrasting physiological range constraints for ponderosa and aspen may imply differing range boundary dynamics over the coming century. Drought avoidance via stomatal closure is a rapid response to water stress (timescale of hours to days), likely helping ponderosa pine avoid extreme spikes in water deficit such as single-year droughts. However, heavy reliance on stomatal closure rather than longer term adjustments may decrease ponderosa pine's ability to reach maturity and/or maintain significant reproductive output under sustained drought or long-term drying trends if low-elevation trees are carbon limited. Long-term decreases in assimilation in low-elevation ponderosas may also increase their susceptibility to bark beetles, both through decreased resin duct formation and decreased resin pressures (Kane & Kolb, 2010). While ponderosa's drought-avoidant physiology would suggest that range shifts driven by increasing drought and long-term aridification should be gradual, the synergistic potential between drought and insect attack could still lead to very rapid range contractions via mass die-off. Indeed, one such die-off-induced range contraction has been documented in ponderosa pine, which occurred in conjunction with an extreme drought as well as a bark beetle outbreak (Allen & Breshears, 1998).

In contrast, trembling aspen's strategy of increasing drought tolerance by building more tolerant organs is a much slower response than the stomatal closure of ponderosa pine (timescale of months to decades). This could allow aspens to acclimate to long-term drying trends but leaves them vulnerable to short-term drought extremes. In the absence of short-term avoidance measures such as stomatal closure, aspen experience catastrophic embolism that can lead to rapid mortality (Anderegg *et al*., 2014), suggesting that aspen range dynamics will be dominated by episodic contractions initiated by short but severe droughts. In addition, aspen and ponderosa pine may be sensitive to different changes in seasonal precipitation. Because it sustains midsummer transpiration, aspen may be sensitive primarily to extreme midsummer moisture stress tied to summer precipitation, growing season length, and temperature-driven evaporative demand. Indeed, a massive aspen die-off across much of the western United States was precipitated in 2002 by the most extreme single summer evaporative and soil moisture deficit of the past century (Anderegg *et al*., 2013a), which caused fatal hydraulic failure in affected aspens (Anderegg *et al*., 2012). Ponderosa pine, on the other hand, can perform 50–70% of its carbon assimilation outside of the growing season (Law *et al*., 2000). Thus, ponderosa pine may respond most strongly to precipitation changes in the fall, winter, and spring that curtail assimilation during the productive 'shoulder seasons'.

These inferences assume that low-elevation trees are carbon limited. Emerging evidence suggests that this may not necessarily be the case for all trees (Körner, 2003; Sala *et al*., 2012). However, the range dynamic implications of a drought-avoidant vs. drought-tolerant strategy are supported by the recent landscape level die-off event at the study site following the extreme

2002 drought mentioned above, which affected aspen but not ponderosa (Worrall *et al*., 2008). The hot 2002 drought predominantly affected stands at aspen's low-elevation range margin (Worrall *et al*., 2008, 2010) indicating probable range contractions. Meanwhile ponderosa pine trees at low elevations showed little or no growth during the drought (LDL Anderegg unpublished data). However, ponderosa pine experienced little mortality at our site and showed elevated mortality elsewhere in the southwestern USA only where beetle outbreaks occurred (Negrón *et al*., 2009). Given the projected drying of the southwestern USA over the next century (Diffenbaugh *et al*., 2008), ponderosa's dry range boundary may slowly contract in response to long-term drying trends that chronically depress assimilation (in the absence of pest outbreak), while aspen may be more prone to rapid and episodic range contractions in response to extreme events.

Acknowledgements

We thank A Baird and D Murray for assistance in the field, as well as G Koch, L Van Volkenburgh, and WRL Anderegg for allowing us to use their equipment. We also thank M Love and M Anderegg for critical logistical support. TM Hinckley, G Quetin, RB Huey, E Linck, and WRL Anderegg provided critical feedback on the manuscript. Fieldwork was supported by a University of Washington Biology Edwards Grant, a Charles Redd Center for Western Studies Summer Research Grant, a Sigma Xi Grant-In-Aid, and an American Alpine Club Research Grant. This material is based upon work supported by the National Science Foundation Graduate Research Fellowship Program under Grant No. DGE-1256082.

References

Adams HD, Kolb TE (2005) Tree growth response to drought and temperature in a mountain landscape in northern Arizona, USA. *Journal of Biogeography*, **32**, 1629–1640.

Adler PB, Salguero-Gómez R, Compagnoni A, Hsu JS, Ray-Mukherjee J, Mbeau-Ache C, Franco M (2014) Functional traits explain variation in plant life history strategies. *Proceedings of the National Academy of Sciences of the United States of America*, **111**, 740–745.

Aitken SN, Yeaman S, Holliday JA, Wang T, Curtis-McLane S (2008) Adaptation, migration or extirpation: climate change outcomes for tree populations. *Evolutionary Applications*, **1**, 95–111.

Albert CH, Thuiller W, Yoccoz NG, Douzet R, Aubert S, Lavorel S (2010) A multi-trait approach reveals the structure and the relative importance of intra- vs. interspecific variability in plant traits. *Functional Ecology*, **24**, 1192–1201.

Allen CD, Breshears DD (1998) Drought-induced shift of a forest-woodland ecotone: rapid landscape response to climate variation. *Proceedings of the National Academy of Sciences of the United States of America*, **95**, 14839–14842.

Anderegg WRL (2014) Spatial and temporal variation in plant hydraulic traits and their relevance for climate change impacts on vegetation. *New Phytologist*, **205**, 1008–1014.

Anderegg WRL, Berry JA, Smith DD, Sperry JS, Anderegg LDL, Field CB (2012) The roles of hydraulic and carbon stress in a widespread climate-induced forest die-off. *Proceedings of the National Academy of Sciences of the United States of America*, **109**, 233–237.

Anderegg LDL, Anderegg WRL, Abatzoglou J, Hausladen AM, Berry JA (2013a) Drought characteristics' role in widespread aspen forest mortality across Colorado, USA. *Global Change Biology*, **19**, 1526–1537.

Anderegg WRL, Plavcová L, Anderegg LDL, Hacke UG, Berry JA, Field CB (2013b) Drought's legacy: multiyear hydraulic deterioration underlies widespread aspen forest die-off and portends increased future risk. *Global Change Biology*, **19**, 1188–1196.

Anderegg WRL, Anderegg LDL, Berry JA, Field CB (2014) Loss of whole-tree hydraulic conductance during severe drought and multi-year forest die-off. *Oecologia*, **175**, 11–23.

Anderegg WRL, Flint A, Huang C-Y *et al*. (2015) Tree mortality predicted from drought-induced vascular damage. *Nature Geoscience*, **8**, 367–371.

Angert AL, Crozier LG, Rissler LJ, Gilman SE, Tewksbury JJ, Chunco AJ (2011) Do species' traits predict recent shifts at expanding range edges? *Ecology Letters*, **14**, 677–689.

Barnard DM, Meinzer FC, Lachenbruch B, McCulloh KA, Johnson DM, Woodruff DR (2011) Climate-related trends in sapwood biophysical properties in two conifers: avoidance of hydraulic dysfunction through coordinated adjustments in xylem efficiency, safety and capacitance. *Plant, Cell & Environment*, **34**, 643–654.

Bartlett MK, Scoffoni C, Sack L (2012) The determinants of leaf turgor loss point and prediction of drought tolerance of species and biomes: a global meta-analysis. *Ecology Letters*, **15**, 393–405.

Bates D, Maechler M, Bolker B, Walker S (2014) lme4: Linear mixed-effects models using Eigen and S4. R package version 1.1-7, Available at: http://CRAN.R-project.org/package=lme4.

Benito-Garzón M, Alía R, Robson TM, Zavala MA (2011) Intra-specific variability and plasticity influence potential tree species distributions under climate change. *Global Ecology and Biogeography*, **20**, 766–778.

Berninger F, Nikinmaa E, Hari P, Mencuccini M (1995) Evaporative demand determines branchiness of Scots pine. *Oecologia*, **102**, 164–168.

Boisvenue C, Running SW (2006) Impacts of climate change on natural forest productivity - evidence since the middle of the 20th century. *Global Change Biology*, **12**, 862–882.

Buckley LB, Kingsolver JG (2012) Functional and phylogenetic approaches to forecasting species' responses to climate change. *Annual Review of Ecology Evolution and Systematics*, **43**, 205–226.

Buckley LB, Waaser SA, MacLean HJ, Fox R (2011) Does including physiology improve species distribution model predictions of responses to recent climate change? *Ecology*, **92**, 2214–2221.

Bunn AG (2010) Statistical and visual crossdating in R using the dplR library. *Dendrochronologia*, **28**, 251–258.

Carnicer J, Barbeta A, Sperlich D, Coll M, Peñuelas J (2013) Contrasting trait syndromes in angiosperms and conifers are associated with different responses of tree growth to temperature on a large scale. *Frontiers in Plant Science*, **4**, 409, 1–19.

Choat B, Jansen S, Brodribb TJ *et al*. (2012) Global convergence in the vulnerability of forests to drought. *Nature*, **491**, 752–755.

Clark JS (2010) Individuals and the variation needed for high species diversity in forest trees. *Science*, **327**, 1129–1132.

Contreras MA, Affleck D, Chung W (2011) Evaluating competitive indices as predictors of basal area increment in Montana forests. *Forest Ecology and Management*, **262**, 1939–1949.

Cregg BM (1994) Carbon allocation, gas exchange, and needle morphology of Pinus ponderosa genotypes known to differ in growth and survival under imposed drought. *Tree Physiology*, **14**, 883–898.

Cregg BM, Olivas-García JM (2000) Provenance variation in carbon isotope discrimination of mature ponderosa pine trees at two locations in the Great Plains. *Canadian Journal of Forestry*, **4**, 883–898.

Dai A (2011) Drought under global warming: a review. *Wiley Interdisciplinary Reviews: Climate Change*, **2**, 45–65.

Daly C, Gibson WP, Taylor GH, Johnson GL (2002) A knowledge-based approach to the statistical mapping of climate. *Climate Research*, **22**, 99–113.

Díaz S, Purvis A, Cornelissen J *et al*. (2013) Functional traits, the phylogeny of function, and ecosystem service vulnerability. *Ecology and Evolution*, **3**, 2958–2975.

Diffenbaugh NS, Giorgi F, Pal JS (2008) Climate change hotspots in the United States. *Geophysical Research Letters*, **35**, L16709.

Doak DF, Morris WF (2010) Demographic compensation and tipping points in climate-induced range shifts. *Nature*, **467**, 959–962.

Domec JC, Gartner BL (2003) Relationship between growth rates and xylem hydraulic characteristics in young, mature and old-growth ponderosa pine trees. *Plant, Cell & Environment*, **26**, 471–483.

Dullinger S, Gattringer A, Thuiller W, Moser D (2012) Extinction debt of high-mountain plants under twenty-first-century climate change. *Nature Climate*, **2**, 619–622.

Fellows AW, Goulden ML (2012) Rapid vegetation redistribution in Southern California during the early 2000s drought. *Journal of Geophysical Research*, **117**, 1–11.

Franks PJ, Drake PL, Froend RH (2007) Anisohydric but isohydrodynamic: seasonally constant plant water potential gradient explained by a stomatal control mechanism incorporating variable plant hydraulic conductance. *Plant, Cell & Environment*, **30**, 19–30.

Gaston KJ (2009) Geographic range limits: achieving synthesis. *Proceedings of the Royal Society B: Biological Sciences*, **276**, 1391–1393.

Handa IT, Körner C, Hättenschwiler S (2005) A test of the treeline carbon limitation hypothesis by in situ CO2 enrichment and defoliation. *Ecology*, **86**, 1288–1300.

Hartmann H (2011) Will a 385 million year-struggle for light become a struggle for water and for carbon? *Global Change Biology*, **17**, 642–655.

Hartmann H, Adams HD, Anderegg WRL, Jansen S, Zeppel MJB (2015) Research frontiers in drought-induced tree mortality: crossing scales and disciplines. *New Phytologist*, **205**, 965–969.

Hegyi F (1974) A simulation model for managing jack pine stands. In: *Growth Models for Tree and Stand Simulations* (ed. Fried J), pp. 74–90. Royal College of Forestry, Stockholm, Sweden.

Huang C-Y, Anderegg WRL (2011) Large drought-induced aboveground live biomass losses in southern Rocky Mountain aspen forests. *Global Change Biology*, **18**, 1016–1027.

IPCC (2014) Climate change 2014: impacts, adaptation, and vulnerability. Part A: global and sectoral aspects. Contribution of Working Group II to the Fifth Assessment Report of the Intergovernmental Panel on Climate Change. (eds Field CB, Barros VR, Dokken D, Mach KJ, Mastrandrea MD, Bilir TE, Chatterjee M, Ebi KL, Estrada YO, Genova RC, Girma B, Kissel ES, Levy EN, MacCracken S, Mastrandrea PR, White LL). pp. 1–1132. Cambridge University Press, Cambridge.

Ishii HR, Azuma W, Kuroda K, Sillett SC (2014) Pushing the limits to tree height: could foliar water storage compensate for hydraulic constraints in Sequoia sempervirens? (ed Watling J). *Functional Ecology*, **28**, 1087–1093.

Kane JM, Kolb TE (2010) Importance of resin ducts in reducing ponderosa pine mortality from bark beetle attack. *Oecologia*, **164**, 601–609.

Kelly AE, Goulden ML (2008) From the Cover: rapid shifts in plant distribution with recent climate change. *Proceedings of the National Academy of Sciences of the United States of America*, **105**, 11823–11826.

Klein T (2014) The variability of stomatal sensitivity to leaf water potential across tree species indicates a continuum between isohydric and anisohydric behaviours. *Functional Ecology*, **28**, 1313–1320.

Koch GW, Fredeen AL (2005) Transport challenges in tall trees. In: *Vascular Transport in Plants* (eds Holbrook NM, Zwieniecki MA), pp. 437–456. Elsevier Academic Press, Burlington, MA, USA.

Körner C (2003) Carbon limitation in trees. *Journal of Ecology*, **91**, 4–17.

Körner C (2015) Paradigm shift in plant growth control. *Current Opinion in Plant Biology*, **25**, 107–114.

Kuznetsova A, Brockhoff PB, Christensen RHB (2014) lmerTest: Tests for random and fixed effects for linear mixed effect models (lmer objects of lme4 package). R package version 2.0-11. Available at: http://CRAN.R-project.org/package=lmerTest.

Lamy J-B, Delzon S, Bouche PS, Alía R, Vendramin GG, Cochard H, Plomion C (2013) Limited genetic variability and phenotypic plasticity detected for cavitation resistance in a Mediterranean pine. *New Phytologist*, **201**, 874–886.

Larcher W, Heber U, Santarius KA (1973) Limiting temperatures for life functions. In: *Temperature and Life* (eds Precht H, Christopherson J, Hensel H, Larcher W), pp. 195–263. Springer-Verlag, Berlin, Heidelberg.

Law BE, Williams M, Anthoni PM, Baldocchi DD, Unsworth MH (2000) Measuring and modelling seasonal variation of carbon dioxide and water vapour exchange of a Pinus ponderosa forest subject to soil water deficit. *Global Change Biology*, **6**, 613–630.

Lens F, Sperry JS, Christman MA, Choat B, Rabaey D, Jansen S (2010) Testing hypotheses that link wood anatomy to cavitation resistance and hydraulic conductivity in the genus Acer. *New Phytologist*, **190**, 709–723.

Levitt J (1980) *Responses of Plants to Environmental Stresses, Volume 2: Water, Radiation, Salt and Other Stresses* (2nd edn). Springer, Berlin.

Lundquist JD, Huggett B (2008) Evergreen trees as inexpensive radiation shields for temperature sensors. *Water Resources Research*, **44**, 1–5.

MacArthur D (1972) *Geographical Ecology: Patterns in the Distribution of Species*. Harper & Row, New York.

Maherali H, DeLucia EH (2000) Xylem conductivity and vulnerability to cavitation of ponderosa pine growing in contrasting climates. *Tree Physiology*, **20**, 859–867.

Maherali H, Williams BL, Paige KN, DeLucia EH (2002) Hydraulic differentiation of Ponderosa pine populations along a climate gradient is not associated with ecotypic divergence. *Functional Ecology*, **16**, 510–521.

Maherali H, Pockman WT, Jackson RB (2004) Adaptive variation in the vulnerability of plants to xylem cavitation. *Ecology*, **85**, 2184–2199.

Martinez-Vilalta J, Cochard H, Mencuccini M *et al*. (2009) Hydraulic adjustment of Scots pine across Europe. *New Phytologist*, **184**, 353–364.

McDowell NG, Phillips N, Lunch C, Bond BJ, Ryan MG (2002) An investigation of hydraulic limitation and compensation in large, old Douglas-fir trees. *Tree Physiology*, **22**, 763–774.

McDowell NG, Allen CD, Marshall L (2010) Growth, carbon-isotope discrimination, and drought-associated mortality across a *Pinus ponderosa* elevational transect. *Global Change Biology*, **16**, 399–415.

McDowell NG, Beerling DJ, Breshears DD, Fisher RA, Raffa KF, Stitt M (2011) The interdependence of mechanisms underlying climate-driven vegetation mortality. *Trends in Ecology & Evolution*, **26**, 523–532.

McGill BJ, Enquist BJ, Weiher E, Westoby M (2006) Rebuilding community ecology from functional traits. *Trends in Ecology & Evolution*, **21**, 178–185.

Medvigy D, Wofsy SC, Munger JW (2009) Mechanistic scaling of ecosystem function and dynamics in space and time: ecosystem Demography model version 2. *Journal of Geophysical Research*, **114**, 1–21.

Mencuccini M, Bonosi L (2001) Leaf/sapwood area ratios in Scots pine show acclimation across Europe. *Canadian Journal of Forest Research*, **31**, 442–456.

Merchant A, Callister A, Arndt S, Tausz M, Adams M (2007) Contrasting physiological responses of six eucalyptus species to water deficit. *Annals of Botany*, **100**, 1507–1515.

Messier J, McGill BJ, Lechowicz MJ (2010) How do traits vary across ecological scales? A case for trait-based ecology. *Ecology Letters*, **13**, 838–848.

Mitchell PJ, Veneklaas EJ, Lambers H, Burgess SS (2008) Leaf water relations during summer water deficit: differential responses in turgor maintenance and variation in leaf structure among different plant communities in south-western Australia. *Plant, Cell & Environment*, **31**, 1791–1802.

Moorcroft PR, Hurtt GC, Pacala SW (2001) A method for scaling vegetation dynamics: the ecosystem demography model (ED). *Ecological Monographs*, **71**, 557–586.

Morin X (2009) Comparing niche-and process-based models to reduce prediction uncertainty in species range shifts under climate change. *Ecology*, **90**, 1301–1313.

Mouillot D, Graham NAJ, Villéger S, Mason NWH, Bellwood DR (2013) A functional approach reveals community responses to disturbances. *Trends in Ecology & Evolution*, **28**, 167–177.

Negrón JF, McMillin JD, Anhold JA, Coulson D (2009) Bark beetle-caused mortality in a drought-affected ponderosa pine landscape in Arizona, USA. *Forest Ecology and Management*, **257**, 1353–1362.

Ogasa M, Miki NH, Murakami Y, Yoshikawa K (2013) Recovery performance in xylem hydraulic conductivity is correlated with cavitation resistance for temperate deciduous tree species. *Tree Physiology*, **33**, 335–344.

Pammenter NW, Vander Willigen C (1998) A mathematical and statistical analysis of the curves illustrating vulnerability of xylem to cavitation. *Tree Physiology*, **18**, 589–593.

Parmesan C, Yohe G (2003) A globally coherent fingerprint of climate change impacts across natural systems. *Nature*, **421**, 37–42.

Pavlick R, Drewry DT, Bohn K, Reu B, Kleidon A (2013) The Jena Diversity-Dynamic Global Vegetation Model (JeDi-DGVM): a diverse approach to representing terrestrial biogeography and biogeochemistry based on plant functional trade-offs. *Biogeosciences*, **10**, 4137–4177.

Pérez-Harguindeguy N, Díaz S, Garnier E *et al*. (2013) New handbook for standardised measurement of plant functional traits worldwide. *Australian Journal of Botany*, **61**, 167.

Quintero I, Wiens JJ (2013) Rates of projected climate change dramatically exceed past rates of climatic niche evolution among vertebrate species (eds Quintero I, Wiens JJ). *Ecology Letters*, **16**, 1095–1103.

R Core Team (2014) *R: A Language and Environment for Statistical Computing*. R Foundation for Statistical Computing, Vienna, Austria. Available at: http://www.R-project.org/.

Reich PB (2014) The world-wide "fast–slow" plant economics spectrum: a traits manifesto. *Journal of Ecology*, **102**, 275–301.

Reich PB, Wright IJ, Cavender Bares J, Craine JM, Oleksyn J, Westoby M, Walters MB (2003) The evolution of plant functional variation: traits, spectra, and strategies. *International Journal of Plant Sciences*, **164**, S143–S164.

Ritchie GA, Hinckley TM (1975) The pressure chamber as an instrument for ecological research. In: *Advances in Ecological Research*, vol. 9 (ed. Macfadden A), pp. 165–254. Academic Press, London.

Root TL, Price JT, Hall KR, Schneider SH, Rosenzweig C, Pounds JA (2003) Fingerprints of global warming on wild animals and plants. *Nature*, **421**, 57–60.

Sack L, Holbrook NM (2006) Leaf hydraulics. *Annual Review of Plant Biology*, **57**, 361–381.

Sáenz-Romero C, Lamy J-B, Loya-Rebollar E, Plaza-Aguilar A, Burlett R, Lobit P, Delzon S (2013) Genetic variation of drought-induced cavitation resistance among

Pinus hartwegii populations from an altitudinal gradient. *Acta Physiologiae Plantarum*, **35**, 2905–2913.

Sala A, Woodruff DR, Meinzer FC (2012) Carbon dynamics in trees: feast or famine? *Tree Physiology*, **32**, 764–775.

Scheiter S, Langan L, Higgins SI (2013) Next-generation dynamic global vegetation models: learning from community ecology. *New Phytologist*, **198**, 957–969.

Sexton JP, McIntyre PJ, Angert AL, Rice KJ (2009) Evolution and ecology of species range limits. *Annual Review of Ecology Evolution and Systematics*, **40**, 415–436.

Soudzilovskaia NA, Elumeeva TG, Onipchenko VG *et al*. (2013) Functional traits predict relationship between plant abundance dynamic and long-term climate warming. *Proceedings of the National Academy of Sciences of the United States of America*, **110**, 18180–18184.

Sperry JS (2000) Hydraulic constraints on plant gas exchange. *Agricultural and Forest Meteorology*, **104**, 13–23.

Sperry JS, Sullivan JE (1992) Xylem embolism in response to freeze-thaw cycles and water stress in ring-porous, diffuse-porous, and conifer species. *Plant Physiology*, **100**, 605–613.

Sperry JS, Donnelly JR, Tyree MT (1988) A method for measuring hydraulic conductivity and embolism in xylem. *Plant, Cell & Environment*, **11**, 35–40.

Sperry JS, Nichols KL, Sullivan J, Eastlack SE (1994) Xylem embolism in ring-porous, diffuse-porous, and coniferous trees of northern Utah and interior Alaska. *Ecology*, **75**, 1736–1752.

Sperry J, Hacke U, Oren R (2002) Water deficits and hydraulic limits to leaf water supply. *Plant, Cell & Environment*, **25**, 251–263.

Stout DL, Sala A (2002) Xylem vulnerability to cavitation in *Pseudotsuga menziesii* and *Pinus ponderosa* from contrasting habitats. *Tree Physiology*, **23**, 43–50.

Violle C, Reich PB, Pacala SW, Enquist BJ, Kattge J (2014) The emergence and promise of functional biogeography. *Proceedings of the National Academy of Sciences of the United States of America*, **111**, 13690–13696.

Von Humboldt A, Bonpland A (1805) *Essai sur la Geographie des Piantes; Accompagne D'un Tableau Physique des Regions Equinoxales*. Fr. Schoell and Tubingen, J.C. Cotta, Paris. [republished 2009, translated by Romanowski S, (ed Jackson ST) Chicago University Press, Chicago, USA & London, UK.]

Wang T, Hamann A, Spittlehouse DL, Murdock TQ (2012) ClimateWNA—high-resolution spatial climate data for western North America. *Journal of Applied Meteorology and Climatology*, **51**, 16–29.

Wheeler JK, Huggett BA, Tofte AN, Rockwell FE, Holbrook NM (2013) Cutting xylem under tension or supersaturated with gas can generate PLC and the appearance of rapid recovery from embolism. *Plant, Cell & Environment*, **36**, 1938–1949.

Whitehead D, Jarvis PG (1981) Coniferous forests and plantations. In: *Woody Plant Communities* (ed. Kozlowski TT), pp. 49–152. Academic Press, New York, NY, USA.

Worrall JJ, Egeland L, Eager T, Mask RA (2008) Rapid mortality of *Populus tremuloides* in southwestern Colorado, USA. *Forest Ecology and Management*, **255**, 686–696.

Worrall JJ, Marchetti SB, Egeland L, Mask RA (2010) ScienceDirect.com – forest ecology and management – effects and etiology of sudden aspen decline in southwestern Colorado, USA. *Forest Ecology and Management*, **255**, 686–696.

Wyckoff PH, Clark JS (2000) Predicting tree mortality from diameter growth: a comparison of maximum likelihood and Bayesian approaches. *Canadian Journal of Forest Research*, **30**, 156–167.

Wyckoff PH, Clark JS (2002) The relationship between growth and mortality for seven co-occurring tree species in the southern Appalachian Mountains. *Journal of Ecology*, **90**, 604–615.

Zhang JW, Feng Z, Cregg BM, Schumann CM (1997) Carbon isotopic composition, gas exchange, and growth of three populations of ponderosa pine differing in drought tolerance. *Tree Physiology*, **17**, 461–466.

Zimmermann MH, Jeje AA (1981) Vessel-length distribution in stems of some American woody plants. *Canadian Journal of Botany*, **59**, 1882–1892.

Zwieniecki MA, Boyce CK (2004) Hydraulic limitations imposed by crown placement determine final size and shape of *Quercus rubra* L. leaves. *Plant, Cell and the Environment*, **27**, 357–365.

Supporting Information

Additional Supporting Information may be found in the online version of this article:

Figure S1. Species relative abundance across elevation at the study site in the La Plata Mountains, (San Juan National Forest, Colorado, USA).
Figure S2. Description of methods for combining Basal Area Increment datasets and Relationship between Hegyi's competitive index (2014 dataset) and number of live trees within 5m (2013 dataset).
Figure S3. Mean annual Basal Area Increment for 2014 data only and combined 2013 & 2014 data.
Figure S4. Xylem vulnerability curves showing raw xylem area specific conductivity (K) as a function of induced xylem tension.
Figure S5. Mean annual Basal Area Increment (BAI) for individual trembling aspen trees as a function of (a) SLA and (b) branch wood density.
Figure S6. Percentage difference from high elevation average A_L:A_S and average median leaf area for individual ponderosa pine trees.
Figure S7. Aspen tree age across elevation from all trees in the full dataset used to calculate BAI for which ages could be estimated from tree cores (n = 86).
Table S1. *Pinus Ponderosa* – Details for linear mixed-effects models of functional trait data.
Table S2. *Populus tremuloides* – Details for linear mixed-effects models of functional trait data.
Table S3. Details from the best linear mixed effects models explaining branch xylem tensions for ponderosa pine and trembling aspen.
Appendix S1–S5. Comma separated value data files for Basal Area Increment analysis (LDLA_JHRL_BasalAreaIncrement_Full-dataset_102115.csv), hydraulic and morphological trait analysis (LDLA_JHRL_Traits_all_final_10_25_15.csv), and xylem vulnerability curves (ponderosa pine: LDLA_JHRL_PIPO_VcurveLong_FinalData_102215.csv, trembling aspen: LDLA_JHRL_POTR_VcurveLong_FinalData_102215.csv). Also includes metadata file with column descriptions for all four data files (LDLA_JHRL_metadata.csv).
Appendix S6. R code (file: AndereggAndHilleRisLambers2015_Code.R) used for analysis, including mixed effects models and figure generation.

Chapter 3: Within-species trait variation challenges our understanding of the causes and consequences of global trait variation

Leander DL Anderegg[1,2,*], Logan T Berner[3], Grayson Badgley[2], Beverly E. Law[3], Janneke HilleRisLambers[1]

Affiliations:
[1] Department of Biology, University of Washington, Seattle, WA
[2] Department of Global Ecology, Carnegie Institute for Science, Stanford, CA
[3] Department of Forest Ecosystems and Society, Oregon State University, Corvallis, OR
[*] Corresponding author: landeregg@carnegiescience.edu, +1 541.790.1096

Short title:
Within-species patterns vs. global trait variation

Key words:
functional trait, leaf economics spectrum, taxonomic scale, intra-specific variation, leaf lifespan, leaf mass per area, leaf nitrogen content

Supplemental Material referenced in text can be found in Appendix E

Abstract:

Functional traits have great potential to stimulate a predictive ecology, providing spatial and temporal scale-independent tools for understanding ecological interactions, community dynamics and ecosystem function. Yet their utility relies in part on three key assumptions: 1) that most trait variation lies between rather than within species, 2) that global patterns of trait covariation are the result of universal evolutionary or physiological trade-offs that are independent of taxonomic scale and 3) that traits respond predictably to environmental gradients. We use an extensive dataset of within-species trait variation and a global dataset of between-species variation to test these key assumptions at a global scale (including 939 plant genera and 214 plant families). We examine three traits central to the leaf economics spectrum, leaf mass per area (LMA), leaf lifespan, and leaf nitrogen content, and quantify patterns of trait variation and trait covariation at multiple taxonomic scales. We also test whether site-level environmental variables reliably predict geographic trait variation within species. We find that log-transformed LMA, leaf lifespan, and mass-based nitrogen content do vary primarily between rather than within species, though area-based leaf nitrogen varies enormously within species (>25% of global variation is within-species). We also find that mass-based leaf nitrogen consistently decreases with LMA and leaf lifespan at all taxonomic scales. However, we find surprisingly different patterns of trait covariation between leaf lifespan, LMA, and area-based nitrogen content within versus between species. The positive global relationship between leaf lifespan and LMA disappears or reverses directions within-species, while the relationship between LMA and area-based nitrogen becomes more constrained within-species. In North American conifers, we find weak intra-specific relationships between site environmental factors and foliar traits. Taken together, our results challenge the 'scale-free' nature of the currently proposed mechanisms

driving leaf trait covariation. However, our results demonstrate the potential power if intra-specific trait variation to deepen our understanding of the causes and consequences of functional trait variation.

Introduction

Trait-based ecology has the potential unify ecological disciplines and decades of ecological study, to provide a predictive framework for community ecology and to drive the development of the next generation of ecosystem models. In particular, plant functional traits have proven extremely useful proxies for both complex ecological 'strategies' and for key niche dimensions such as biotic stress tolerance. Some notable successes of plant functional ecology include the identification of the 'global leaf economics spectrum' (Wright *et al.*, 2004) and the linking of various functional traits to demographic outcomes (e.g. Kraft *et al.*, 2010; Adler *et al.*, 2014; Falster *et al.*, 2015) or climatic stress tolerance Maherali *et al.*, 2004; Skelton *et al.*, 2015).

However, emergent challenges have begun to force a re-evaluation of functional traits as a taxonomy-independent, scale-transcending silver bullet for simplifying the complex ecologies and life histories that drive ecological interactions and ecosystem function (Shipley *et al.*, 2016). An increasing awareness of the size and importance of within-species trait variation that is traditionally ignored (Clark, 2010; Jung *et al.*, 2010; Albert *et al.*, 2010a; 2010b; Violle *et al.*, 2012; Reich *et al.*, 2014; Siefert *et al.*, 2015). Ecosystem models often rely on a particularly fraught assumption that traits vary more between 'Plant Functional Types' (PFTs) than within PFTs (Wright *et al.*, 2005; Poorter *et al.*, 2009; Anderegg, 2014). Additionally, the

'functionality' of plant traits has proven surprisingly weak in a number of contexts, such as explaining differences in observed species range shifts (Buckley & Kingsolver, 2012), predicting sapling demographic rates (Paine *et al.*, 2015), or explaining plant species coexistence (Kraft *et al.*, 2015).

These emerging complexities highlight three key, yet largely untested assumptions in trait-based plant ecology. First, most applications assume that trait variation within species (or for ecosystem models, within PFTs) is negligible compared to trait variation between species. Second, it is assumed that global spectra of trait co-variation are taxonomically scale independent, and result from universal physiological or evolutionary trade-offs. Third, traits are assumed to vary in a consistent and predictable way across environmental gradients. Here we use a large dataset of global leaf trait measurements and intensive within-species trait measurements from the northwestern U.S.A. to test these three assumptions.

The study of trait variation within-species rather than between species has great potential to shed light on these fundamental assumptions about functional traits. From an evolutionary perspective, intra-specific trait variation is the very cloth out of which natural selection is cut. Heritable variation between individuals in a population is the core requirement of evolutionary change. Unfortunately, the sampling intensity needed to quantify within-species variation is often prohibitive, resulting on a pervasive focus on between-species trait variation. Yet within-species patterns of trait variation have the huge advantage of holding constant many axes of life history variation that might otherwise obscure ecological patterns or create spurious, non-causal trait-trait, trait-environment, or trait-performance correlations. Additionally, within-species trait variation can potentially speak to evolutionary trade-offs at the scale at which we understand evolution to occur, namely between individuals or populations in a species. An understanding of

within-species trait variation is critical in order to understand trait variation across spatial, temporal, and taxonomic scales. For example, if we wish to build trait-based ecosystem models that capture key evolutionary and physiological trade-offs rather than simply modeling static Plant Functional Types informed primarily by plant physiognomy (e.g. Pavlick *et al.*, 2013; Scheiter *et al.*, 2013), we must first develop a robust framework that can explain evidently conflicting patterns of foliar traits within individual canopies versus across species (Poorter *et al.*, 2009; Bonan *et al.*, 2012). Finally, intra-specific trait variation could prove particularly valuable for linking trait variation directly to environmental variation, because within-species comparisons naturally control for phylogenetic/biogeographic variation that can confound patterns across communities.

Ultimately, a strong understanding of the patterns of trait variation, the mechanisms driving this variation, and the links between this variation and organismal performance are critical foundation stones of plant functional ecology. We explore trait variation in leaf mass per area, leaf lifespan, and leaf nitrogen content (on either a mass or area basis) as an example of functional traits widely applied in the literature. These leaf traits are central to the leaf economics spectrum, the main between-species axis of leaf trait co-variation defining a continuum between 'fast' leaves with low LMA, short leaf lifespan, high mass-based nitrogen content, and high photosynthetic and metabolic rates; and 'slow' leaves with high LMA, long leaf lifespan, low nitrogen and slow physiological rates (Wright *et al.*, 2004; 2005; Reich, 2014). Here, we examine the magnitude of trait variation within versus between species in a large collection of published and unpublished trait data encompassing 4051 measurements of 1991 plant species from around the globe. Next we assess trait co-variation at multiple taxonomic scales to test

whether trait spectra are universal. We test whether foliar traits show consistent responses to environmental gradients within individual, extensively sampled species.

We find surprisingly high within-species variation in some traits, particularly area-based leaf nitrogen content. We then identify conflicting patterns of between- versus within-species trait variation that challenge the 'scale-free' ubiquity of putative physiological and evolutionary trade-offs invoked to explain global patterns of trait co-variation. We also find that within-species, key foliar traits of the leaf economics spectrum vary weakly across environmental gradients, and do not necessarily respond to the same environmental factors across traits or species.

Methods:

To assess trait variation and covariation at a variety of taxonomic scales, we collected leaf trait data from multiple published and unpublished datasets encompassing 4051 measurements of at least two foliar traits, including measurements from 1991 species, 939 genera, and 214 families. In total, we were able to compile within-species trait variation data for 44 species (mean of 37 trait measurements per species). We focused on three leaf traits: leaf lifespan, leaf mass per area (LMA), and leaf nitrogen content (either on a mass basis - N_{mass}, or an area basis - N_{area}). We principally analyzed $\log_{10}$-transformed traits, due to the roughly log-normal distribution of these traits. However, because raw trait values are also widely used, particularly in vegetation modeling, we also performed a subset of analyses with raw trait values. These three foliar traits were common across all datasets, less dependent on the (typically unreported) measurement conditions than leaf gas exchange traits, and related to common plant parameters in Earth System

models. Moreover, these traits are central to the 'Leaf Economics Spectrum' (Wright *et al.*, 2004) but yet only loosely mechanistically linked in our current understanding (Osnas *et al.*, 2013; Blonder *et al.*, 2015). A brief outline of datasets used follows:

GLOPNET data

This database contains leaf trait data from 175 sites and 2021 plant species from around the world (Wright *et al.*, 2004; 2005). We utilized a subset of the dataset that had either both leaf lifespan and LMA measurements, both leaf lifespan and leaf % Nitrogen measurements, or both LMA and % Nitrogen. We associated the GLOPNET data with taxonomic data using the R package *taxize* to querry both the ITIS and NCBI taxonomic databases. Aliases and misspellings were looked up and corrected by hand, or removed from analyses (total of 48 species).

PNW conifer data

Leaf trait data were also acquired from the TERRA-PNW foliage, productivity and soil database (Berner & Law, 2016), henceforth PNW data, from 239 sites in Oregon and northern California. This database contains foliage traits (leaf lifespan, LMA, C:N ratio, %C and %N) from 35 tree and shrub species, primarily focusing on dominant conifer trees. A total of 16 species had more than 10 trait measurements and were sampled at more than five sites (See Table S1 in Appendix E). All individual trait measurements from these species were included in within-species trait analyses. Trait values were also averaged to species for all 35 species in the dataset and included in genus-level, family-level and global trait analyses with the GLOPNET species.

Foliar traits were measured on one year-old needles from mid-canopy, sun exposed branches from the south side of the canopy of the dominant woody species at each site. Multiple stand characteristics were either measured at the site (soil properties from soil cores, stand surveys, Leaf Area Index measurements, and annual biomass growth) or extracted from gridded data products (elevation, 30 year climate normal). To our knowledge, this is the largest dataset of consistently collected tree leaf traits documenting within-species trait variation to date, and is associated with high quality site and stand metadata. Full methods descriptions can be found in Berner & Law (2016) and Law et al. (2008).

Additional data

Data on geographic variation in leaf traits was also drawn for *Populus tremuloides* from (Anderegg & HilleRisLambers, 2015) (LMA) and for cultivated *Coffea arabica,* from (Martin *et al.*, 2016) (LMA and N_{mass}). Unpublished data on geographic variation in leaf traits in *Quercus gambelii* (LMA) and 2 *Eucalyptus* species (LMA and N_{mass}) collected by LDL Anderegg (unpublished) were also included. These datasets include elevational or landscape-scale trait variation, often with replicate measurements within individual. Leaf lifespan data for *Populus tremuloides* and *Quercus gambelii* were extracted from remotely sensed NDVI phenologies that can distinguish the elevational variation in growing season length. All data that were collected at scales smaller than the individual (i.e. leaf or branch) were averaged to the individual for analysis to be consistent with the above datasets.

Variance Decomposition

We first performed a variance decomposition analysis to determine the dominant taxonomic scales of trait variation. We used linear mixed effects models with only a fixed intercept term and nested random effects for different taxonomic levels. The random effects variance parameters are directly comparable across random effects in a linear model with normally distributed random variance components.

Using all individual measurements from all datasets, we determined within-species, within-genus, within-family and between family variance components of both $\log_{10}$-transformed and raw LMA, leaf lifespan, and N_{mass}. Next, we assessed how trait variation is distributed within a single Plant Functional Type, the well-sampled needle-leaf conifers in the PNW dataset. We included trait measurements from all needle-leaf conifers that were dominant canopy species (made up at least 30% of the basal area in at least one site). Because the PNW dataset contains replicated measurements at a site, we decomposed within-PFT variation in the five foliar traits in the dataset (LMA, leaf lifespan, C/N ratio, % leaf carbon content, and % leaf nitrogen content/N_{mass}) into within-plot, between plots within species, between species and between genus variation.

Trait co-variation

We assessed the strength of the covariance between leaf traits at multiple taxonomic scales by comparing the distributions of correlation coefficients and of standardized major axis (SMA) regression slopes, which account for error in both the x and y variables, within various taxa at increasing taxonomic scales. First, we created a dataset of within-species trait variation including all species in the global dataset used for variance decomposition that had more than five trait records (n = 44 species, 1624 trait measurements). Then, we averaged all data in the

GLOPNET, PNW and other data to the species level, all species-level averages to the genus level, and all genus level-averages to the family level (see Table S2 in Appendix E for total sample sizes for all trait pairs). We fit SMA regressions to the trait data within each species, each genus and each family that had at least five trait measurements (e.g. at least five measurements within a species, five species within a genus, or five genera within a family). We also calculated the trait-trait correlations and SMA regressions as across the family means of all families with at least three species and globally across all species means. We tested for significant differences of SMA slopes and correlation coefficients for within-species comparisons versus higher taxonomic levels using unweighted linear models and t-tests, or models weighted by the within-taxon trait variances or within-taxon sample size. We also created funnel plots (plotting individual SMA slopes and correlation coefficients as a function of the within-taxon variance or sample size) to visually verify that patterns were not driven by differences in sample sizes between taxonomic groups.

Trait-environment relationships

We quantified the effect of site environmental factors on dominant conifer leaf lifespan, LMA and N_{area} for the six well sampled conifer species in the PNW dataset that had nearly complete site soil and LAI data. We fit linear mixed effects models with climate variables (see below), soil nitrogen content, log(stand age), stand Leaf Area Index, and stand annual biomass increment (see Berner & Law, 2016) and Law et al. 2008 for detailed methods of stand about stand characterization), as fixed effects and a stand level intercept random effect. All predictors were mean centered and z-score standardized so that effect sizes are comparable between predictors. We performed model selection on models including all possible variable

combinations using AIC. We report the most parsimonious model for each trait for each species. Because multiple models had similar AICs for many traits and species, we also calculated the variable importance values and model-averaged standardized effects sizes derived from a model ensemble of all models that had a ΔAIC of less than four from the best model. This provides a robust estimation of the relative importance of the stand-level predictors.

Before including climate variables as predictors, we performed a PCA based on the PRISM 30 yr climatologies of mean annual temperature, mean annual precipitation, climate moisture index (potential evapotranspiration – mean annual precipitation), maximum vapor pressure deficit, and the mean soil moisture content of the topmost soil layer and the full soil column from the Variable Infiltration Capacity hydrology model. We used the first two principal components, which explained ~90% of the total variance, as the two climate predictors in the mixed effects models. The first principle component ('climPC1') explained 72% of the total variance and loaded strongly with precipitation, soil moisture, vapor pressure deficit and climate moisture index (Appendix E, Table S3). Thus, we refer to this PC as generally characterizing stand 'wetness'. The second principle component ('climPC2') explained 18% of the total variance and loaded almost entirely with mean annual temperature and slightly with vapor pressure deficit. We refer to 'climPC2' as describing stand 'warmth'.

All analysis was performed in the R statistical environment (R Core Team 2016, version 3.2.4). We fit standard major axis regressions using the 'lmodel2' function from the *lmodel2*. Mixed models were fitted using the *lme4* and *lmerTest* packages in R (Bates et al. 2015, Kuznetsova et al. 2016), and model averaging was performed using the *MuMIn* package in R (Kamil Bartoń 2016).

Results

Variance Decomposition

Analysis of our combined dataset of 4051 measurements of leaf lifespan, LMA, and leaf nitrogen content from 1991 species showed that inter-specific variation is typically larger than intra-specific variation. However, the proportion of intra-specific variation was remarkably high in area-based Nitrogen content (N_{area}), and was more variable in raw traits than $\log_{10}$ transformed traits (Figure 1). Global variation in $\log_{10}$ transformed LMA, leaf lifespan and N_{mass} was generally driven first by variation between families with a decreasing proportion of the total variance deriving from successively lower taxonomic scales (Figure 1a). Between family differences contributed between 38% (LMA) and 48% (N_{mass}) of the global variation in $\log_{10}$ trait variation, while within-species differences contributed between 12% (leaf lifespan) and 15% (N_{mass}). Area-based nitrogen, on the other hand, showed almost the reverse pattern of taxonomic variation, with 27% of total variation falling within-species, and the proportion of variance decreasing at the highest taxonomic scales (30% of variance was within genera, 25% within families and only 19% across families).

The importance of intra-genus and intra-specific variation was much larger for raw, untransformed LMA and leaf lifespan, though our parameter estimates are likely more uncertain for raw traits (see Discussion). The taxonomic distribution of variance was relatively similar for $\log_{10}(N_{mass})$ and N_{mass}, but intra-genus variation made up the majority (54%) of raw LMA variation and intra-specific variation made up the majority (63%) of raw leaf lifespan variation. This discrepancy between log-transformed and raw variance decompositions implies that intra-generic and intra-specific variation increases markedly for genera and species with large LMA and long leaf lifespan. Within-species variation remained the dominant source of N_{area} variation,

with the contrast between N_{mass} and N_{area} becoming even stronger in raw versus log_{10} transformed traits.

Within the evergreen needle-leaf conifer PFT, a PFT that dominates much of the northern hemisphere in many models, within-species variation was large. In the well-sampled PNW dataset we found that intra-specific trait variation (the sum of within-plot and between-plot

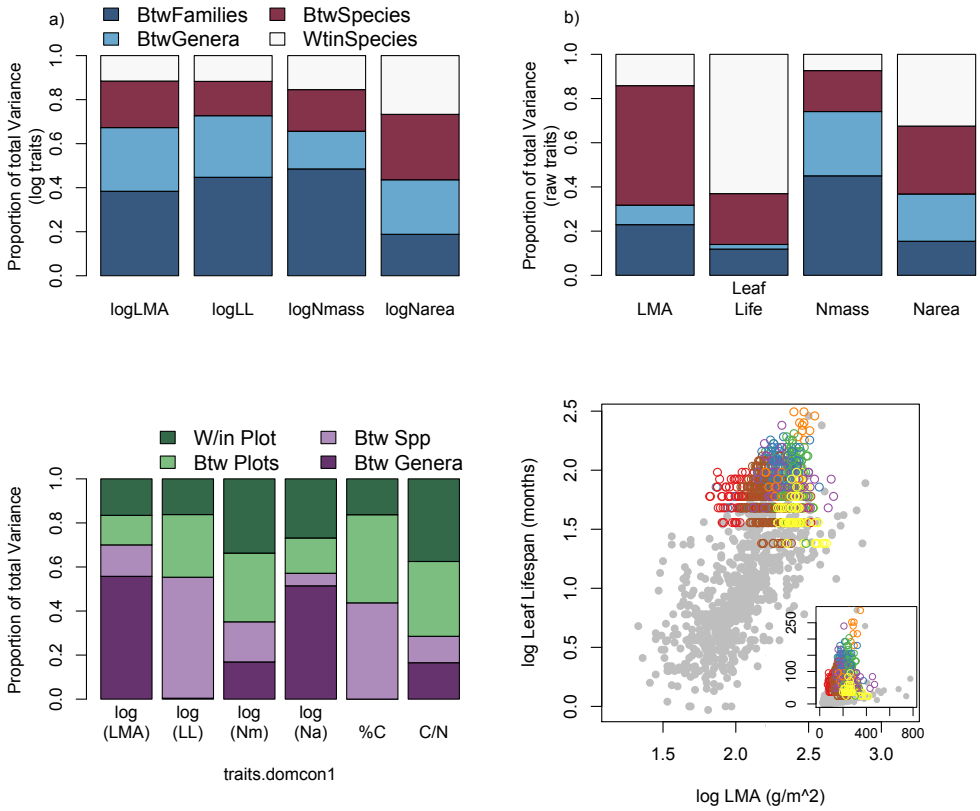

Figure 1: *Variance decomposition of log_{10} (a) and raw (b) Leaf Mass per Area (LMA), leaf lifespan, mass-based nitrogen (Nmass), and area-based nitrogen (Narea) across different taxonomic scales. 'WtinSpecies' : within species variation, 'BtwSpecies': variation between species in a genus, 'BtwGenera': variation between genera in a family, 'BtwFamilies': trait variation between plant families. (c) The variance decomposition of leaf traits in the ' evergreen needle-leaf conifer' Plant Functional Type represented by the PNW dataset, where intra-specific variation is high. (d) The proportion of global log_{10}(leaf lifespan) and log_{10}(LMA) traits space covered by these conifers (PNW species are open colored points, GLOPNET data are in grey, inset shows raw trait values).*

variation) made up 30% $\log_{10}$LMA variation and >40% of log-trait variation in all other traits (Figure 1c). This is particularly pronounced in leaf chemical traits involving nitrogen, traits often used as physiological input parameters in ecosystem models. Within-species variation made up 65% of variation in $\log_{10}$ N_{mass} and over 71% of the variation of (raw) leaf C:N ratio. In fact, variation within an individual plot made up >25% of the intra-PFT variation in $\log_{10}$ N_{mass}, $\log_{10}$ N_{Area}, and C:N ratio. In total, this dominant needle-leafed conifer dataset covers a large fraction of global trait variation in $\log_{10}$(leaf lifespan) and $\log_{10}$(LMA) (Figure 1d) and the majority of global raw leaf lifespan and LMA variation (Figure 1d inset).

Trait covariation

We find that some of the trait relationships central to the leaf economics spectrum consistently scale across taxonomic levels, consistent with a 'scale-free' interpretation of the LES. In particular, the relationship between nitrogen content on a per-mass basis (N_{mass}) is consistently negative with increasing LMA and leaf lifespan (Figure 2, Table 1) at all levels of taxonomic aggregation. The average slopes of the Standardized Major Axis SMA regression between N_{mass} and both LMA and leaf lifespan do not differ statistically across taxonomic levels. This pattern is consistent in both unweighted linear models or linear models weighted by the variance in N_{mass} or LMA/leaf lifespan (Figure 2a,b, Table S4 in Appendix E). The mean within-taxon correlation between N_{mass} and LMA/leaf lifespan does decrease at lower taxonomic groupings (Fig 2a,b, Table S4 in Appendix E), but this is likely an artifact of the restricted within-taxon variation in N_{mass} at lower taxonomic levels (Figure 2c,d). Funnel plots showing the strength of individual correlations plotted against the variance in N_{mass} contained in each comparison indicate that the trait correlations tend to converge on the global between-species

correlation as within-taxon N_{mass} variance increases, regardless of the taxonomic level of aggregation.

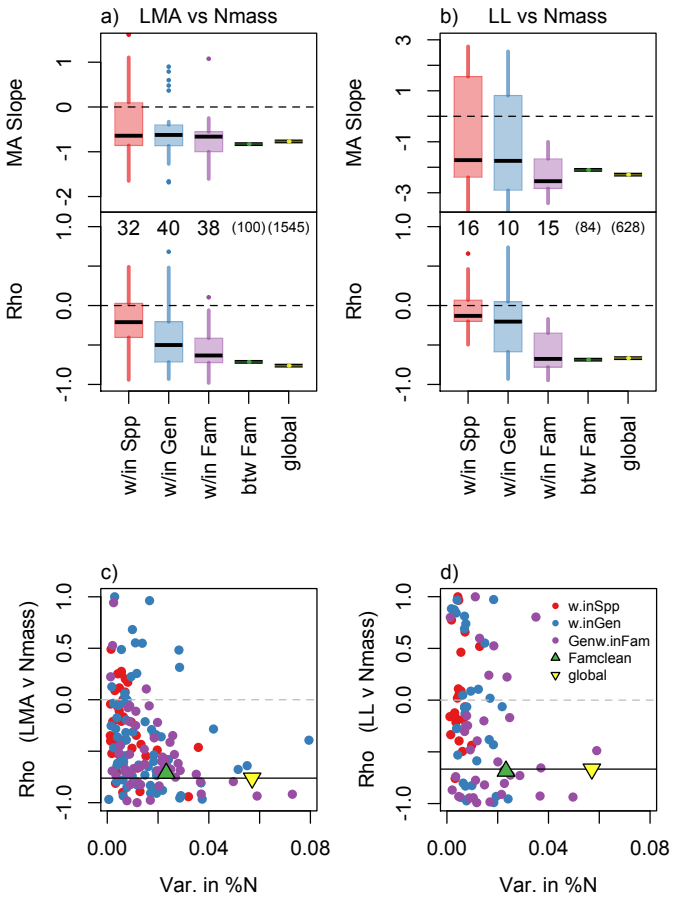

Figure 2: *The average SMA regression slope between log_{10}-transformed N_{mass} and either LMA (a) or leaf lifespan (b) does not differ significantly across taxonomic levels and is roughly similar to the global between species-relationship. The strength of the correlations between N_{mass} and other leaf traits increases significantly with increasing taxonomic scale. However, based on the patterning of correlation coefficients of individual taxonomic comparisons with the variance in N_{mass} encompassed by the comparison, the increasing correlation strength is likely due to the increasing trait variance encompassed by higher taxonomic comparisons (c – correlations between N_{mass} and LMA, d – correlations between N_{mass} and leaf lifespan). The solid line in c and d shows the strength of the global between-species relationship. Numbers in a & b show the number of taxa included in each taxonomic level, parenthetical numbers show total sample size for between-family and global between-species trait relationships.*

The similarities between species level traits and the global LES end there. While the globally strong positive correlation between log_{10}(leaf lifespan) and log_{10}(LMA) manifests within genera, within families and between families, it weakens and even reverses sign within

species (Figure 3, Table 1). The statistically significant difference between inter-and intra-specific leaf lifespan and LMA co-variation is robust across weighting methods (Appendix E, Table S4), and is unlikely to be an artifact of small sample sizes or low trait variances at the within-species level (Appendix E, Figure S2).

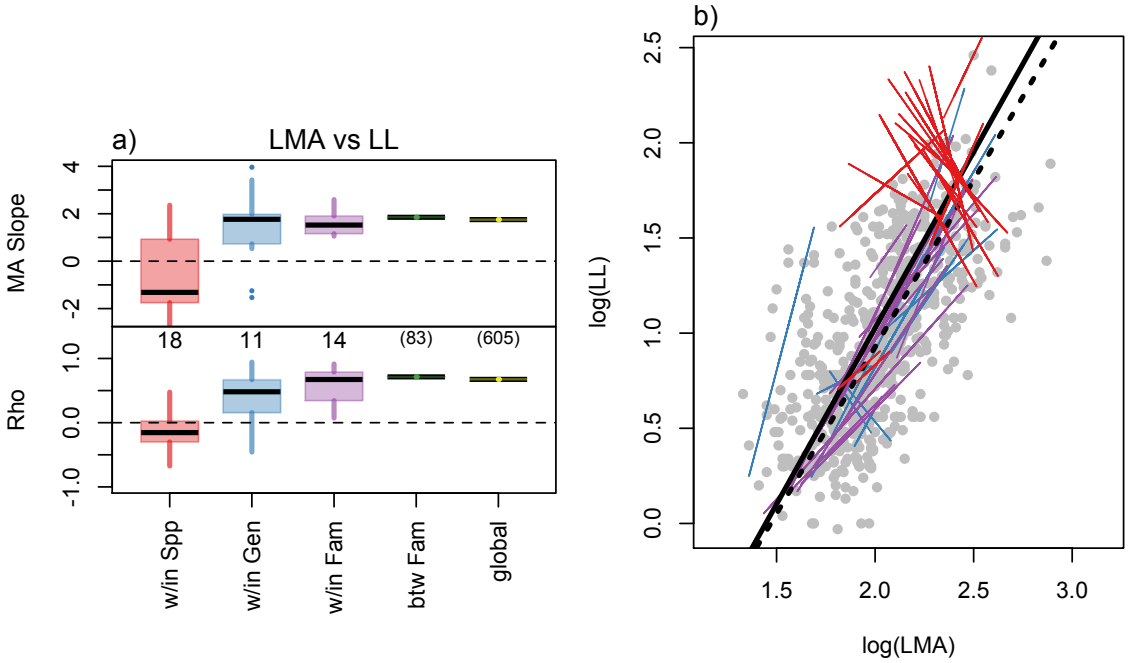

Figure 3: *Species level relationships between log_{10}(Leaf Lifespan) and log_{10}(LMA) are the opposite of those seen in the leaf economics spectrum. (a) across the 18 species with >5 records the mean within-species Standardized Major Axis regression slope and correlation coefficient significantly differ from zero, and from the mean regression slopes/correlations within individual genera, and within families. Numbers indicate the number of individual within-taxon relationships fitted at each taxonomic level (parenthetical numbers show the number of families and species in the between family and global-between species relationships, respectively). (b) Scatterplot of log(LMA) versus log(leaf lifespan) from the global GLOPNET dataset (gray points), with the trait relationships for individual species shown as red lines, individual genera as blue lines, and families as purple lines. The relationship across families is shown in solid black, and the global between-species relationship is shown as a dotted black line.*

In addition, the relationship between log_{10}-transformed nitrogen on an area basis (N_{area}) and log_{10}-transformed LMA is remarkably strong within-species, and becomes weaker at higher taxonomic levels (Figure 4a,b). The Standardized Major Axis (SMA) regression slope within-species is 1.25±0.02 (mean ± SE), but only 0.88±0.08 within genera, 0.86±0.08 across genus

means within families and only 0.65 globally across the entire GLOPNET dataset. SMA slopes differed significantly across taxonomic scale with all but the N_{area} variance-weighted model formulations (Table S4 in Appendix E), and contrasts between within-species SMA slopes and higher taxonomic level slopes were significant in all model formulations. Moreover, the correlation between LMA and N_{area} was similarly strong across all taxonomic levels (Figure 4b), which is striking given the tendency towards weaker correlations at lower taxonomic levels in all other trait relationships. Moreover, because of the reversal of the LMA~leaf lifespan relationship and strong link between LMA and Narea within-species, the globally weak positive relationship between leaf lifespan and N_{area} becomes a reasonably strong negative relationship within species (Figure 4c,d).

Trait-environment Relationships

Contrary to the general assumption, stand climate, nutrient availability, and light environment were neither strong nor consistent predictors if intra-specific trait variation in log(LMA) and log(N_{area}), and only mediocre predictors of log(leaf lifespan) (Figure 5, Table 2). In six well-sampled conifers species in the PNW dataset, the mean marginal R^2 of the best trait-environment model was 0.34 for leaf lifespan, 0.17 for LMA and only 0.12 for N_{area}. Few climate variables had large effect sizes for any species or trait (Figure 5a). Leaf lifespan was the only trait that showed consistent responses to any environmental variable across species, decreasing with increasing 'warmness' (PC2 of the climate PCA), and increasing with stand Leaf Area Index. Moreover, there was little consistency in which environmental variables proved important across species, or across traits (Table 2, Figure 5b). No climate variable was consistently included in the best trait model for all species (Table 2). 'Warmth' (climate PC2) and Leaf Area

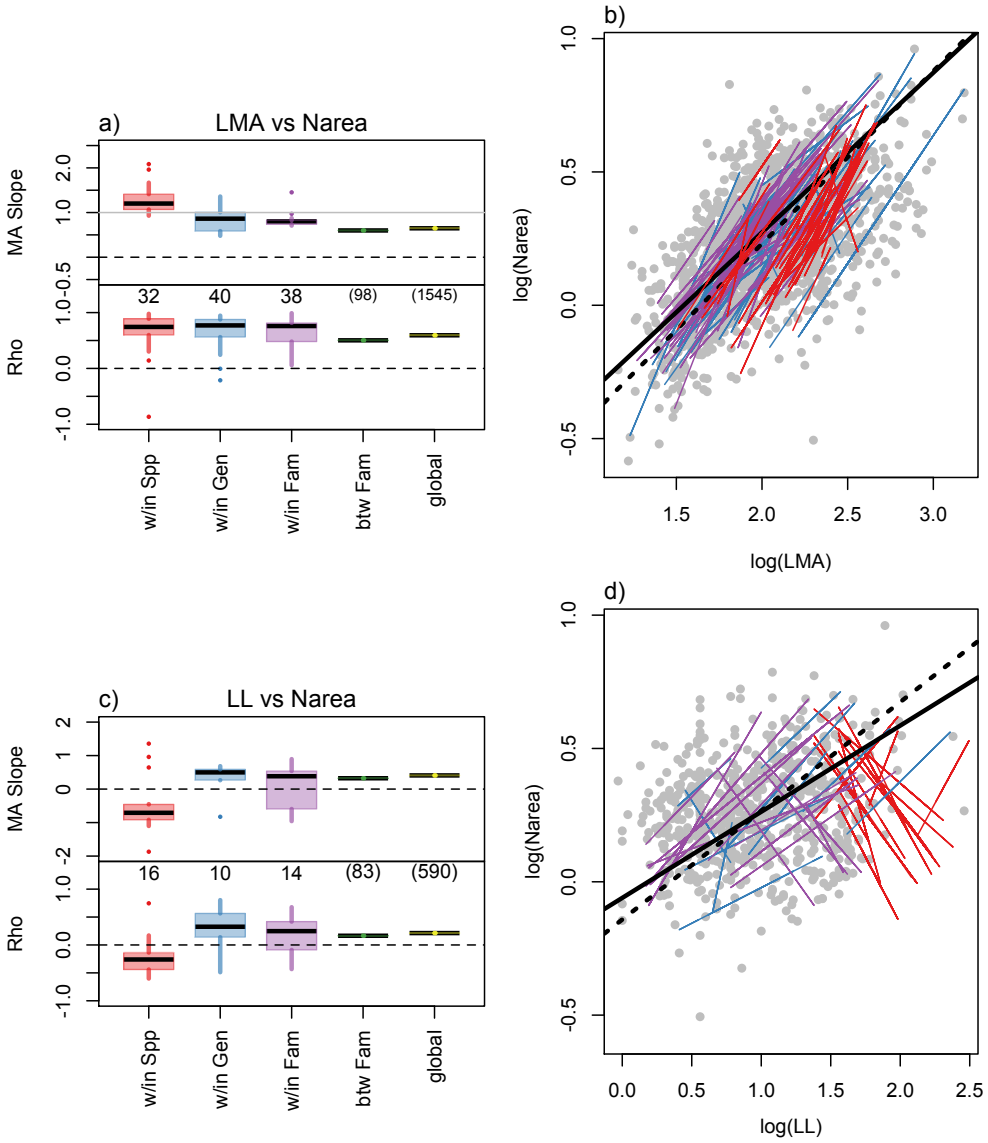

Figure 4: *Log-transformed area-based leaf nitrogen (N_{area}) is strongly positively correlated with log-transformed leaf LMA within species, and shows a stronger scaling slope within-species than at higher levels of taxonomic aggregation. Meanwhile, $\log_{10}$(leaf lifespan) shows a week positive relationship with $\log_{10}(N_{area})$ within higher taxa, but a negative relationship within-species (a, c) Boxplots of the distributions of Standardized Major Axis regression slopes and correlation coefficients fit to individual species, genera, and families, as well as the relationship across all plant families and the global between-species relationship. Numbers indicate the number of individual within-taxon relationships fitted at each taxonomic level (parenthetical numbers show the number of families and species in the between family and global-between species relationships, respectively). Grey line in panel (a) indicates isometric (1:1) scaling. (b) Scatterplot of log(LMA) versus log(Narea) or (d) log(LL) versus log(Narea) from the global GLOPNET dataset (gray points), with the trait relationships for individual species shown as red lines, individual genera as blue lines, and families as purple lines. The relationship across families is shown in solid black, and the global between-species relationship is shown as a dotted black line.*

Index had fairly high average variable importance for leaf lifespan, and 'warmth' had a high average variable importance for LMA (Figure 5b). But most other environmental variables were inconsistently important and did not even have a consistent direction of effect. Results were qualitatively similar for raw trait values and $\log_{10}$ transformed trait values, so only results for $\log_{10}$ transformed variables are shown.

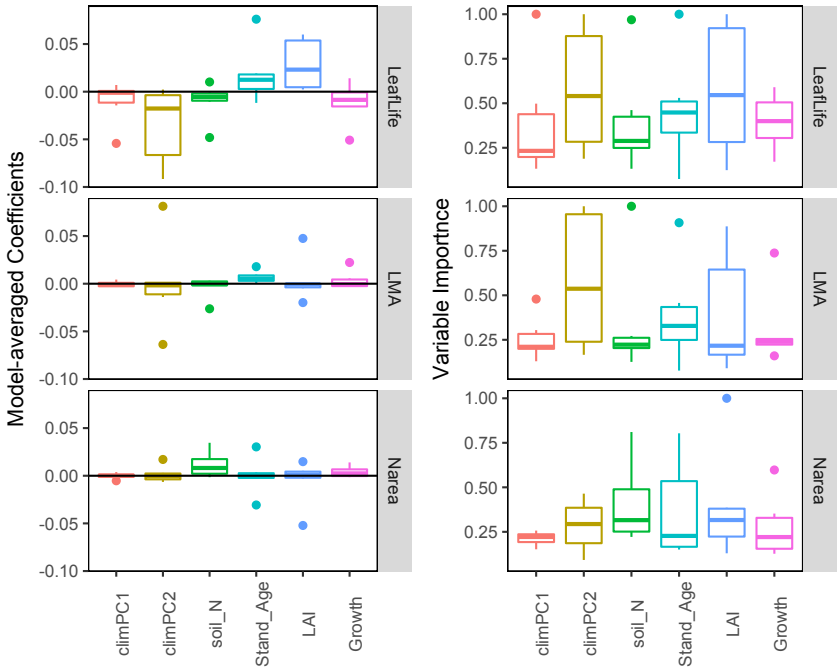

Figure 5: *Site environmental characteristics rarely had large effects on or were consistently useful in explaining foliar trait variation. Distribution of standardized, model-averaged effect sizes (a) and variable importance (b) for six environmental variables from linear mixed effects models relating a leaf traits to site environmental factors for each of six conifer species. Model averaged effect sizes and variable importance were derived from the subset of all model formulations that had a ΔAIC of less than 4 from the best model for each species for each trait. Variable importances show which variables were consistently included in the top models across species (even if they had small effect sizes).*

Discussion

Using an extensive global dataset documenting leaf trait variation with and between species, we tested four critical assumptions in plant functional ecology: 1) that within-species trait variation is small compared to between species variation, 2) that global trait spectrums are scale independent and represent universal physiological and/or evolutionary trade-offs, and 3) that trait variation can be linked to environmental variation.

Small, but variable, intra-specific trait variation

We found that three traits central to the global 'leaf economics spectrum' do generally show more variation between than within species. Log_{10}-transformed LMA, leaf lifespan and N-per-unit-mass (N_{mass}) owed 40+% of their global variation to variation between plant families, and less than 20% of their global variation to intra-specific variation (Figure 1). For N_{mass} and LMA, this variance decomposition held true for raw trait values as well (though within-genus variation became much more important for raw LMA). This may imply that N_{mass} and LMA variation of sun leaves is fairly constrained within species, despite the well-documented large plasticity of LMA (Poorter *et al.*, 2009). However, a fourth trait not originally part of the leaf economics spectrum, nitrogen content on a per-area basis (N_{area}), showed very large within-species variability on both a log_{10} scale and a raw scale. Across species, leaf nitrogen content has been suggested to be primarily distributed on a per-area rather than per-mass basis (Osnas *et al.*, 2013), in which case the small inter-specific variability of N_{mass} may largely be the result of the fairly small intra-specific variation in LMA. Regardless, the consistent and large within-species variation in N_{area} poses a significant challenge to the assumption of larger inter- than intra-specific variation. Leaf lifespan, a trait with extreme leverage over ecosystem function (Reich *et*

al., 2014), showed low intra-specific variation on a log basis, but potentially very high unlogged intra-specific variation. This may partially be a result of the fundamentally log-normal distribution (or perhaps more phenomenalogically gamma distributed) of leaf lifespan, and to a certain extent LMA, that hinders our ability to estimate variance components for raw trait values. However, it also suggests that proportional trait variation tends to be small within species and genera for LMA and leaf lifespan, but by extension the amount of absolute trait variation increases at higher trait values. An annual herb and conifer may both reasonably vary their leaf lifespan by 20%, but this translates into a difference of days for the herb and years for the conifer. But the implication for applications such as ecosystem modeling that rely on raw trait values is important and unappreciated. Greater rigor is needed to understand hierarchical variation in raw trait values.

Focusing in on the evergreen needle-leafed conifer Plant Functional Type, which makes up ~30% of global forest cover (Reich *et al.*, 2014), we found that intra-specific trait variation was a considerable fraction of within-PFT trait variation, and almost 50% of the variation in leaf chemical composition (N_{area}, leaf carbon content, and C:N ratio, Figure 1c). This PFT contains a considerable fraction of global leaf $\log_{10}$-trait variation and an even larger fraction of raw trait variation (Figure 1d) (Wright *et al.*, 2005; Poorter *et al.*, 2009; Anderegg, 2014), a considerable fraction of which can be found within a species or even within an individual population. In fact, a full 30% of the variation in N_{area} is found within individual sites (Figure 1c). This further supports our conclusion that 'trait-based' ecosystem modeling approaches (e.g. Scheiter *et al.*, 2013) require a new, synthetic understanding of foliar nitrogen variation that can scale across environmental gradients ranging from within a canopy to across communities. Due to the relatively low species diversity of the temperate/boreal conifer PFT and the continental range

sizes of many of most dominant conifers, it is possible that within-species variation makes up an abnormally large proportion of this PFT compared to other PFTs. However, we suspect that within-species trait variation may be substantial in other PFTs as well. Because discretization of biological complexity will always be necessary for land surface modeling (meaning PFTs are, in some senses, unavoidable), understanding the underlying functional variation to be discretized is critical for determining where and how we can safely simplify functional complexity. The large fraction if intra-PFT trait variance made up by within-species trait variance that we document here highlights a need for taxonomy-independent theories of trait variation in order to develop more flexible and 'trait-based' PFT concepts for vegetation modeling.

We note that the variance decompositions presented here are likely conservative estimates of intra-specific variation. Branch selection in the PNW dataset was designed to avoid within-canopy leaf variation while approximating the canopy mean foliar traits. Thus, even this extensive dataset is likely a conservative estimate of within-site trait variation in any species. At the global scale, the species with replication in the GLOPNET dataset represent site mean trait values from multiple sites. Thus, they represent only site-to-site variability, and are quite conservative as an indicator of total intra-specific variation.

Scale dependence of the Leaf Economics Spectrum

We found that some axes of trait co-variation that define the leaf economics spectrum are relatively consistent across taxonomic scales, but that the strong link between leaf lifespan and LMA breaks down within species. In general, LMA and leaf lifespan both retain their negative relationships with mass-based Nitrogen content (N_{mass}) at all taxonomic scales. These relationships are hypothesized to represent a physiological trade-off between structural biomass

and photosynthetic biomass (N_{mass} decreases as LMA increases, driving down the mass-based photosynthetic rate at high LMA) and an evolutionary trade-off between photosynthetic rates and leaf lifespans (leaves with low N_{mass} have low photosynthetic rates, and thus require long leaf lifespans to pay back their structural investment costs). The exact mechanisms of the physiological trade-offs that underlie these trait correlations with mass-based nitrogen content and assimilation rate are still under debate (Vasseur *et al.*, 2012; Blonder *et al.*, 2013; Osnas *et al.*, 2013; Sack *et al.*, 2013; Blonder *et al.*, 2014; Sack *et al.*, 2014; Blonder *et al.*, 2015). However, the link between LMA and leaf lifespan is not a physiological trade-off but an evolutionary one, which is independent of normalization (Osnas *et al.*, 2013) and not a result of mass-based physiological rates. Rather, it is the result of a theoretical evolutionary cost to structurally resilient leaves: high LMA leaves are costly to build and tend to have low photosynthetic rates, and therefore require long lifespans to pay off.

It is therefore surprising that we found a breakdown and even reversal of the positive relationship between leaf lifespan and LMA at the scale at which we understand evolution to occur, namely within individuals of a species. We found that, on average, leaf lifespan and LMA were slightly negatively related within individual species (Figure 3, Table 1). This poses a challenge to the evolutionary argument that leaf construction costs increase the 'carbon payoff' period that controls leaf lifespan, as we found no such trade-off at the scale at which evolution occurs (within-species). This also challenges the hypothesis that the strong evolutionary coupling between leaf lifespan and LMA has caused the 'contrariness' of conifers (shade needles have lower LMA than sun needles on the same individual, but shade tolerant conifers have higher LMA than light-demanding conifers, (Lusk *et al.*, 2008).

This negative intra-specific LMA~leaf lifespan trend may be unique to conifers, or unique to evergreen trees. Unfortunately, data on within-species variation in leaf lifespan is extremely limited except for conifers, which have easily counted annual bud scars. Our dataset includes intra-specific leaf lifespan data for only three angiosperms (*Populus tremuloides*, *Quercus gambelii*, and *Quercus chrysolepis*). The evergreen oak *Q. chrysolepis* showed a negative LMA~LL relationship similar to gymnosperms (SMA slope = -1.5, Pearson's r = -0.63), but deciduous *Q. gambelii* and *P. tremuloides* showed slightly positive LMA~LL relationships (SMA slopes of 0.97 and 0.92, Pearson's r of 0.24 and 0.27 respectively). Additionally, an extensive growth chamber experiment with *Arabidpsis thaliana* found a positive relationship between leaf lifespan and LMA across *A. thaliana* lines and mutants (Blonder *et al.*, 2015). However, more data on within-species variation in leaf lifespan is sorely needed. Indeed, given that leaf lifespan was the only trait that reliably correlated to stand environmental variables and was linked with stand relative growth rate in our analysis (see Figure S3 in Appendix E), we advocate for renewed study of leaf lifespan in non-gymnosperms.

At the same time that the link between $\log_{10}$ LMA and $\log_{10}$ leaf lifespan weakens within species, we found an increasingly tight link between $\log_{10}$ LMA and log area-based nitrogen content N_{area} (Figure 4). At a global scale, LMA and N_{area} are more weakly linked than LMA and mass-based nitrogen content (correlation 0.58 for N_{area} and -0.75 for N_{mass}, (Wright *et al.*, 2004), similar in our expanded dataset, Table 1). However, taxonomic analysis revealed an increasingly strong scaling between $\log_{10}$ LMA and $\log_{10}$ N_{area} within lower taxonomic groupings. The slope of log-log relationships, or 'scaling exponents', indicate the proportionality of pairwise trait relationships. Within-species, we found that the scaling factor between N_{area} and LMA was slightly greater than one (1.17±0.01), meaning LMA and N_{area} scaled allometrically rather than

'isometrically' (i.e. in direct proportion to one another). In other words a 10% increase in LMA yields roughly a 12% increase in N_{area} (i.e. raw N_{area} scales with $LMA^{1.18}$). However this allometric scaling falls below one rapidly at all higher taxonomic levels. The mean scaling slope across species means within genera is 0.85 (a 10% increase in LMA results in an 8.5% increase in N_{area}), and globally across all species mean trait values log N_{area} scales with log LMA with a SMA slope of 0.65. This implies that, within-species, increasing LMA requires devoting a progressively larger fraction of total leaf nitrogen to leaf structure. However, between species the scaling slope of less than 1 implies that increasing LMA can be achieved while shifting allocation away from structural sources and maintaining nitrogen in photosynthetic and cytosolic pools.

This intra-specific shift of the LMA-N_{area} scaling relationship could be the results of two processes: either an evolutionary constraint or a physiological/anatomical constraint. First, the pattern could result from an evolutionary constraint, with LMA proving a relatively canalized trait while N_{area} is much more evolutionary labile and/or plastic within a species. If this were true, we would expect to see strong phylogenetic signal in LMA across clades, and relatively weak phylogenetic signal in N_{area} (Crisp & Cook, 2012). The large proportion of global N_{area} variation and N_{area} variation in needle-leafed conifers that falls within species would also support the evolutionary constraint interpretation (Figure 1). However, this explanation seems unlikely because 1) LMA is known to be an extremely plastic trait even within the canopy of a single individual depending on light environment (Poorter *et al.*, 2009), 2) the strong correlation between LMA and N_{area} would still require a physiological constraint linking LMA and nitrogen content in order to so consistently manifest within-species as well as across species, genera and families.

The second possibility is that N_{area} variation within species is strongly constrained by leaf cellular anatomy, such that the anatomical shifts that lead to increased LMA are mechanistically linked to increasing leaf nitrogen per unit leaf area. A recent extensive synthesis of the physiological and structural trade-offs that underpin the leaf economics spectrum found that the mass of cell walls per unit leaf area increases extremely strongly with LMA, with a scaling slope of 1.37 (Onoda *et al.*, 2017). Because neither the nitrogen content of cell walls nor the mass of nitrogen allocated to rubisco are related to LMA, this results in a strong increase in the amount of nitrogen in cell walls per unit leaf area with increasing LMA and a concomitant increase in the proportion of total N_{area} that is found in cell walls (rather than photosynthetic machinery) at higher LMA (Onoda *et al.*, 2017). In light of these global patterns, strong scaling of N_{area} with LMA within species is likely the result of a fixed nitrogen composition of cell walls (or perhaps bulk leaf structural tissue) and anatomically constrained mechanisms for increasing LMA within species. This is consistent with a strong intra-specific link between LMA and N_{area} and a relatively weak link between LMA and N_{mass}. If nitrogen allocation between phostosynthetic and cytosolic pools is fairly plastic within species but the nitrogen content of cell walls is relatively fixed, then the relationship between LMA and N_{mass} would be expected to be more variable than the LMA~N_{area} relationship, particularly if N allocation to photosynthetic and cytosolic pools is governed by different environmental cues than LMA. This aligns well observations of considerable reallocation of photosynthetic nitrogen (except for nitrogen in chlorophyll) even over the lifespan of individual leaves/needles, as foliage produced in high light becomes shaded (Brooks *et al.*, 1994; 1996).

Using the terminology Osnas et al. (2013), it appears that nitrogen is distributed strongly 'mass proportional' within-species, but is largely 'area proportional' between species. In light of

this, the negative within-species relationship between $\log_{10} N_{area}$ and $\log_{10}$ leaf lifespan (Figure 4,d) is principally driven by nitrogen's strong relationship with LMA and LMA's negative relationship with leaf lifespan. We suspect that this shift from area- to mass-proportionality is the result of constraints on the within-species variation in the leaf cellular anatomy. We hypothesize that many aspects of leaf cellular anatomy vary considerably more between than within species, leading to an anatomic constraint on nitrogen allocation within species that switches to biochemical or transport constraint on metabolic and photosynthetic rates at higher taxonomic levels and larger scales of anatomical variation. More research is needed on within-species variation in assimilation and respiration rates in relation to leaf mass, leaf area, and critically leaf anatomy and leaf rubisco content (e.g. within-species extensions of Onoda *et al.*, 2017 and Poorter *et al.*, 2013) to elucidate the mechanisms behind the LMA, leaf lifespan and nitrogen patterns documented here.

Weak trait-environment relationships even within species

Our findings of relatively weak relationships between environmental variables and foliar traits challenge some fundamental assumptions about the functionality of leaf economics spectrum traits. According to the definition of functional trait forwarded by (Violle *et al.*, 2007), a functional trait is a morphological, physiological or phenological trait that influences some aspect of plant performance/fitness (i.e. growth, reproduction or survival) and that displays different values (either within or between species) across environmental gradients. By this definition, we found limited 'functionality' of leaf lifespan, LMA and N_{area} within species, because they neither relate strongly to easily measured stand-level environmental variables. We found that leaf lifespan was the most sensitive to environmental variables, with site climate, soil

and competition-related metrics explaining up to half the total variation in leaf lifespan in some species (Table 2).

Consistent with previous studies of conifer needle longevity, we found that temperature (PC2 of our climate PCA) was generally negatively related to leaf lifespan, though its effect was considerably less ubiquitous than in the boreal-focused literature (Figure 5, Table 2 versus Reich *et al.*, 2014). We also found that leaf lifespan tended to increase with stand leaf area index, which is consistent with observed patterns of leaf longevity in sun exposed versus shaded plants (Vincent, 2005). However, leaf lifespan was only slightly negatively related to stand biomass growth rate, which we hypothesized would be a good proxy for rate of self shading which should decrease leaf lifespan. This suggests that spatial variation in leaf lifespan within-species may partially result from the higher probability of sampling partially shaded branches in stands with higher LAI (Berner & Law, 2016).

LMA and N_{area}, on the other hand, were quite weakly related to stand-level environmental variables. LMA was slightly negatively related to temperature for most species (Figure 5), similar to previously report LMA patterns in the evergreen *Quercus ilex* (Niinemets, 2014). However, the effects of all other environmental variables were both weak and somewhat inconsistent across species. Ultimately, environmental variables explained at most 38% of total LMA variation within a species (mean marginal $R^2 = .16$) and the null model was the most parsimonious model for two of the six species. LMA is very plastic trait that has been found to vary consistently across environmental gradients in some species (e.g. Anderegg & HilleRisLambers, 2015, Niinemets, 2014, Vilà-Cabrera *et al.*, 2015) and experimentally responds strongly to light and temperature gradients and somewhat to water stress and nutrient availability (Poorter *et al.*, 2009). However, at least in these needle leaf conifers, LMA was fairly insensitive

to environmental variation even across the large geographic scales covered by the PNW dataset. N_{area} was even less well explained by environmental variables than LMA, which is consistent with the few other studies that have explore intra-specific N_{area} variation across environmental gradients (Auger & Shipley, 2012; Vilà-Cabrera *et al.*, 2015).

There may be at least two reasons for these weak trait-environment relationships. First, very local conditions (microclimate of the site, within-canopy variation in light availability) may be more important for some traits than larger scale environmental predictors at the stand scale. This seems particularly likely, given that within-stand variability actually exceeds between stand trait variability in LMA and N_{area} (Figure 1c). Even with a consistent branch selection protocol over the entire PNW dataset, variation in N_{area} between replicate samples in a plot was twice as large as variation between plots (30% of total variance within plots versus 15% between). Similar levels of large within-plot variation have been found in other systems as well, including Australian eucalypts (LDL Anderegg, unpublished data), deciduous aspen trees (Anderegg & HilleRisLambers, 2015), French alpine perennials (Albert *et al.*, 2010a), and cultivated coffee (Martin *et al.*, 2016). It is clear from studies of sub-canopy heterogeneity that leaves adjust their morphology and physiology to their hyperlocal environement (Field, 1988; Williams *et al.*, 1989), so a large fraction of intra-specific trait variation can be expected *a priori* to be unexplainable from site environment.

Second, LMA and N_{area} are compound traits that result from multiple anatomical and physiological leaf attributes that respond to environmental gradients in complicated and sometimes compensating ways. For instance, LMA is the emergent result of leaf thickness, leaf density, cell size, and a host of leaf anatomical characteristics (Poorter *et al.*, 2009). Each of these characteristics may vary semi-orthogonally in response to temperature, water or light

limitation (Baird et al. *in press*). Meanwhile, N_{area} is the result of nitrogen availability mediated by multiple allocation decisions, between structural tissue, cytosolic demands and photosynthetic machinery (Onoda *et al.*, 2017). The result is that both traits do not necessarily show clean and unambiguous responses to different environmental stresses. As such, it is perhaps unsurprising that LMA and N_{area} are difficult to predict, even within species. It is, however, rather striking that the average within-species explanatory power found in this analysis is roughly similar to the weak trait-environment relationships that a recent global analysis found between species across multiple biomes (Maire *et al.*, 2015). Indeed, the composite nature of LMA is likely also responsible at least in part for the unexpected reversal of the LMA~leaf lifespan relationship within species. LMA increases to boost leaf physical resilience to mechanical stress have been hypothesized to mechanistically link LMA and leaf lifespan (Wright *et al.*, 2004; 2005; Lusk *et al.*, 2008; Reich *et al.*, 2014). But our results indicate that these alterations cannot be the main driver of LMA variation within species.

The above weak trait-environment relationships indicate that the 'functionality' of LMA and leaf nitrogen content is somewhat fraught. These traits may capture important aspects of a plant's foliar strategy, but their relative unresponsiveness to environmental gradients either between or within species makes them at best an imperfect characterization of some niche axis for community ecological purposes. While we lack data on individual performance (e.g. growth, reproduction, survival) with which to test the importance of these traits for organismal fitness, stand level trait averages were poo0r predictors of stand average growth in single species stands in the PNW dataset (see Figure S3 in Appendix E). Foliar traits were poorly predicted from stand environment, but also poor predictors of tree performance. Using two different formulations of stand growth rate, we found that stand mean log LMA and log N_{area} of mono-dominant stands

were unrelated to growth, while leaf lifespan was significantly related to one growth metric and only marginally related a second. This stand level analysis no doubt loses considerable power through its aggregation to the stand level, and additional research is needed on the fitness consequences of these leaf foliar traits. But their weak responses to environmental gradients and non-existent relationships with performance in long-lived woody organisms may limit their functionality in the evolutionary sense.

Conclusion

We found that (1) within-species trait variation is often but not universally small compared to between species variation, except for area-based nitrogen content (2) some critical trait relationship underpinning the leaf economic spectrum change with taxonomic scale, and (3) trait variation within-species is only weakly linked to environmental variation. These results highlight the need for additional study of within-species trait variation, particularly with respect to leaf nitrogen content, and for modeling the boreal conifer cover type where intra-specific variation represents a large fraction of total trait variation. Our results also challenge the strong evolutionary trade-off between leaf lifespan and leaf mass per area, as this trade-off does not manifest at the within-species scale at which evolution occurs. We also find a strong link between LMA and area-based nitrogen within species that has been overlooked due to their weaker global relationship. This link presents exciting avenues for further illuminating fundamental physiological links between structure and function that are hidden at higher taxonomic scales. Finally, our findings that, in conifers, LMA and leaf nitrogen content are less 'functional' than leaf lifespan emphasize the need for renewed study of leaf lifespan as a global functional trait, particularly in angiosperms where it is difficult to quantify.

	Within Species		Global	
Correlation	LMA	LL	LMA	LL
LL	-0.15±0.02	-	0.67	-
Nmass	-0.2±0.01	-0.06±0.02	-0.76	-0.67
Narea	0.67±0.01	-0.21±0.02	0.59	0.21

SMA Slope	LMA	LL	LMA	LL
LL	-0.85±0.1	-	1.75	-
Nmass	-0.37±0.03	-0.8±0.14	-0.77	-2.29
Narea	1.17±0.02	-0.51±0.05	0.65	0.41

Table 1: Mean within-species trait correlations and SMA slopes versus global between-species relationships.

LEAF LIFESPAN										
Species	mean log(LL)	PC1	PC2	soil N	log (Stand Age)	LAI	Biomass Growth	Marg R2	Cond R2	n
Pseudotsuga menziesii	1.77	-0.053			0.078	0.032		0.48	0.79	221
Pinus ponderosa	1.74		-0.040	-0.024			0.027	0.19	0.36	97
Pinus contorta	1.96		-0.082			0.100	-0.089	0.52	0.60	34
Pinus jeffreyii	1.86		-0.092					0.36	0.54	45
Abies concolor	2.00					0.061		0.22	0.64	88
Tsuga heterophylla	1.79			-0.050	0.027			0.26	0.32	60
LMA										
Species	mean log (LMA)	PC1	PC2	soil N	log (Stand Age)	LAI	Biomass Growth	Marg R2	Cond R2	n
Pseudotsuga menziesii	2.22		-0.017	-0.027	0.015	-0.031	0.034	0.15	0.34	220
Pinus ponderosa	2.38				0.021			0.14	0.36	135
Pinus contorta	2.39							0.00	0.00	34
Pinus jeffreyii	2.37		0.091			0.056		0.33	0.33	45
Abies concolor	2.32							0.00	0.48	88
Tsuga heterophylla	2.05		-0.068					0.38	0.58	60
Narea										
Species	mean log (N_{area})	PC1	PC2	soil N	log(Stand Age)	LAI	Biomass Growth	Marg R2	Cond R2	n
Pseudotsuga menziesii	0.25							0.00	0.19	220
Pinus ponderosa	0.45		-0.015					0.03	0.25	135
Pinus contorta	0.41			0.035				0.11	0.11	34
Pinus jeffreyii	0.36			0.040	0.052			0.21	0.21	45
Abies concolor	0.25						0.022	0.06	0.35	88
Tsuga heterophylla	0.07			0.039	-0.036	-0.052		0.31	0.50	60

Table 2: Best linear mixed effects models relating geographic variation in foliar traits to site environmental factors for six conifer species. All predictors are z-score standardized to facilitate comparisons across environmental factors. 'Mean' column indicates the intercept term (with all predictors mean centered). 'PC1' is the first principle component of a climate PCA, generally representing site wetness. 'PC2' is the second climate principle component, generally representing site warmth. 'Soil N' was measured from multiple soil cores per plot (see (Berner & Law, 2016), while stand age, Leaf Area Index (LAI), and biomass growth were assessed with stand surveys and tree cores. 'Marg R2' indicates the marginal R^2 of the best model (i.e. the R^2 of only the fixed portion of the model), while the conditional R^2 ('Cond R2') indicates the R^2 of both the fixed and random portions of the model.

Works cited

Adler PB, Salguero-Gómez R, Compagnoni A, Hsu JS, Ray-Mukherjee J, Mbeau-Ache C, Franco M (2014) Functional traits explain variation in plant life history strategies. *Proceedings of the National Academy of Sciences of the United States of America*, **111**, 740–745.

Albert CH, Thuiller W, Yoccoz NG, Douzet R, Aubert S, Lavorel S (2010a) A multi-trait approach reveals the structure and the relative importance of intra- vs. interspecific variability in plant traits. *Functional Ecology*, **24**, 1192–1201.

Albert CH, Thuiller W, Yoccoz NG, Soudant A, Boucher F, Saccone P, Lavorel S (2010b) Intraspecific functional variability: extent, structure and sources of variation. *Journal of Ecology*, **98**, 604–613.

Anderegg LD, HilleRisLambers J (2015) Drought stress limits the geographic ranges of two tree species via different physiological mechanisms. *Global Change Biology*, **22**, 1029–1045.

Anderegg WRL (2014) Spatial and temporal variation in plant hydraulic traits and their relevance for climate change impacts on vegetation. *New Phytologist*, **205**, 1008–1014.

Auger S, Shipley B (2012) Inter-specific and intra-specific trait variation along short environmental gradients in an old-growth temperate forest (ed de Bello F). *Journal of Vegetation Science*, **24**, 419–428.

Bates D, Maechler M, Bolker B, Walker S (2015). Fitting Linear Mixed-Effects Models Using lme4. *Journal of Statistical Software*, 67(1), 1-48. doi:10.18637/jss.v067.i01.

Bartoń K (2016). MuMIn: Multi-Model Inference. R package version 1.15.6. https://CRAN.R-project.org/package=MuMIn

Berner LT, Law BE (2016) Plant traits, productivity, biomass and soil properties from forest sites in the Pacific Northwest, 1999–2014. *Scientific Data*, **3**, 160002.

Blonder B, Vasseur F, Violle C, Shipley B, Enquist BJ, Vile D (2015) Testing models for the leaf economics spectrum with leaf and whole-plant traits in Arabidopsis thaliana. *AoB PLANTS*, **7**.

Blonder B, Violle C, Enquist BJ (2013) Assessing the causes and scales of the leaf economics spectrum using venation networks in Populus tremuloides (ed Cornelissen H). *Journal of Ecology*, **101**, 981–989.

Blonder B, Violle C, Bentley LP, Enquist BJ (2014) Inclusion of vein traits improves predictive power for the leaf economic spectrum: a response to Sack et al. (2013). *Journal of Experimental Botany*, **65**, 5109–5114.

Bonan GB, Oleson KW, Fisher RA, Lasslop G, Reichstein M (2012) Reconciling leaf physiological traits and canopy flux data: Use of the TRY and FLUXNET databases in the Community Land Model version 4. *Journal of Geophysical Research*, **117**, n/a–n/a.

Brooks JR, Hinckley TM, Sprugel DG (1994) Acclimation responses of mature Abies amabilis sun foliage to shading. *Oecologia*, **100**, 316–324.

Brooks JR, Sprugel DG, Hinckley TM (1996) The effects of light acclimation during and after foliage expansion on photosynthesis ofAbies amabilis foliage within the canopy. *Oecologia*, **107**, 21–32.

Buckley LB, Kingsolver JG (2012) Functional and Phylogenetic Approaches to Forecasting Species' Responses to Climate Change. *Annu Rev Ecol Evol Syst*, **43**, 205–226.

Clark JS (2010) Individuals and the variation needed for high species diversity in forest trees. *Science*, **327**, 1129–1132.

Crisp MD, Cook LG (2012) Phylogenetic niche conservatism: what are the underlying

evolutionary and ecological causes? - Crisp - 2012 - New Phytologist - Wiley Online Library. *New Phytologist*, **196**, 681–694.
Falster D, COOMES DA, Hui F et al. (2015) Plant functional traits have globally consistent effects on competition. *Nature*, 1–15.
Field CB (1988) On the role of photosynthetic responses in constraining the habitat distribution of rainforest plants. *Functional Plant Biology*.
Jung V, Violle C, Mondy C, Hoffmann L, Muller S (2010) Intraspecific variability and trait-based community assembly. *Journal of Ecology*, **98**, 1134–1140.
Kraft NJB, Godoy O, Levine JM (2015) Plant functional traits and the multidimensional nature of species coexistence. *Proceedings of the National Academy of Sciences of the United States of America*, **112**, 797–802.
Kraft NJB, Metz MR, Condit RS, Chave J (2010) The relationship between wood density and mortality in a global tropical forest data set. *New Phytologist*, **188**, 1124–1136.
Kuznetsova A, Brockhoff PB, Bojesen Christensen RH (2016). lmerTest: Tests in Linear Mixed Effects Models. R package version 2.0-30. https://CRAN.R-project.org/package=lmerTest
Lusk CH, Reich PB, Montgomery RA, Ackerly DD, Cavender-Bares J (2008) Why are evergreen leaves so contrary about shade? *Trends in Ecology & Evolution*, **23**, 299–303.
Maherali H, Pockman WT, Jackson RB (2004) Adaptive variation in the vulnerability of plants to xylem cavitation. *Ecology*, **85**, 2184–2199.
Maire V, Wright IJ, Prentice IC et al. (2015) Global effects of soil and climate on leaf photosynthetic traits and rates. *Global ecology and biogeography*, **24**, n/a–n/a.
Martin AR, Rapidel B, Roupsard O, Van den Meersche K, de Melo Virginio Filho E, Barrios M, Isaac ME (2016) Intraspecific trait variation across multiple scales: the leaf economics spectrum in coffee (ed Barton K). *Functional Ecology*.
Niinemets U (2014) Is there a species spectrum within the world-wide leaf economics spectrum? Major variations in leaf functional traits in the Mediterranean sclerophyll Quercus ilex. *New Phytologist*, **205**, 79–96.
Onoda Y, Wright IJ, Evans JR et al. (2017) Physiological and structural tradeoffs underlying the leaf economics spectrum. *New Phytologist*, **113**, 4098.
Osnas JLD, Lichstein JW, Reich PB, Pacala SW (2013) Global Leaf Trait Relationships: Mass, Area, and the Leaf Economics Spectrum. *Science*, **340**, 741–744.
Paine CET, Amissah L, Auge H et al. (2015) Globally, functional traits are weak predictors of juvenile tree growth, and we do not know why (ed Gibson D). *Journal of Ecology*, n/a–n/a.
Pavlick R, Drewry DT, Bohn K, Reu B, Kleidon A (2013) The Jena Diversity-Dynamic Global Vegetation Model (JeDi-DGVM): a diverse approach to representing terrestrial biogeography and biogeochemistry based on plant functional trade-offs. *Biogeosciences*, **10**, 4137–4177.
Poorter H, Lambers H, Evans JR (2013) Trait correlation networks: a whole-plant perspective on the recently criticized leaf economic spectrum. *New Phytologist*.
Poorter H, Niinemets U, Poorter L, Wright IJ, Villar R (2009) Causes and consequences of variation in leaf mass per area (LMA): a meta-analysis. *New Phytologist*, **182**, 565–588.
R Core Team (2016). R: A language and environment for statistical computing. R Foundation for Statistical Computing, Vienna, Austria. URL https://www.R-project.org/.
Reich PB (2014) The world‐wide "fast–slow"plant economics spectrum: a traits manifesto. *Journal of Ecology*.
Reich PB, Rich RL, Lu X, Wang YP, Oleksyn J (2014) Biogeographic variation in evergreen

conifer needle longevity and impacts on boreal forest carbon cycle projections. *Proceedings of the National Academy of Sciences of the United States of America*, **111**, 13703–13708.
Sack L, Scoffoni C, John GP, Poorter H, Mason CM, Mendez-Alonzo R, Donovan LA (2013) How do leaf veins influence the worldwide leaf economic spectrum? Review and synthesis. *Journal of Experimental Botany*, **64**, 4053–4080.
Sack L, Scoffoni C, John GP, Poorter H, Mason CM, Mendez-Alonzo R, Donovan LA (2014) Leaf mass per area is independent of vein length per area: avoiding pitfalls when modelling phenotypic integration (reply to Blonder et al. 2014). *Journal of Experimental Botany*, **65**, 5115–5123.
Scheiter S, Langan L, Higgins SI (2013) Next-generation dynamic global vegetation models: learning from community ecology. *New Phytologist*, **198**, 957–969.
Shipley B, Bello F, Cornelissen JHC, Laliberté E, Laughlin DC, Reich PB (2016) Reinforcing loose foundation stones in trait‐based plant ecology. *Oecologia*, **180**, 923–931.
Siefert A, Violle C, Chalmandrier L et al. (2015) A global meta-analysis of the relative extent of intraspecific trait variation in plant communities (ed Chase J). *Ecology letters*, **18**, 1406–1419.
Skelton RP, West AG, Dawson TE (2015) Predicting plant vulnerability to drought in biodiverse regions using functional traits. *Proceedings of the National Academy of Sciences of the United States of America*, 201503376.
Vasseur F, Violle C, Enquist BJ, Granier C, Vile D (2012) A common genetic basis to the origin of the leaf economics spectrum and metabolic scaling allometry (ed Maherali H). *Ecology letters*, **15**, 1149–1157.
Vilà-Cabrera A, Martinez-Vilalta J, Retana J (2015) Functional trait variation along environmental gradients in temperate and Mediterranean trees. *Global ecology and biogeography*, **24**, 1377–1389.
Vincent G (2005) Leaf Life Span Plasticity in Tropical Seedlings Grown under Contrasting Light Regimes. *Annals of botany*, **97**, 245–255.
Violle C, Enquist BJ, McGill BJ et al. (2012) The return of the variance: intraspecific variability in community ecology. *Trends in Ecology & Evolution*, **27**, 244–252.
Violle C, Navas M-L, Vile D, Kazakou E, Fortunel C, Hummel I, Garnier E (2007) Let the concept of trait be functional! *Oikos*, **116**, 882–892.
Williams K, Field CB, Mooney HA (1989) Relationships among leaf construction cost, leaf longevity, and light environment in rain-forest plants of the genus Piper. *The American Naturalist*.
Wood, S.N. (2011) Fast stable restricted maximum likelihood and marginal likelihood estimation of semiparametric generalized linear models. *Journal of the Royal Statistical* Society (B) 73(1):3-36
Wright IJ, Reich PB, Cornelissen JHC et al. (2005) Assessing the generality of global leaf trait relationships. *New Phytologist*, **166**, 485–496.
Wright IJ, Reich PB, Westoby M et al. (2004) The worldwide leaf economics spectrum. *Nature*, **428**, 821–827.

Chapter 4: Supplemental Materials for Chapters 1-3

Appendix A: Supplemental Data and Analysis, climate/competition tradeoffs
Supplemental Material for Chapter 1

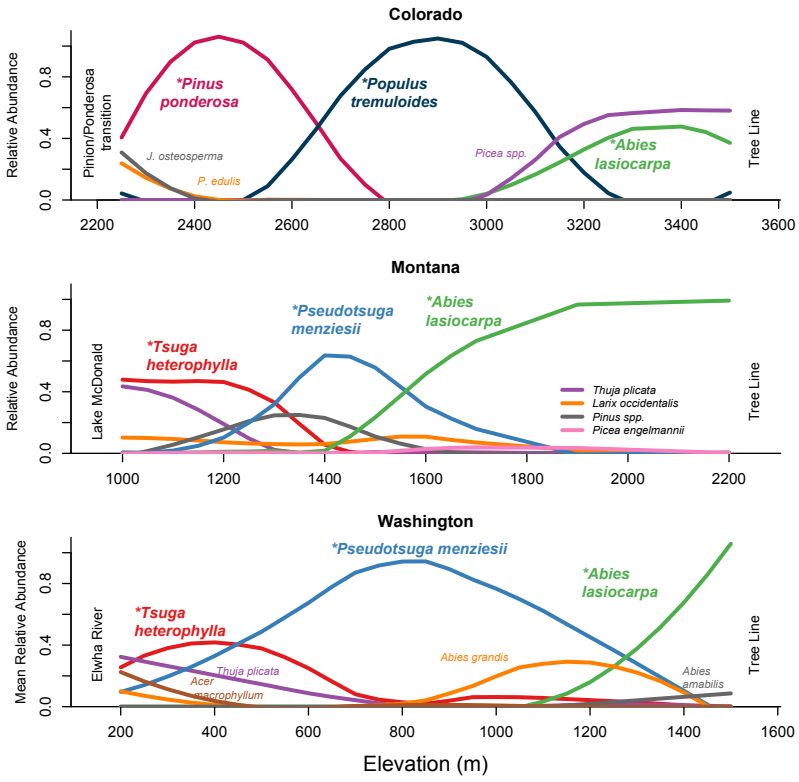

Figure S1: Relative abundance of canopy tree species across ~1000m elevation gradients on the three study mountains: Shark's Tooth in San Jaun National Forest, Colorado (top), Mt. Brown in Glacier National Park, Montana (middle), and Hurricane Ridge in the Olympic National Park, Washington (bottom). Relative abundance was assessed via three to six 5x50m strip transects approximately every 50m of elevation gain. Sampled species are denoted with an asterisk (*). All transects ended at high elevation tree line.

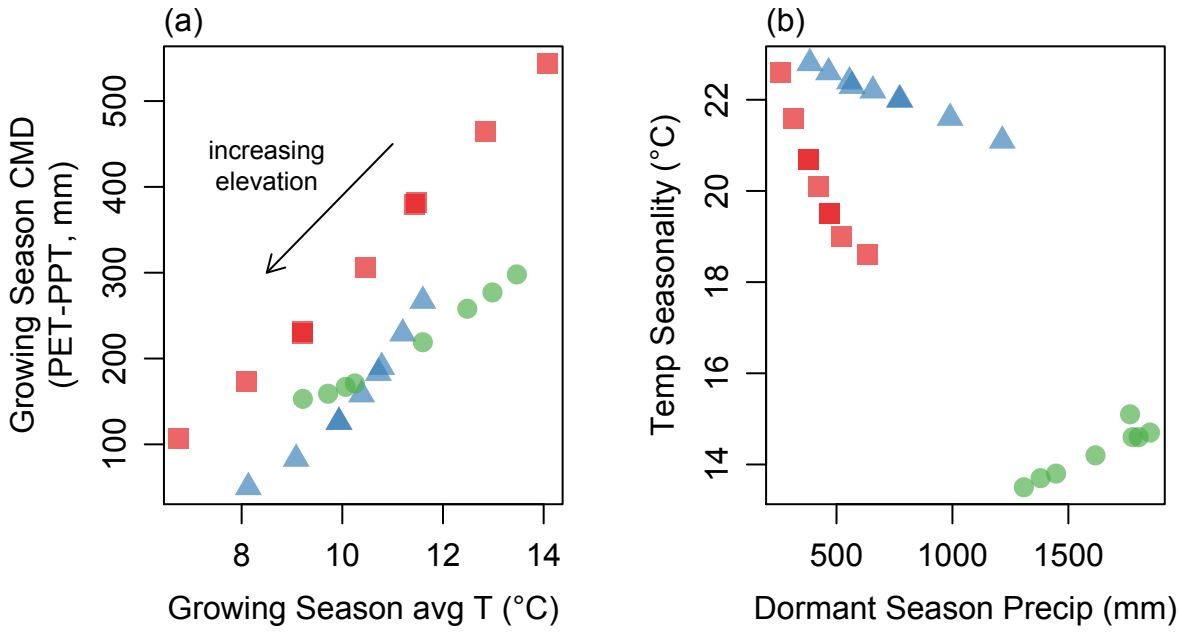

Figure S2: (a) Growing season (May-Oct) average T and average grown season (May-Oct) Climate Moisture Deficit (CMD = potential evapotranspiration – precipitation) of the transect – summer temperature and water stress decrease with elevation on all three mountains. (b) Dormant season (Nov-Apr) precipitation and temperature seasonality (difference between mean warmest month temperature and mean coldest month temperature) of each transect – transects differ considerably in winter precipitation and seasonal temperature variation. Climate normal were calculated for each elevation band using the ClimateWNA downscaling algorithm of the gridded CRU T 1970-2000 climate normals (Wang et al. 2016).

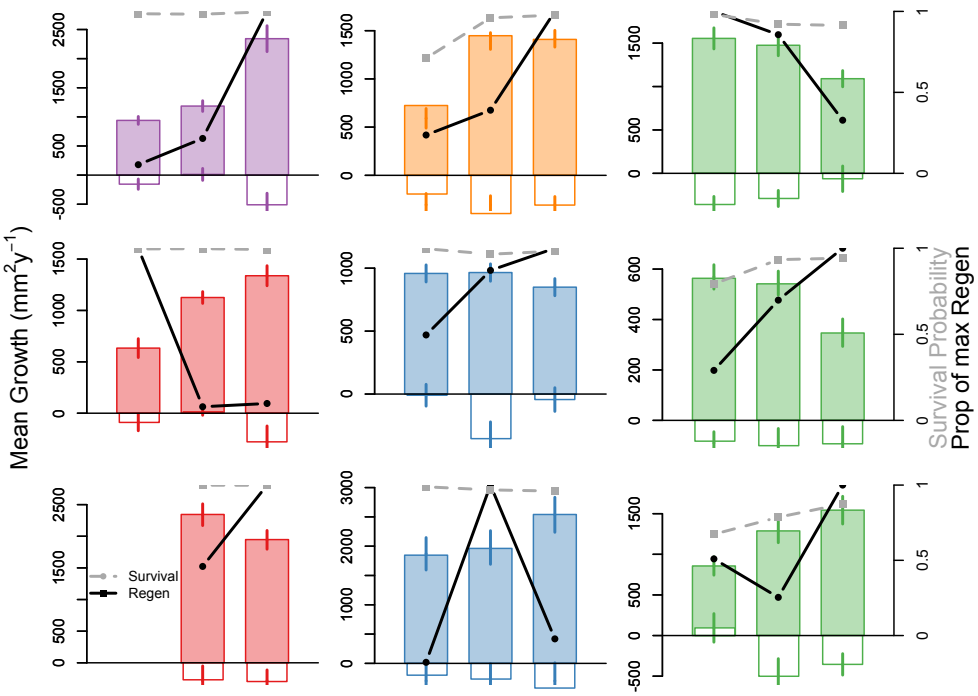

Figure S3: Size- and competition-specific population mean annual basal area growth rate (filled bars, mm^{2}yr^{-1}) and strength of competitive suppression (open bars) for all nine species-replicates. Competitive suppression indicates the amount by which growth of a tree of mean size is reduced by increasing neighborhood density one standard deviation. Black points indicate proportion of maximum seedling/sapling density (at mean competitive density). Gray squares indicate proportion of max conspecific mortality documented from variable radius plots around focal trees. See Tables S2-S4 for statistical significance of changes between the range margins and range center for each species-replicate.

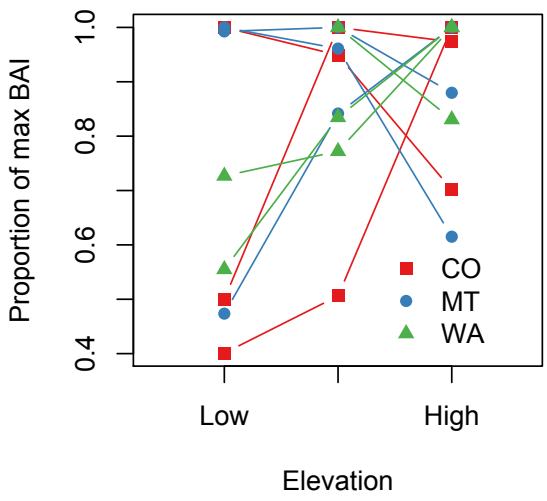

Figure S4: Species-site mean size and competition-standardized basal area increment as a proportion of species-site maximum growth across elevation. Harsh (slow growing) range margins occurred at both the upper and lower range margins of species on all three transects.

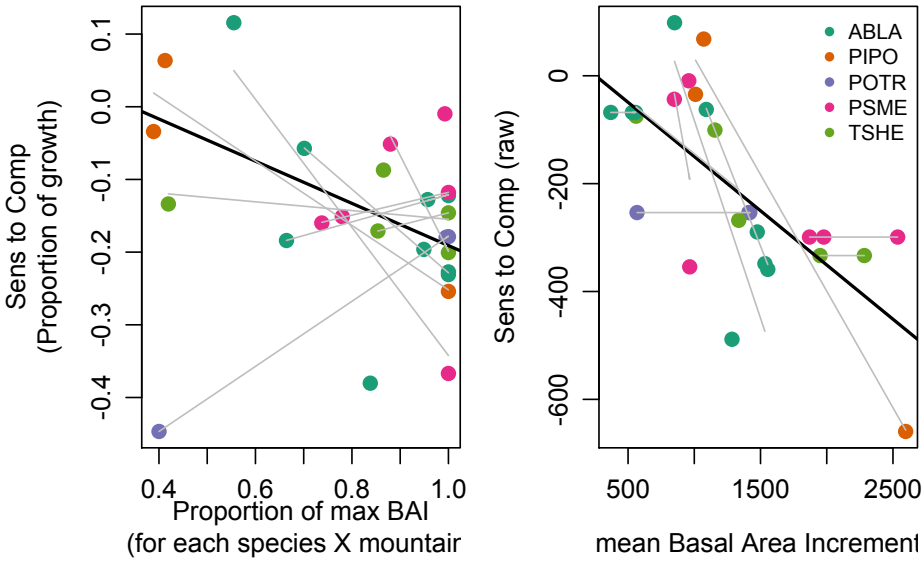

Figure S5: Comparison of the global relationship between mean populations growth rate and strength of competitive suppression (negative denotes stronger competitive suppression), assessed with proportional values (a) versus raw values (b). In (a), competitive suppression has been divided by the population mean growth rate to yield a growth suppression as a proportion of mean growth. Mean growth has been standardized by the mean growth of the fastest growing population (the benign range margin population) for each species-replicate. The trends are qualitatively similar, though the main effect is non-significant for proportional competitive

sensitivity (se-weighted linear mixed effects model, p=0.35) and significant for raw competitive sensitivity (p=0.001)

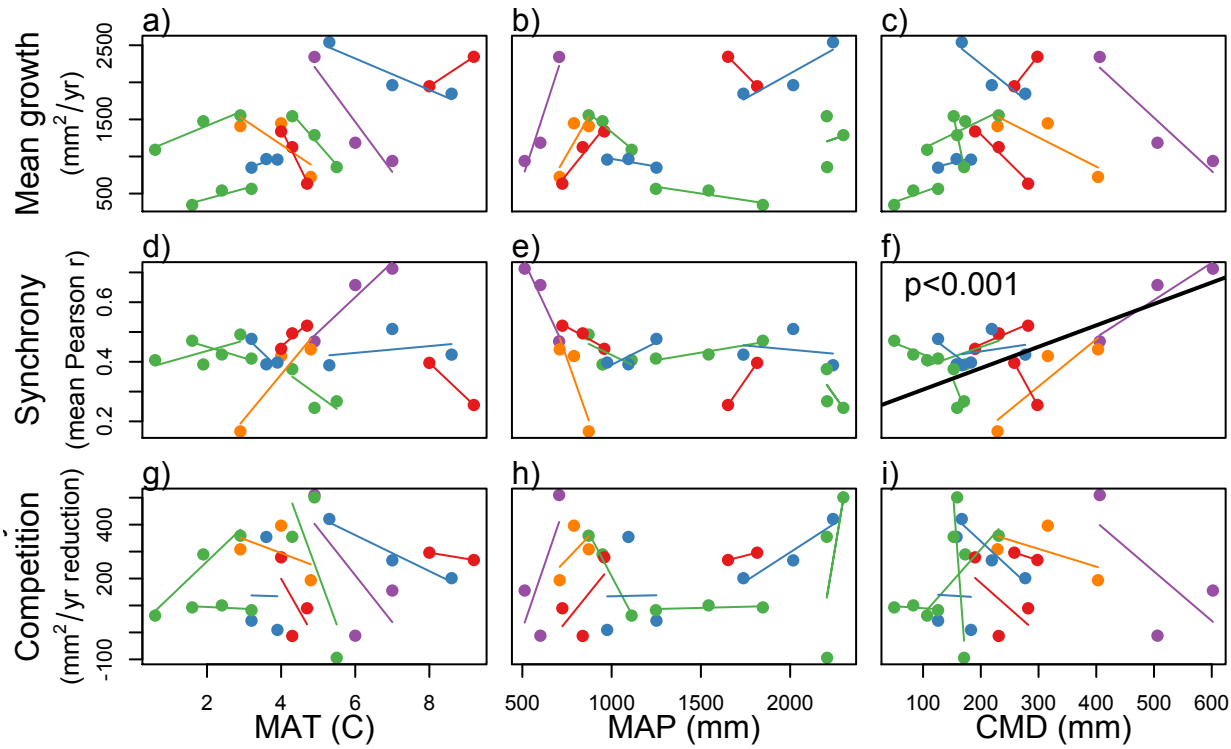

Figure S5: Mean growth (a-c), growth synchrony (d-f) and sensitivity to competition (g-h) of each species/site against Meant annual Temperature, Mean annual precipitation, and Climatic Moisture Deficit (PET – MAP). Only the Synchrony~CMD relationship was significant. Colored lines show the trend for each species/site.

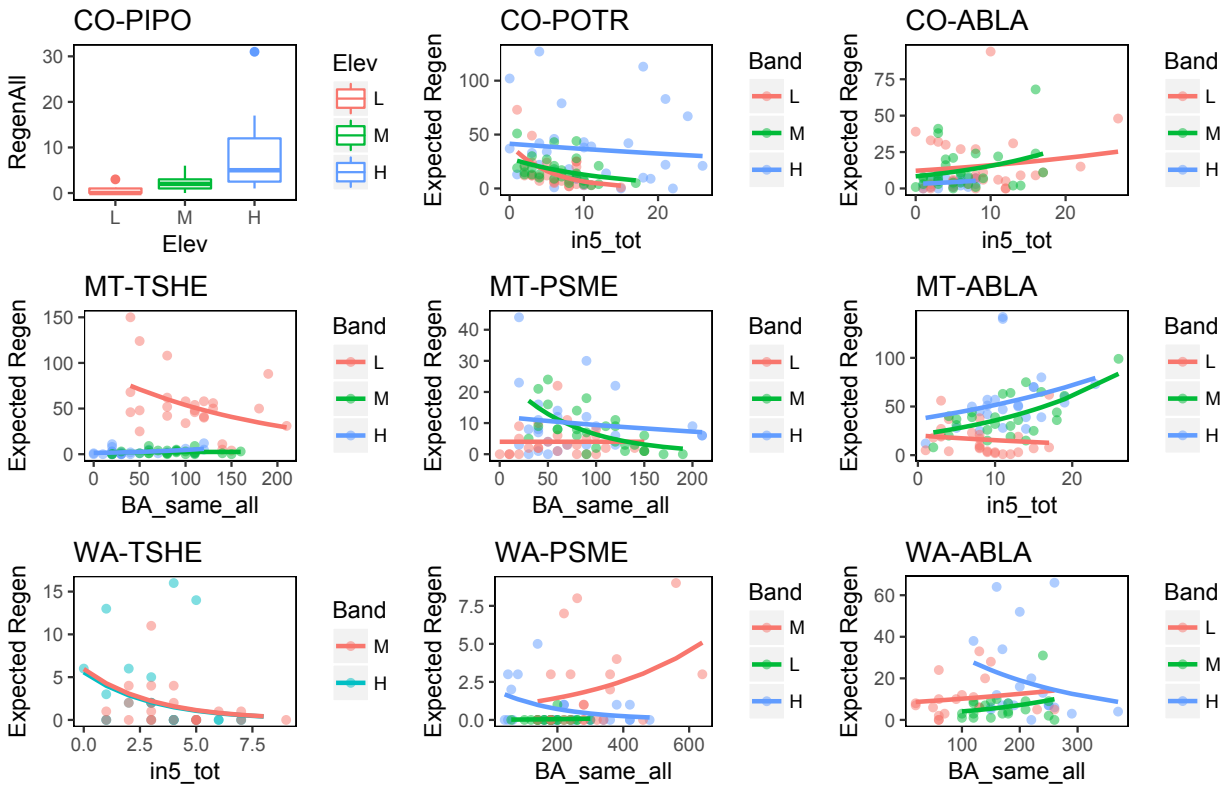

Figure S7: Regeneration dynamics across elevation and competitive environment for all species-replicates. Pinus ponderosa densities were assessed through supplemental regeneration transects, and thus cannot be analyzed as a function of competition, only elevation.

Table S1: Summary statistics (mean ± sd) for the low, mid and high elevation bands sampled for each of nine species-replicates (low elevation band was not sampled for *Tsuga heterophylla* in Washington because its range extends to sea level). PIPO = *Pinus ponderosa*, POTR = *Populus tremuloides*, ABLA = *Abies lasiocarpa*, TSHE = *Tsuga heterophylla*, PSME = *Pseudotsuga menziesii*. 'Dist w/in pair' referse to distance between paired trees (one in a high and one in a low competitive environment). 'Dist btw pairs' refers to the distance between centroids of all 10-15 tree pairs in an elevation band. 'ACF' refers to tree active crown fraction (% of tree height with foliage).

State	Species	Dist w/in pair (m)	Dist btw pairs (m)	DBH (cm)	Height (m)	Elev (m)	Basal Area (m^2/h)	Trees in 5m	ACF (%)
CO	**PIPO**	18.4±12.6	2134±1452	42.3±5.4	18.4±3.9	2280±31	19±10	4±3.1	0.66±0.16
CO	**PIPO**	25.9±12.7	932±662	46.6±8.3	23.6±3.7	2468±25	28±11	4.2±4	0.49±0.14
CO	**PIPO**	31.5±24.7	1776±1130	56.2±9.7	21.7±3	2682±18	14±7	5±3.6	0.69±0.12
CO	**POTR**	29.3±17.6	1831±1038	27.4±5.7	16.1±3.3	2693±21	17±8	6.4±3.2	0.39±0.11
CO	**POTR**	14±7.4	803±859	36.5±8.7	20.8±4.5	2876±23	38±14	6.7±3.9	0.44±0.13
CO	**POTR**	27.2±15.3	1341±927	36.9±8.9	23.1±3.8	3085±13	40±17	10.9±7.5	0.35±0.14
CO	**ABLA**	31.9±18.2	1439±1001	39.5±9.9	21.1±3.9	3087±16	42±16	8.7±6.3	0.67±0.2
CO	**ABLA**	32.9±21.5	1386±1154	38.4±7.7	22.2±4.5	3291±11	43±20	6.3±4.8	0.65±0.21
CO	**ABLA**	41.1±28.8	563±503	31.2±7.4	14.7±4.3	3487±28	24±13	4±2.4	0.85±0.14
MT	**TSHE**	26.4±10.5	379±212	47.4±5.4	29.1±3.6	1025±12	41±13	2.5±1.8	0.44±0.1
MT	**TSHE**	16.9±7.6	263±135	31.2±7.2	21.1±3.8	1164±27	39±12	8±4.4	0.57±0.14
MT	**TSHE**	21.3±9.6	294±173	29.2±3.8	18.3±3.6	1299±29	32±10	7.5±4.4	0.75±0.18
MT	**PSME**	15.8±9.2	315±179	40.4±11.7	25±3.4	1323±33	33±12	6.8±4.8	0.49±0.14
MT	**PSME**	14.6±7.6	167±77	36.1±3.9	21.7±3.9	1446±26	32±12	5.5±2.9	0.5±0.07
MT	**PSME**	16.7±10.6	197±101	36.1±10.4	21.9±4.6	1610±25	36±11	7.2±4.2	0.53±0.15
MT	**ABLA**	15.8±5	181±99	23.6±4	18.5±3.2	1607±24	33±11	8.2±4.5	0.57±0.15
MT	**ABLA**	13.9±7.1	114±53	24.8±5	15.8±3.1	1906±22	29±10	11.3±5.7	0.71±0.1
MT	**ABLA**	10.5±5.1	179±104	21.2±4.2	5.7±1	2219±45	18±7	12±4.8	0.78±0.14

WA	**TSHE**	NA	NA	NA	NA	NA	NA	NA	NA
WA	**TSHE**	20.7±11.1	152±82	51.8±13.9	37.5±8.6	221±30	59±19	4±2	0.56±0.14
WA	**TSHE**	18.2±9	161±85	54.1±8	40.2±7.6	550±28	62±13	3.5±2	0.51±0.12
WA	**PSME**	28.5±12	212±95	81.8±15.2	38.1±10.2	394±43	75±14	3.8±2.3	0.53±0.09
WA	**PSME**	19.4±9.5	135±66	75.1±24.9	32.8±8.9	857±23	68±27	4.2±2	0.51±0.14
WA	**PSME**	22±9.4	126±51	93.8±21.9	28.7±7	1298±33	67±28	4.5±2.3	0.58±0.12
WA	**ABLA**	15.1±12.5	74±37	35.3±9.8	19.5±5.1	1250±22	38±10	4.3±3.2	0.56±0.13
WA	**ABLA**	13.4±9	115±57	42.4±14.2	19.6±4.2	1393±16	37±10	8±4.1	0.5±0.15
WA	**ABLA**	10.5±6.3	120±67	38.5±10.4	16.9±3.4	1506±16	43±11	8.3±4.4	0.73±0.13

Table S1 *cont.*: Summary statistics (mean ± sd) for the low, mid and high elevation bands sampled for each of nine species-replicates (low elevation band was not sampled for *Tsuga heterophylla* in Washington because its range extends to sea level). PIPO = *Pinus ponderosa*, POTR = *Populus tremuloides*, ABLA = *Abies lasiocarpa*, TSHE = *Tsuga heterophylla*, PSME = *Pseudotsuga menziesii*. 'Dist w/in pair' referse to distance between paired trees (one in a high and one in a low competitive environment). 'Dist btw pairs' refers to the distance between centroids of all 10-15 tree pairs in an elevation band. 'ACF' refers to tree active crown fraction (% of tree height with foliage).

Table S2: Summary of linear models and linear mixed models of mean growth (mean Basal Area Increment from 2003-2012, mm^2) and beta regression models of growth synchrony. Mean Basal Area Increment (BAI) was modeled as a potential function of tree size ('DBH'), competitive environment ('ACF' = active crown fraction or the % of tree height with green foliage; 'N_Cr' = number of tree crowns touching the focal tree; 'BA_tot' = total basal area of living and recent dead trees around the focal tree assessed with a wedge prism), elevation band ('Elev') and DBH and competition's potential interactions with elevation band (indicated by a '*'). "Pair random effect" indicates whether a mixed model with a random effect of tree pair was included in the best model. "Variance Structure" indicates if variance was modeled as a function (either power or exponential) of either the fitted values or tree DBH. 't' indicates a variance function coefficient, while ' | Elev' indicates a different variance coefficient was fitted for each elevation band. Random effect, variance and fixed effect structure were selected with an iterative model selection approach based minimizing model AIC (See Methods). "L contrast" and "H contrast" indicate significant differences between the low elevation band or high elevation band (respectively) and the mid elevation range center, assessed using t-tests (with Satterthwaite's estimated degrees of freedom for mixed models). The "Sensitivity to Competition" columns indicate whether there was a significant interaction between the best competitive index and elevation band ("LRT" = significance of interaction based on a likelihood ratio test, "L int" and "H int" indicate significant differences between competitive effects at the low and high elevation range margins compared to the mid elevation range center assessed via t-tests). For growth synchrony models, all pairwise correlation coefficients between every pair of detrended tree growth chronologies in an elevation band (n=20-30 trees) were transformed to be bounded between 0 and 1 and then modeled as a function of elevation band using a beta-regression.

		Mean Growth and growth sensitivity to competitive environment			Mean Growth (differences from Mid elevation)		Sensitivity to Competition (difference from Mid elevation			Growth Synchrony (differences from Mid elevation)	
State	Species	Pair random effect	Variance Structure	Best model	L contrast	H contrast	LRT	L int	H int	L contrast	H contrast
CO	PIPO	no	fitted^2t	DBH + ACF + N_Cr * Elev	**0.0071**	**<0.0001**	**0.0003**	**0.0484**	**0.0041**	**2.70E-07**	**< 2e-16**
CO	POTR	yes	exp(2*t*DBH)	DBH + ACF + BA_tot + Elev	**<0.0001**	0.84	>.05	-	-	0.0816	**< 2e-16**
CO	ABLA	no	fitted^2t	DBH + Elev * BA_tot	0.6434	**0.0124**	**0.0146**	0.6048	**0.0631**	**1.63E-14**	0.251
MT	TSHE	no	DBH^2t | Elev	DBH + Elev * BA_tot	**<0.0001**	**0.0362**	**0.047**	0.1428	**0.0042**	**0.0326**	**3.46E-06**
MT	PSME	no	none	Elev * ACF	0.94	0.23	**0.035**	**0.0116**	**0.0203**	0.68	**2.98E-11**
MT	ABLA	yes	DBH^2t	DBH * Elev + ACF	0.727	**0.0092**	>0.05	-	-	0.3345	**0.00139**
WA	TSHE	no	exp(2*t*DBH)	DBH + ACF + Elev	NA	0.0723	>0.05	-	-	NA	**2.00E-16**
WA	PSME	yes	DBH^2t	DBH + BA_tot + Elev	0.1139	0.1946	>0.05	-	-	**4.48E-07**	**1.55E-11**
WA	ABLA	no	fitted^2t	DBH + BA_tot*Elev	**0.02**	0.2563	**0.003**	**0.0063**	0.4622	**0.00777**	**6.74E-06**

Table S3: Model results of generalized linear mixed models (bionomial error distribution with logit link, and tree as a random effect) modeling ~5 yr survival of conspecific trees falling within the variable-radius plot measured around each cored tree used to assess stand basal area. Trees were considered 'recent dead' in the model if the maintained dead foliage in their canopy or if they retained all bark and fine branches. These trees were assumed to have died within approximately the last five years. Trees without bark or fine branches were considered 'snags' and excluded from the analysis. Wedge prism basal area factor was selected to include 15-25 trees in each plot (including non-conspecifics) to derive a robust estimate of stand basal area, and the minimum number of conspecific trees assessed per elevation band was 54 (mean 260 trees per elevation, max of 511). "L difference" and "H difference" indicate the sign of the survival difference at each range margin compared to the mid elevation range center, and p-values indicate the statistical significance of these differences based on t-tests of model parameters using on Satterthwaite's approximate degrees of freedom. The column "Follows Adult BAI?" indicates whether survival patterns mirror mean growth patterns across elevation (See Figure S2). If growth correlates with survival within each species-replicate, survival is expected to be lowest at the slowest growing or 'harsh' range boundary, and highest at the fastest growing or 'benign' range boundary. 'Yes' indicates that both margins show the expected sign of difference compared to the range center and at least one margin shows a significant difference. 'Partially' indicates that one range boundary shows the expected difference from the range center, while the other shows the opposite of the expected difference. 'no pattern' indicates no significant differences in survival between elevation bands. 'No' indicates that both range margins showed the opposite of the expected difference from the range center (these species-replicates are highlighted in red in Figure 5a).

State	Species	L difference	p-value	H difference	p-value	Follows Adult BAI?
CO	PIPO	+	0.677	+	0.067	Partially
CO	POTR	**-**	**<0.001**	+	0.267	Yes
CO	ABLA	**+**	**0.012**	-	0.914	Yes
MT	TSHE	-	0.655	-	0.3462	no pattern
MT	PSME	**+**	**0.02**	+	0.215	Partially
MT	ABLA	**-**	**<0.001**	+	0.517	No
WA	TSHE	NA	NA	-	0.784	no pattern
WA	PSME	+	0.175	-	0.826	No
WA	ABLA	**-**	**0.011**	**+**	**0.018**	Yes

Table S4: Model results of poisson regressions modeling density of seedlings/saplings within 5m of cored trees as a potential function of elevation band, metrics of competitive environment (in5_tot = total number of adult trees within 5m of cored tree, BA_same = Basal area of conspecific trees near cored tree determined via a wedge prism, BA_tot = Basal area of all adult trees near cored tree determined via a wedge prism), and an interaction between elevation band and competition. Best models were selected based on AIC. 'L/H int sign' indicates whether, for models which include an elevation X competition interaction, the competition coefficient increased (+) or decreased (-) from the mid elevation range center to the low/high range margin (p-value indicates significance of this change based on a t-test). Because the competitive effects are generally negative, a decrease in the competitive coefficient (-) indicates an increased sensitivity of regeneration density to competitive environment.

			Density at mean competitive environment					Sensitivity to Competition (difference from Mid elevation)			
State	Spp	Best model	L dif	p-value	H dif	p-value	Follows Adult BAI?	L int sign	p-value	H int sign	p-value
CO	PIPO	Elev	-	**0.007**	**+**	**<0.001**	Yes				
CO	POTR	Elev * in5_tot	-	**<0.001**	**+**	**<0.001**	Yes	-	**<0.001**	**+**	**<0.001**
CO	ABLA	Elev * in5_tot	+	**0.002**	**-**	**<0.001**	Yes	-	**0.003**	+	0.927
MT	TSHE	Elev * BA_same	**+**	**<0.001**	**+**	**0.025**	No	-	0.092	**+**	**0.015**
MT	PSME	Elev * BA_same	-	**<0.001**	+	0.085	No	**+**	**<0.001**	**+**	**<0.001**
MT	ABLA	Elev * in5_tot	-	**<0.001**	**+**	**<0.001**	No	-	**<0.001**	-	**0.0106**
WA	TSHE	Elev + in5_tot + BA_same	NA	NA	-	0.79	No trend	NA	NA		
WA	PSME	Elev * BA_same	-	**<0.001**	-	**<0.001**	Partially	+	0.78	-	**0.012**
WA	ABLA	Elev * BA_same	**+**	**<0.002**	**+**	**<0.001**	Partially	-	0.082	-	**<0.001**

Appendix B: Supplemental Methods, Mean growth and growth sensitivity Supplemental Material for Chapter 1

We quantified environmental harshness and growth sensitivity to competition based on the relationship between mean annual Basal Area Increment (mm^2) from the 2003-2012 period and tree size, range position and competitive environment. Using an iterative model selection technique based on the suggestions of Zurr et al. 2008, we first determined for each species-site whether tree pair was needed as a random effect (to account for edaphic similarities between trees in a pair) using an 'over-the-top' fixed-effect structure fit with restricted maximum likelihood and Likelihood Ratio Tests (tree pair was included as a random effect for four of nine species/sites, the remaining five did not require mixed-modeling). We then examined residual plots, removed extreme outliers (five trees total) and iteratively tested different variance structures (allowing error variance to change as some function of tree DBH, some function of the response variable, allowing different variances per elevation or some combination of the above). For each variance structure, we fit a large number of candidate models including combinations of elevation band, tree DBH, and one or more (non collinear, i.e. Variance Inflation Factor <2) competitive environment metrics and interactions between elevation and DBH or elevation and competitive metrics using maximum likelihood estimation. Potential competitive environment metrics included stand basal area (from a variable radius plot measured using a wedge prism), number of trees within 5m of the focal tree, active crown fraction of the focal tree (proportion of tree height that held foliage), and number of crowns touching the focal tree. We used AIC to select the best model for each variance structure, and then compared the AICs of the best models (which typically converged on identical fixed-effects structures) to determine the optimal variance structure. We then verified that that adding or deleting terms (including quadratic DBH and competition terms and interactions with elevation) did not improve the model, and refit the final model using restricted maximum likelihood estimation (Zurr et al. 2008).

Models with were fit using the *lme* (where a random effect for pair was required) or *gls* (where no random effect was needed) functions from the *{nlme}* packaged in R, or in the simplest case using the *lm* function from the *{stats}* package if no random effect or complex variance structure was required. Significance of Elevation term and Elevation * Competition interactions were tested using Likelihood Ratio Tests against reduced models without these terms. In all models, mid elevation/range center was set as the model intercept so that built in model contrasts tested for differences in BAI between approaching range margins with t-tests (using Satterthwaite estimated degrees of freedom for mixed models). All predictor variables were converted to z-scores so that model coefficients can be directly compared between variables (i.e. model coefficients represent the BAI change for a one standard deviation change in any competitive metric). Mean growth estimates (elevation band intercepts) thus represent the mean basal area increment predicted for a tree of species-replicate mean DBH and species-replicate mean competitive environment. Growth Sensitivity to Competition was calculated as the predicted reduction in growth associated with a one standard deviation increase in competitive environment (for all competitive metrics included in the best model) using the *predictSE* function from the *{AICcmodavg}* package. Reported standard errors are prediction errors. Best model formulations and statistics are reported in Table S2. Parameter estimates for mean size- and competition-standardized growth and Growth Sensitivity to Competition shown in Figures 2&3 in the main text were calculated using the full model (fixed effects of Band,

competition, and Band x competition interaction) for each species/site, but best model formulations, significance statistics, and elevation contrasts are reported in Table S2.

Appendix C: Supplemental Methods, Alternative metrics of climate sensitivity Supplemental Material for Chapter 1

We applied multiple alternative methods to quantify growth sensitivity to climate, in addition to the growth synchrony metrics reported in the main text. We paired detrended and pre-whitened Ring Width Index chronologies (either for each tree or robust bi-weighted mean chronologies for each population) with monthly 20th century climate data from various sources (see below). We then qualitatively assessed climate sensitivity to monthly climate variables following the traditional dendrochronological technique of plotting all individual correlations between population mean chronologies and 24 monthly climate variables from September of the growth year (when growth was assumed to have ceased) to October of the year prior to growth. These correlations are shown for each species-site in Figures S8-S16. Because these individual correlations are not independent (i.e. monthly climate is temporally autocorrelated with previous months and many different climate variables are strongly collinear), these monthly correlations cannot easily be summarized into a metric of total climate sensitivity across months and climate variables. The qualitative inferences that these plots reveal are that:

1) The seasonality of climate sensitivity varies enormously between species-replicates, even for species-replicates on the same mountain. For example, compare the CMD sensitivity of *Pinus ponderosa* versus *Abies lasiocarap* in CO (Figs S8c and S10c); or the temperature sensitivity of *Pseudotsuga menziesii* versus *Tsuga heterophylla* in MT (Figs. S11a and S12a).
2) Seasonal metrics (winter, spring, summer, or growing season vs dormant season) rarely capture important periods of climate sensitivity, and are in no way universal across all species-replicates.
3) Lagged climate effects are reasonably common (e.g. to moisture availability in all MT species-replicates, Figures S11-13 b,d), and sometimes are of opposite sign to current year growth sensitivities to the same variable (e.g. late summer precipitation sensitivity in *Abeis laisocarpa* in MT, Fig 13b,d; or summer temperature sensitivity in *Abies lasiocarpa* in WA, Fig. S16a,c).
4) Differences in climate sensitivity across elevation are obvious for some species-replicates (e.g. temperature sensitivity of *Abies lasiocarpa* in CO, Fig. S10a,c), but difficult to objectively integrate across months and years to derive a total climate sensitivity for many species-replicates (e.g. precipitation sensitivity of *Abies lasiocarpa* in CO where low elevation is more sensitivity to precipitation in the growth year, but mid elevation is more sensitivity to precipitation in the previous year, Fig. S10b,d).

Thus, we explored multiple statistical methods using linear mixed effects models (on individual tree growth chronologies) or linear models (on population master chronologies) to quantify total climate sensitivity and climate sensitivity to specific climate variables. We employed various model selection techniques, and numerous summary metrics as alternatives to quantify total climate sensitivity or climate sensitivity to particular climate stresses. However,

the inferences about climate sensitivities at range margins compared to range centers were often not robust across different modeling techniques, summary metrics, climate datasets, or climate covariate selection rationals. Due to the lack of robust inference from any particular modeling approach, we instead used growth synchrony (see Methods of Chapter 1) as the least problematic and easiest to interpret metric of growth sensitivity to climate.

Figures S8-S16: Correlations between monthly climate variables, (a- mean temperature, b- total precipitation, c- Growing Degree Days, d- Climate Moisture Deficit or Potential evaoptranspriation minus precipitation) beginning with the September of the growth year and moving back through time through two water years (pySep indicates the September of the year previous to the growth year). Red lines indicate correlations with the master RWI chronology of the low elevation range margin, purple lines show correlations with the mid elevation/range center master chronology, and green lines show correlations with the high elevation range margin chronology. Points indicate correlations that were significant (alpha = 0.05, no correction more multiple tests). Vertical solid line divides the growth year (on the right) from the previous year (on the left). Red shading shows the growth year summer (June-Aug), green shading shows the growth year spring (Mar-May), and blue shows growth year winter (Dec-Feb).

Figure S8: *Pinus ponderosa* in Colorad0

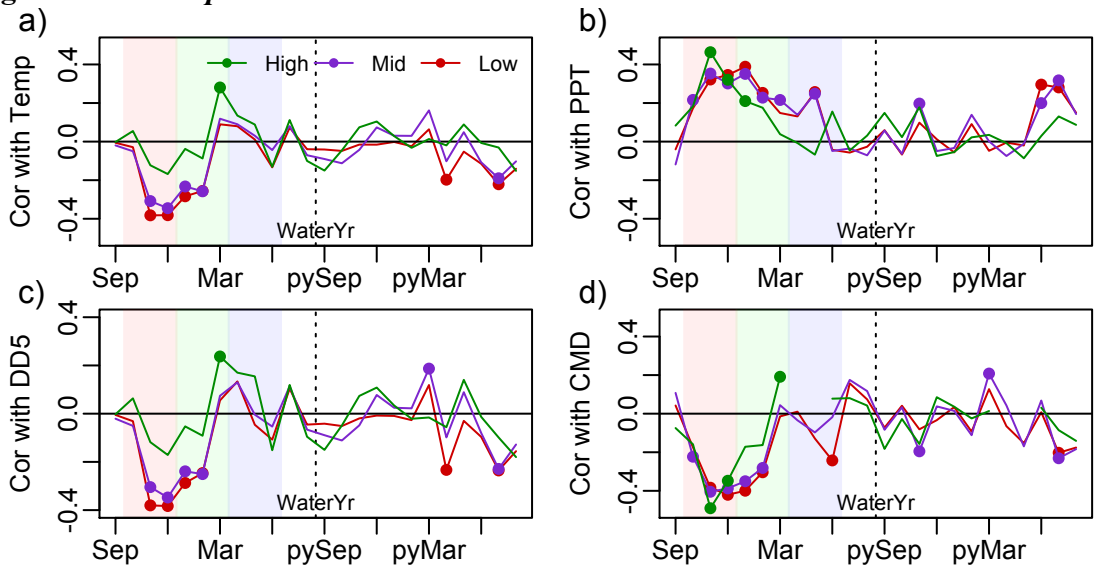

Figure S9: *Populus tremuloides* in Colorado

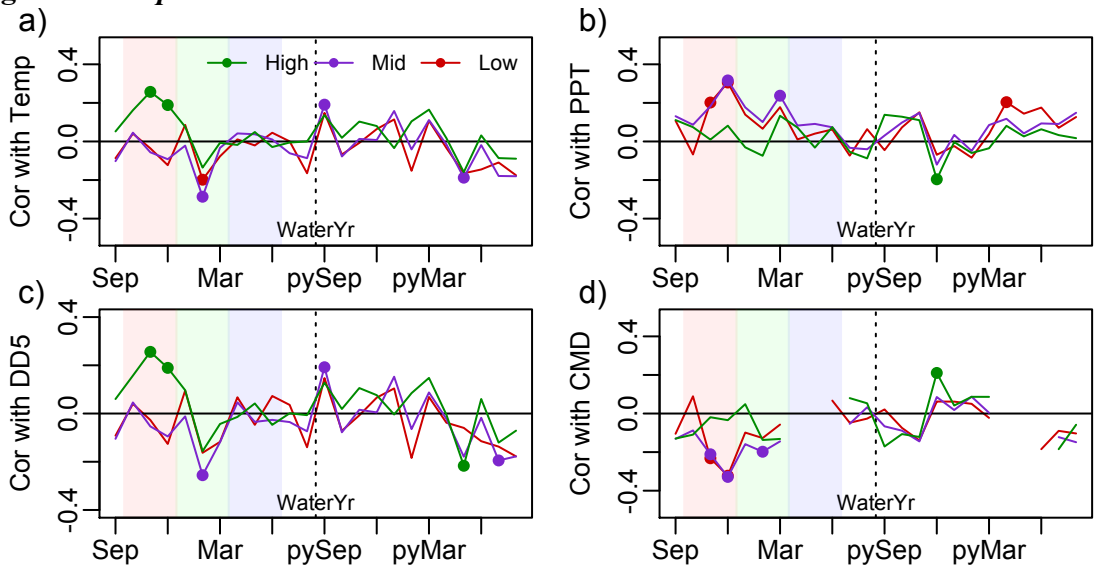

Figure S10: *Abies lasiocarpa* in Colorado

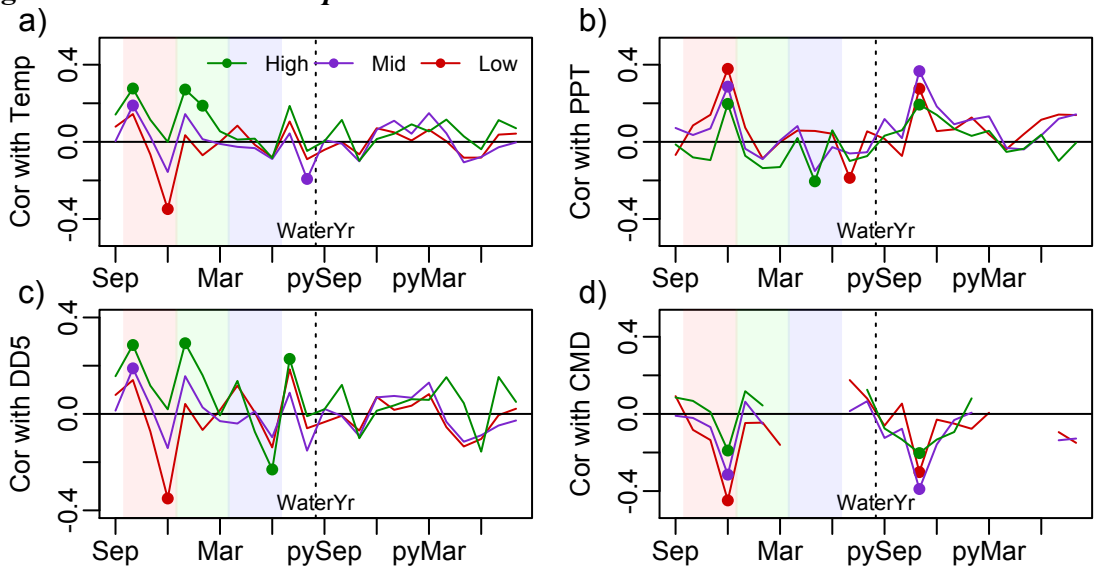

Figure S11: *Tsuga heterophyla* in Montana

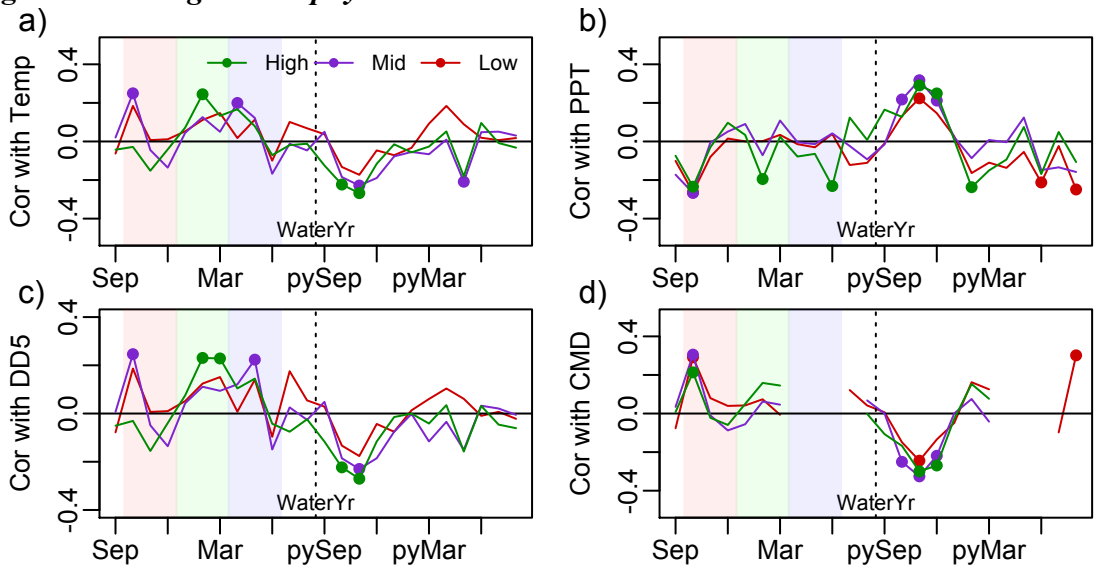

Figure S12: *Pseudotsuga menziesii* in Montana

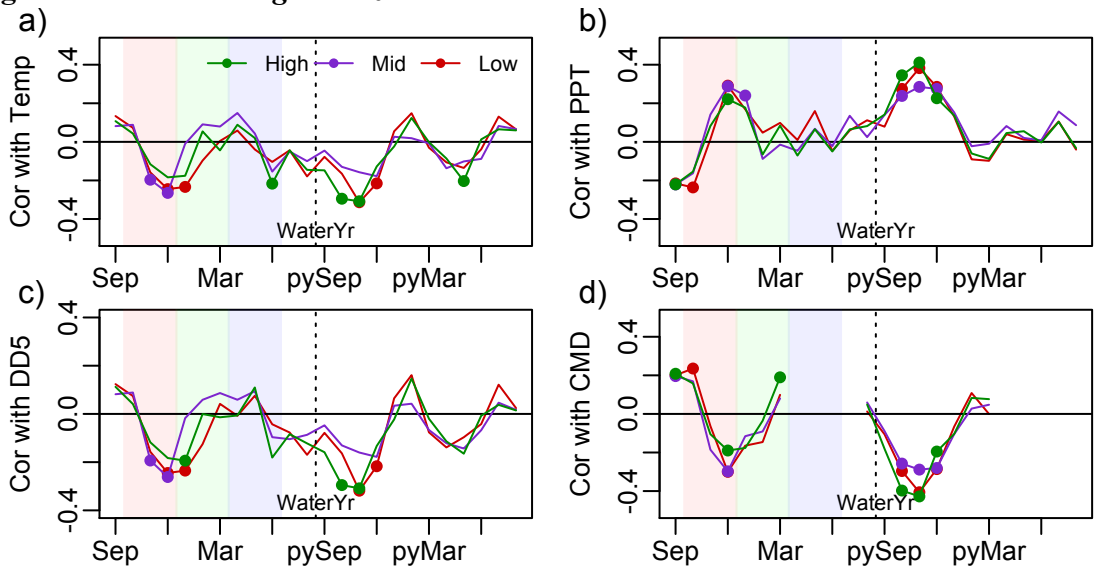

Figure S13: ***Abies lasiocarpa*** **in Montana**

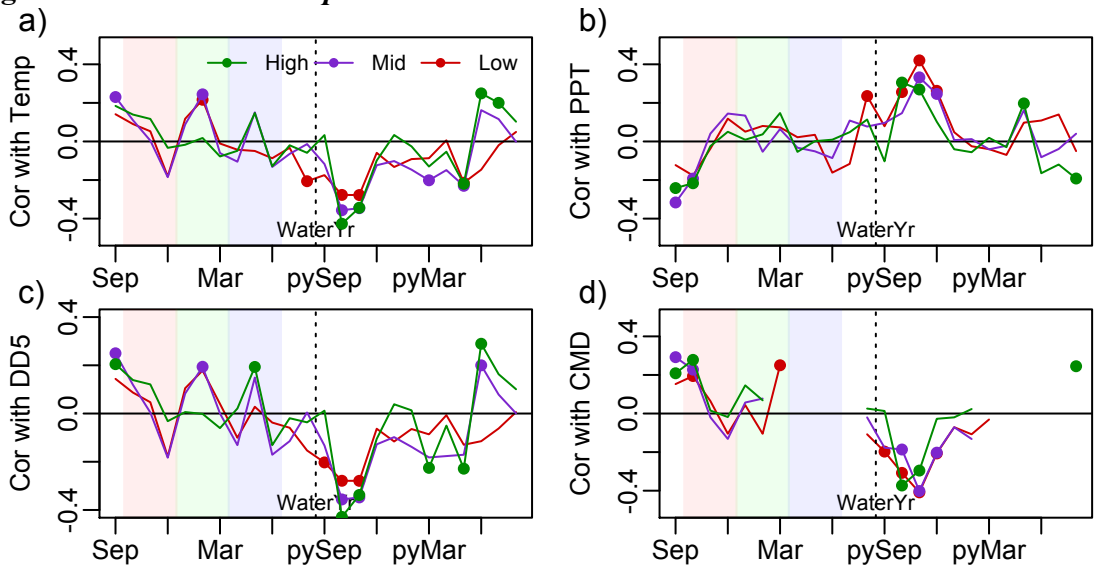

Figure S14: ***Tsuga heterophylla*** **in Washington**

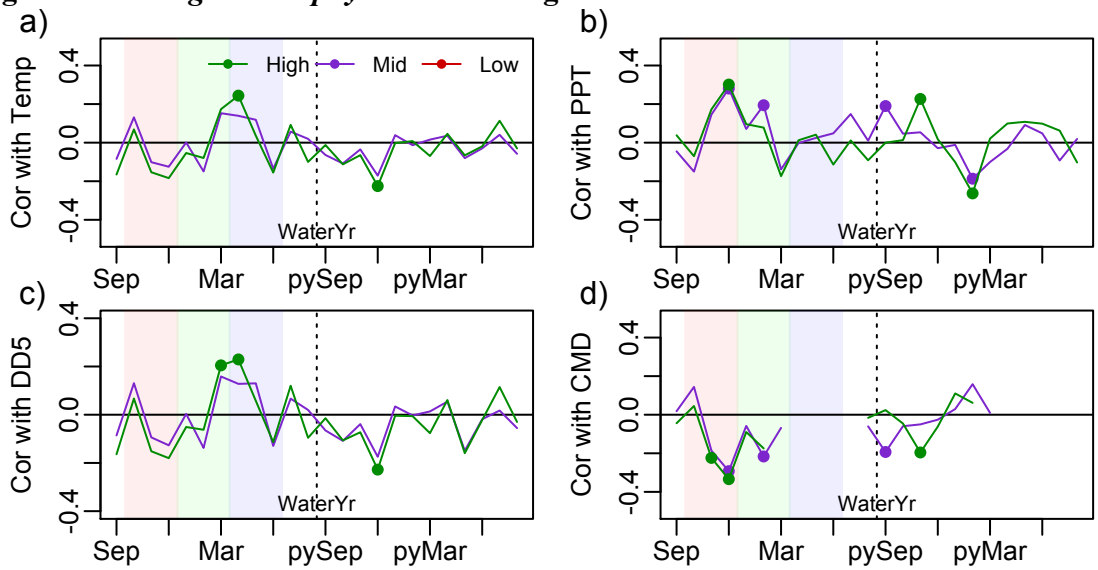

Figure S15: *Pseudotsuga menziesii* in Washington

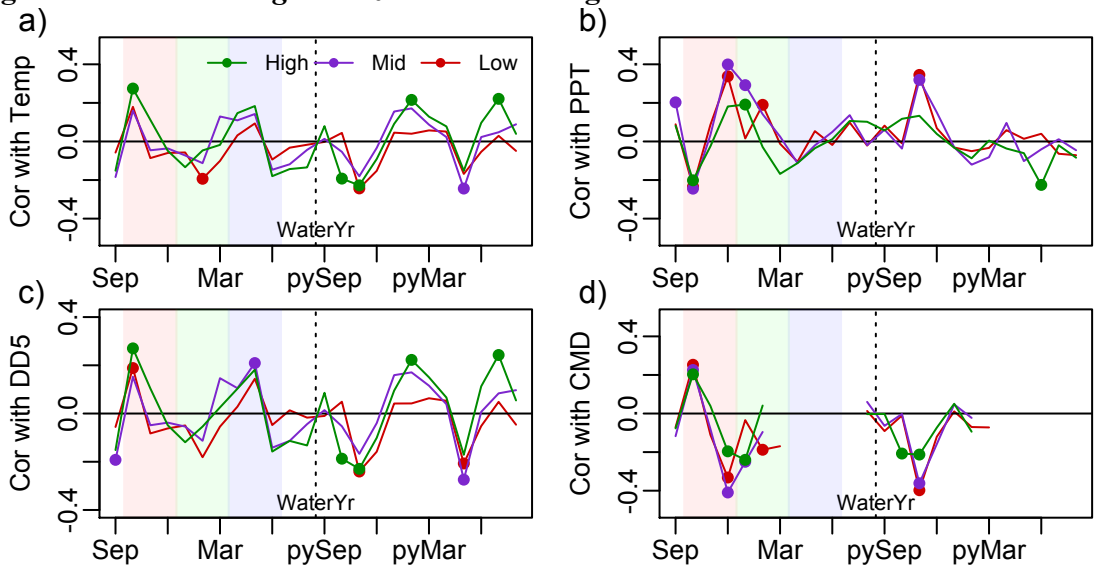

Figure S16: *Abies lasiocarpa* in Washington

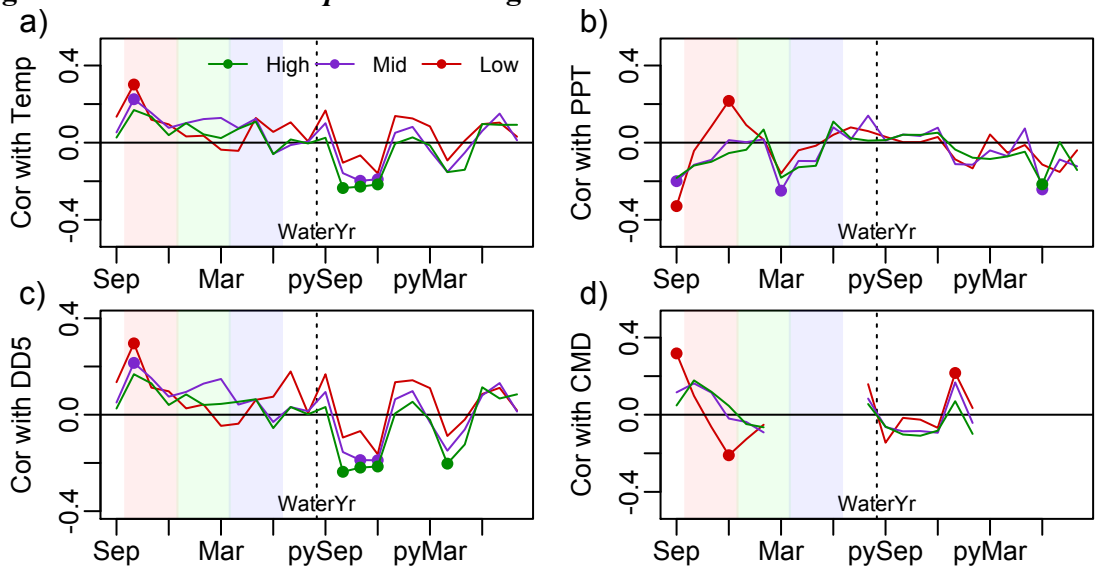

Climate data:

To determine the identity of the key climatic constraints on growth and to assess how these constraints vary across elevation for each species, we compared annual tree RWI chronologies with annual climate variables from 1902 to 2012. Monthly climate variable time series were acquired from three independent data sources. First, the CRU TS 3.1 gridded historical climate time series(Mitchell & Jones 2005) were interpolated to the midpoint of each elevation band for each species-replicate using the 1961-1990 PRISM climate normals (Daly et al. 2008) and the scale-free interpolation technique of ClimateWNA (ClimateWNA version 5.21, Wang et al. 2012). Additionally, NOAA monthly Divisional climate time series (divisions WA-1, MT-1, CO-2) were downloaded for each mountain from http://www7.ncdc.noaa.gov/CDO/CDODivisionalSelect.jsp (5 May 2016). Finally, monthly time series (1950-2012) were extracted from the 4km PRISM dataset (Daly et al. 2008), and monthly soil moisture values at three soil depths were derived by averaging daily values from the Variable Infiltration Capacity Model (Livneh et al. 2015). Monthly climate variables were also aggregated into seasonal (wt, sp, sm, at), growing/dormant season (gs and ds), and water year (previous year Oct through current year Sept) summaries.

Correlations between climate variables from the different data products were usually strong but not perfect (Figure S17). The relationships between data products were also not consistent between climate variables (e.g. annual precipitation in Colorado was most strongly correlated between CRU and PRISM, but mean annual temperature in Colorado was most strongly correlated between CRU and NOAA Divisional Climate, Figure S17), nor were correlations between products consistent across mountains. We had little knowledge a-priori about which data product was likely the most accurate for each mountain, and thus included variables from all three products in most model selection approaches. However, we never allowed the same exact climate variable from multiple products to be included in candidate models.

Figures S17-S19: Correlations between climate time series from CRU TS 3.1, PRISM 4km, and NOAA Divisional Climate summary data. Data shown from CRU and PRISM are for the mid elevation population of the mid elevation species for each mountain. Pairplots on the left show relationships between annual Precipitation (PPT_an = CRU, PPTPR_an = PRISM, PPTDiv_an = NOAA Divisional Climate), while pairplots on the left show relationships between mean annual temperature (Tave_an = CRU, TavePR_an = PRISM, TaveDiv_an= NOAA Divisional Climate). Note: CRU and PRISM are in metric units while NOAA divisional climate is in English units.

Figure S17: COLORADO

Annual Precipitation

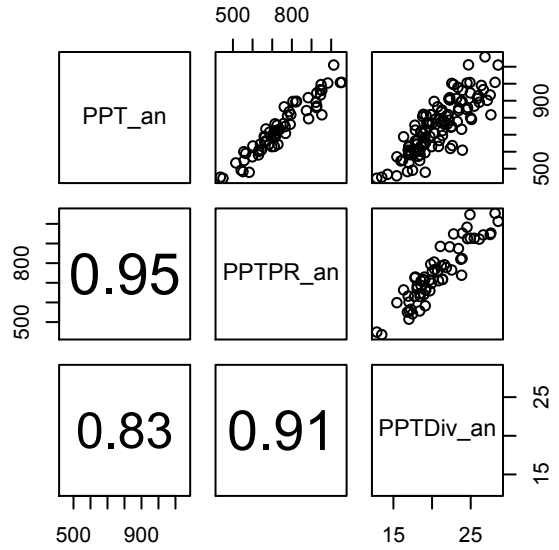

Mean Annual Temperature

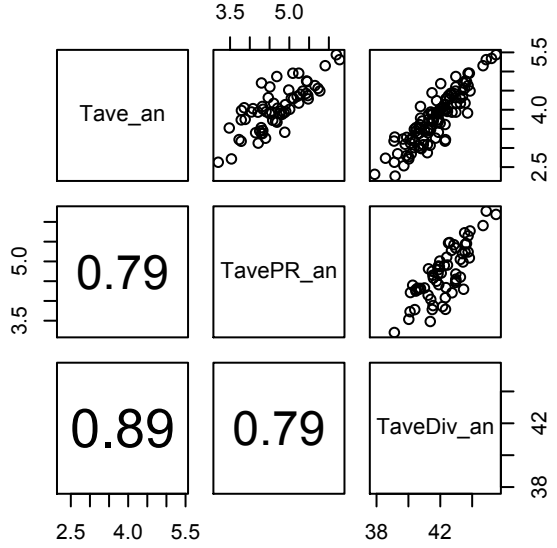

Figure S18: MONTANA

Annual Precipitation

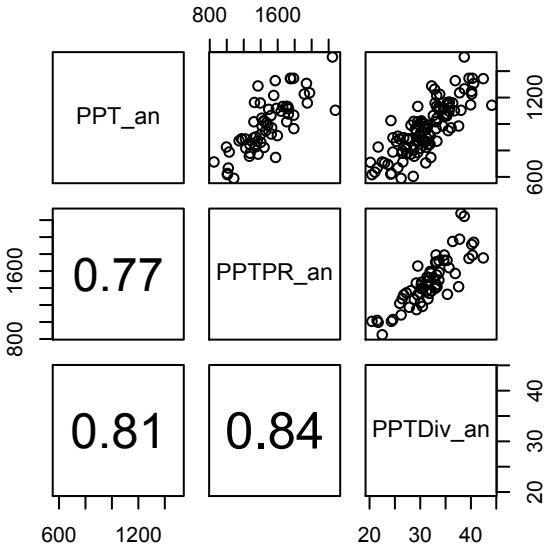

Mean Annual Temperature

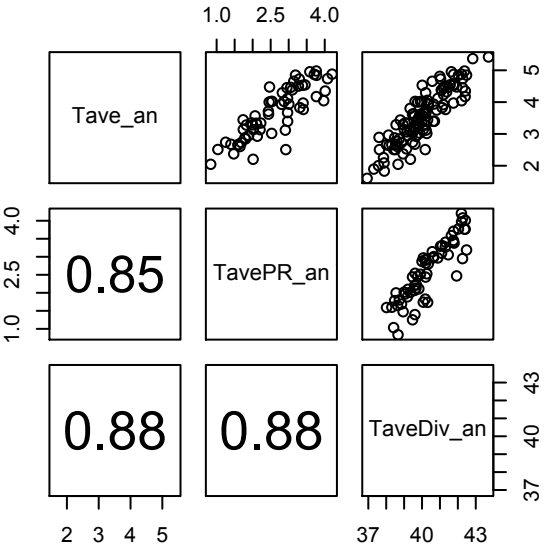

Figure S19: WASHINGTON

Annual Precipitation

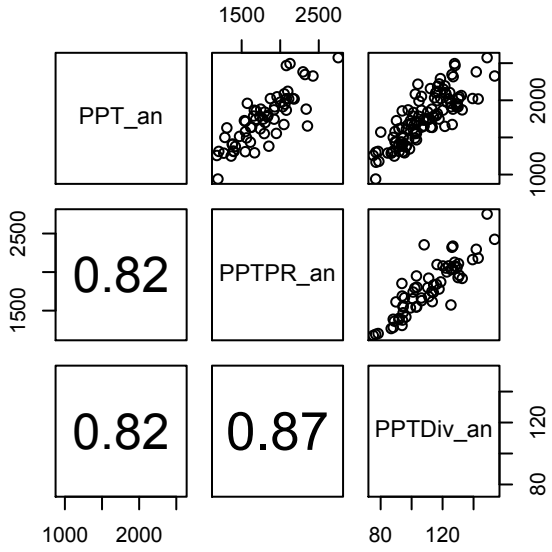

Mean Annual Temperature

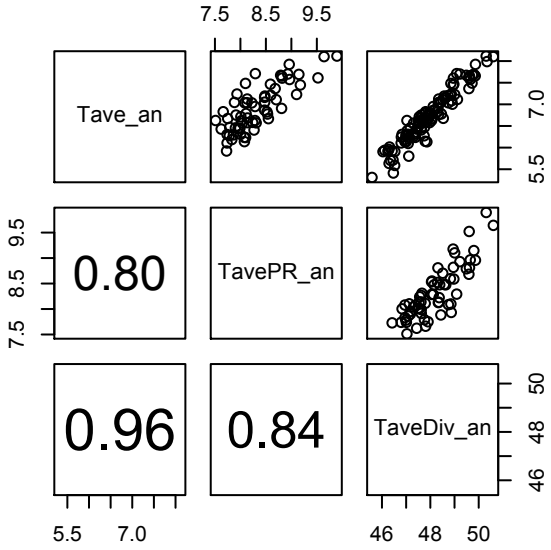

Appendix D: Supplemental Data and Analysis, differing methods drive tree range limits
Supplemental Material for Chapter 2

Figure S1: Species relative abundance (Loess smoothed) across elevation at the study site in the La Plata Mountains, (San Juan National Forest, Colorado, USA). Relative abundance of all stems >5cm DBH was assessed via 3-6 strip transects (50m long by 5m wide) every 50m of elevation gain.

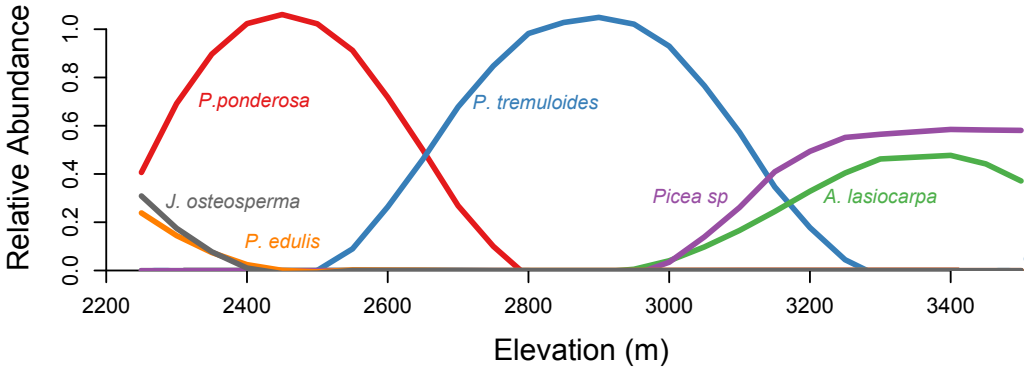

Methods for combining Basal Area Increment datasets:
We combined estimates of Basal Area Increment from the trees sampled in this study (see Methods section) with nearby trees previously cored for a different study. In 2013, tree cores were collected from 20 to 30 trees per elevation at the range center and upper and lower range margins of ponderosa pine and trembling aspen for climate sensitivity analysis. These elevation bands were identical to the elevation bands used for stand selection in this study, cored trees were close (<500m) to the plots used in this study, and core collection and processing was identical to this study (see Methods section). Tree selection in 2013 was very similar to tree selection used in 2014 for this study (e.g. mature, healthy canopy trees far from visible drainages), except that, rather than being grouped in plots, trees were grouped in pairs comprised of one tree in a high competitive environment and one tree in a low competitive environment. Trees within a pair were <20m apart, and pairs were >40m apart (Anderegg & HilleRisLambers *in prep.*). In 2013, competitive environment was quantified using a variety of metrics including: number of trees within 5m of the focal tree, number of crowns touching the focal tree, active grown fraction (fraction of tree height with live foliage), and stand basal area estimated using a wedge prism. Based on 30 present in both datasets, we constructed linear models relating all of these measures (individually and together) to Hegyi's competitive index. Based on AIC, number of trees within 5m alone was the best predictor of Hegyi's competitive index and explained 64% of the variance (Figure S2). We then used this linear relationship to estimate Hegyi's competitive index for all trees cored in 2013 in order to combine the 2013 and 2014 datasets. However, results were qualitatively very similar using only the data from 2014 (Figure S3), though with the decreased sample size the mixed-effects model including elevation as an explanatory variable was not significantly better than the null model (containing only competitive index and DBH) for aspen (ponderosa LRT p=0.0019, aspen LRT p=0.21).

Figure S2: Linear relationship between Hegyi's competitive index (distance and size dependent metric of competitive environment measured in 2014) and the number of live trees within 5m of the focal tree, which was a better predictor of Hegyi's CI than any other single competitive index or combination of competitive indices measured in 2013.

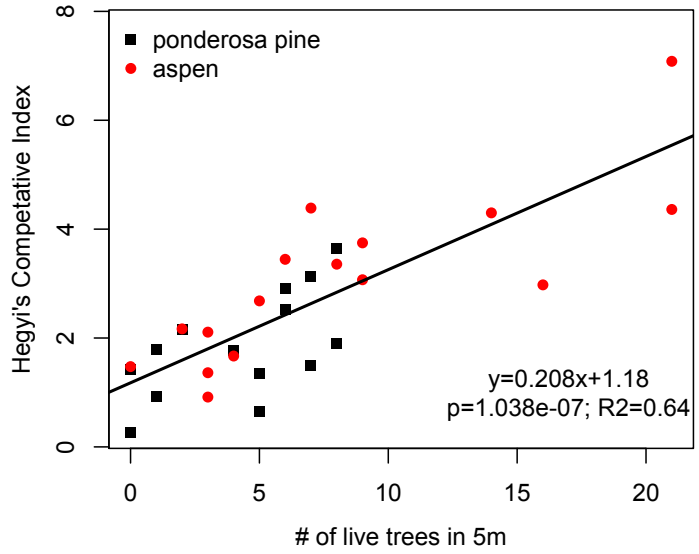

Figure S3: Raw mean annual basal area increment (not standardized by tree size or competitive environment) for the 2002-2012 period. (a) only trees cored in 2014 (b) combined dataset of trees cored in 2013 and 2014. Results are qualitatively similar between datasets but sample size and thus statistical power are greatly increased in the combined dataset, resulting in a significant effect of elevation on BAI for both species in the combined dataset. Boxplots show the median (bar), interquartile range (box), range (lines) and outliers (circles). "*" indicates a margin significantly different from the range center based on mixed-effects models with elevation coded categorically.

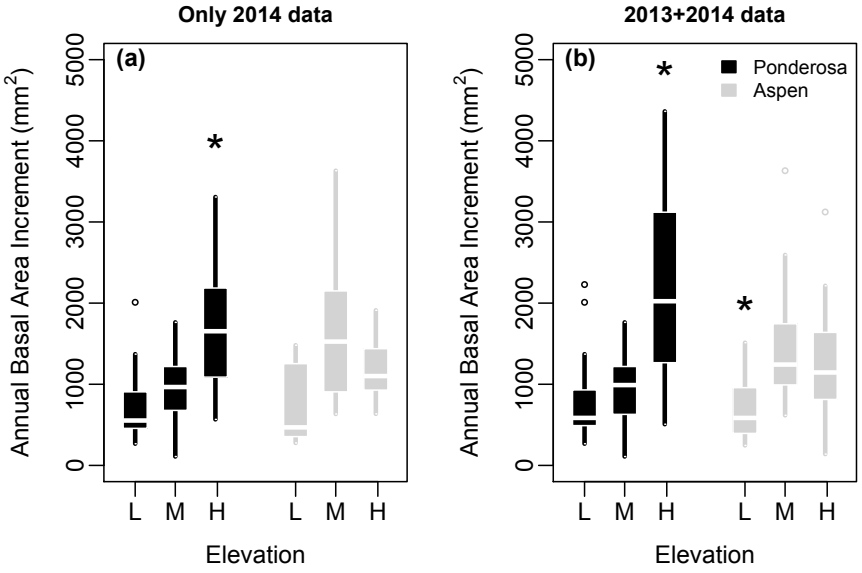

Figure S4: Xylem vulnerability curves showing raw xylem area specific conductivity (K) as a function of induced xylem tension. Conductance at 0 MPa is K_{max} measured after embolism was removed via vacuum infiltration.

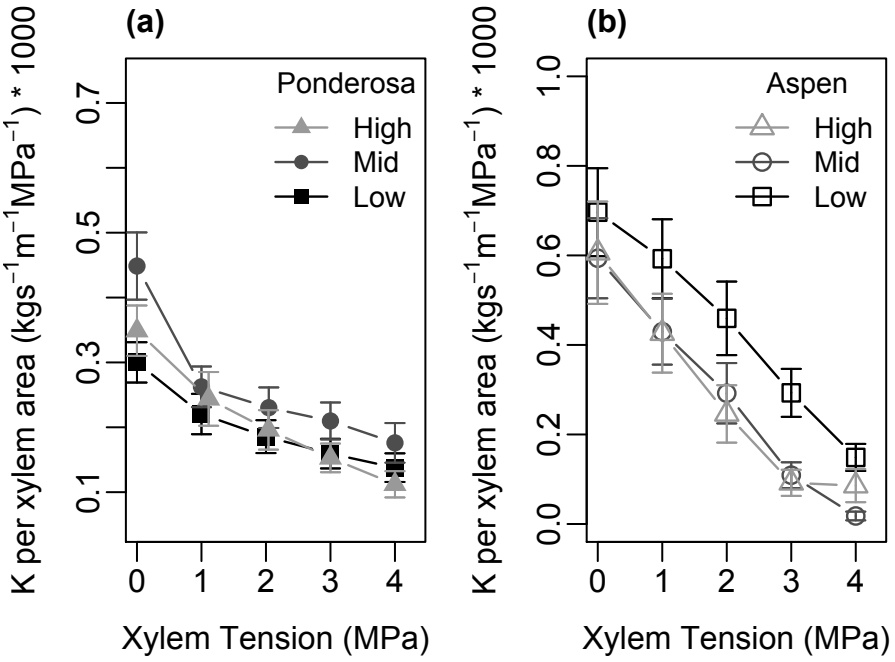

Figure S5: Mean annual Basal Area Increment (BAI) for individual trembling aspen trees as a function of (a) SLA and (b) branch wood density. Statistics show the p value of Likelihood Ratio Tests comparing linear mixed effects models including only tree DBH and competitive environment (null) to models with DBH, competitive environment and either SLA or wood desnity (BAI was square root transformed for normality). Trend lines are added to indicate the slope of the relationship. Point colors denote tree elevation. Tissues with high carbon density (low SLA, high wood density) are associated with slow radial growth.

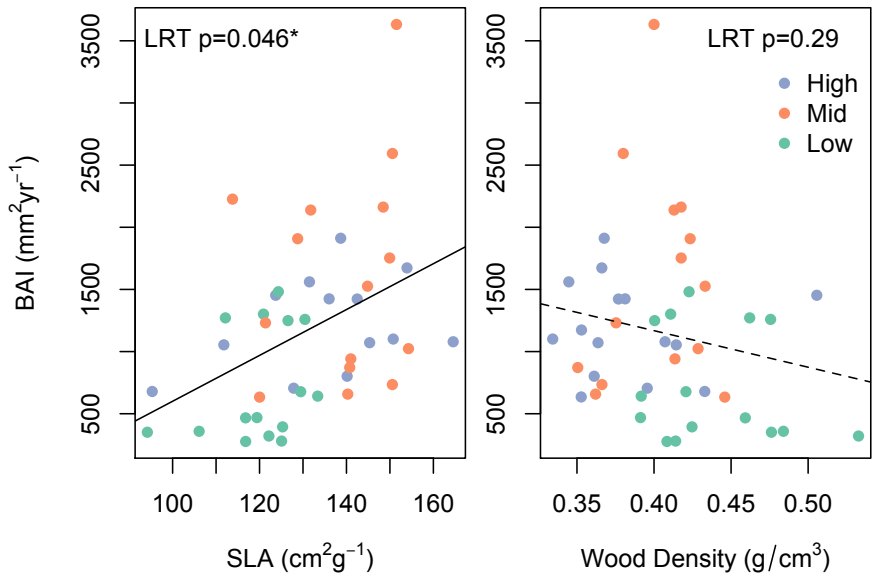

Figure S6: Percentage difference from high elevation average A_L:A_S and average median leaf area for individual ponderosa pine trees. A_L:A_S values were corrected for the effect of stem diameter. Dotted line shows the 1:1 line, while solid line shows the total least squares regression line.

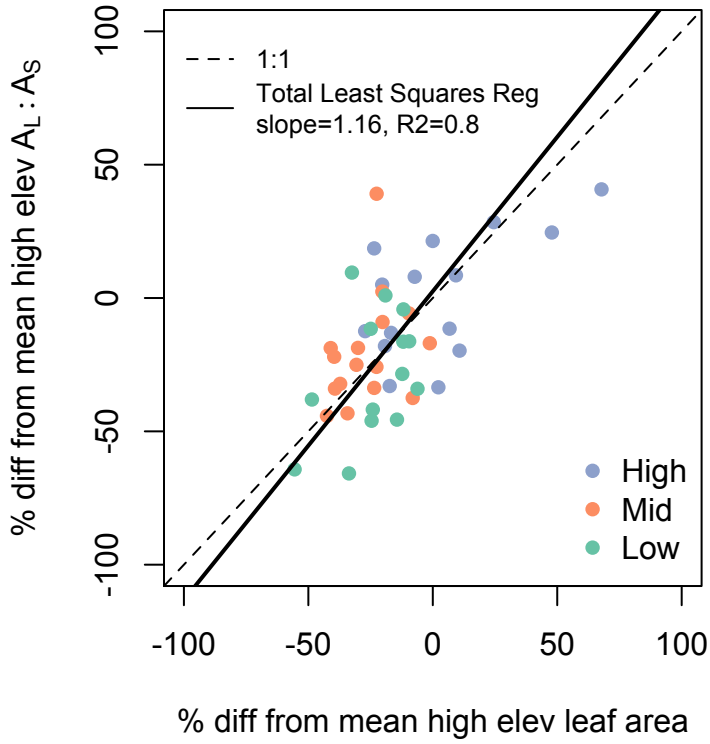

Figure S7: Aspen tree age across elevation from all trees in the full dataset used to calculate BAI (see Methods for calculating Basal Area Increment) for which ages could be estimated from tree cores (n=86). Letters denote significant differences between elevation based on Tukey's Honest Significant Differences test (alpha = 0.05). Trees in the dataset were selected to capture a representative size distribution of dominant canopy trees at each elevation.
A large increase in tree age at low elevation might indicate increased survival in slow growing trees indicative of 'demographic compensation' that could offset the consequences of greatly decreased mean annual growth at the dry range margin. Mid elevation showed significantly decreased tree age compared to high elevation, but low (slowest growing) and high elevation (fastest growing) trees showed no significant difference (p=0.84). As all ponderosas in the area regenerated following complete clearcut ~100 years ago, tree ages are artificially uniform in this species.

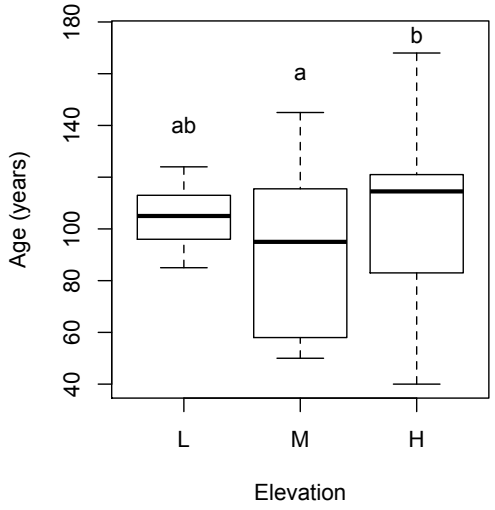

Table S1: *Pinus Ponderosa* – Details for linear mixed-effects models of functional trait data. "Data Transformation" indicates if/how trait data were power transformed to achieve normality prior to model fitting. "Covariates included in model" lists any covariates controlled for during model construction. "LRT from null model" shows the likelihood ratio test p-value comparing a model with Elevation to a null model. If elevation was significant in a likelihood ratio test, "Low Elev p-value"/"High Elev p-value" show post-hoc differences between the lower/upper range margin and the range center assessed via the Satterthwaite approximation of marginal fixed effect significance using the mixed-effects model with elevation. "btw stand : w/in stand variation" shows ratio of the variance estimated between stands and variance within stands (between individual variation + measurement error) in the best fit mixed-effects model (0 indicates no variance assigned to stand random effect).

Trait	**Data Transfor-mation**	**Covariate included in model**	**LRT from null model**	**Final sample size**	**Low Elev p-value**	**High Elev p-value**	**btw stand : w/in stand variation**
10yr mean annual BAI	lambda=0.25	DBH + comp. Index	***3.3e-8**	96	0.16	***0.000001**	**0**
Median leaf size	-	-	***0.0018**	49	0.57	***0.01**	0.10
Height	-	-	0.2856	51	-	-	0.84
A_L:A_S	-	Stem diameter	***0.0257**	45	0.49	***0.0253**	0.28
SLA	lambda = -1	log(stem diameter)	0.4584	47	-	-	0.23
Wood Density	-	Stem diameter	0.2044	46	-	-	0.04
K_{nat_Leaf}	lambda = -0.5	log(stem diameter)	0.4714	35	-	-	0.01
K_{max}	lambda = 0.5	log(stem diameter)	***0.0012**	42	***0.020**	0.45	0
Safety margin	-	-	***3e-7**	46	***0.001**	***0.001**	0.05
PLC		-	0.102	37	-	-	0.40
g_s	log transform	-	***0.0028**	33	0.097	0.18	0.60

Table S2: *Populus tremuloides* – Details for linear mixed-effects models of functional trait data. "Data Transformation" indicates if/how trait data were power transformed to achieve normality prior to model fitting. "Covariates included in model" lists any covariates controlled for during model construction. "LRT from null model" shows the likelihood ratio test p-value comparing a model with Elevation to a null model. If elevation was significant in a likelihood ratio test, "Low Elev p-value"/"High Elev p-value" show post-hoc differences between the lower/upper range margin and the range center assessed via the Satterthwaite approximation of marginal fixed effect significance using the mixed-effects model with elevation. "btw stand : w/in stand variation" shows ratio of the variance estimated between stands and the variance within stands (between individual variation + measurement error) in the best fit mixed-effects model (0 indicates no variance assigned to stand random effect).

Trait	**Data Transfor-mation**	**Covariates included in model**	**LRT from null model**	**Final sample size**	**Low Elev p-value**	**High Elev p-value**	**btw stand : w/in stand variation**
10yr mean annual BAI	lambda=0.5	DBH + comp. Index	***0.0006**	117	***0.005**	0.70	0.74
Median leaf size	-	-	0.17	45	-	-	0.52
Height	-	-	***2.9e-5**	45	***0.0002**	0.98	0.95
A_L:A_S	-	-	0.57	46	-	-	0
SLA	-	-	***0.0102**	45	***0.0138**	0.65	0.43
Wood Density	lambda= -2	-	***0.0007**	44	***0.0214**	***0.088**	0
K_{nat_Leaf}	lambda = 0.5	-	0.30	40	-	-	1.33
K_{max}	lambda = 0.25	-	0.49	41	-	-	0.66
Safety margin	-	-	***4.3e-9**	39	***2e-7**	0.43	0.76
PLC	lambda = 0.5	-	***0.001**	36	***0.004**	0.27	0
g_s	log transform	-	0.2761	36	-	-	1.27

Table S3: Details from the best linear mixed effects models explaining branch xylem tensions with the possible explanatory variables of Time (predawn vs midday), Elevation (coded as a continuous variable), and a Time * Elevation interaction with a random effect of stand and tree. Possible models included null, Time only, Elevation only, Time + Elevation, and Time + Elevation + Time * Elevation. Model selection was performed using AIC, and the significance of the best model over the next simplest model was tested using a likelihood ratio test. The Satterthwaite approximation of marginal fixed effect significance was then used to estimate the significance of individual model coefficients. Significant p values (alpha = 0.05) are in bold and denoted by "*".

Species	**Best model**	**Δ AIC from null model**	**Δ AIC from next best model**	**LRT from next best**	**Time**	**Elev**	**Time * Elev**
Ponderosa pine	Time + Elev + Time * Elev	112.6	23.0 (from Time + Elev)	***2.7e-7**	***<0.0001**	***<0.0001**	***<0.0001**
Trembling aspen	Time + Elev + Time * Elev	256.6	5.7 (from Time + Elev)	***0.005**	***<0.0001**	***0.0076**	***0.006**

Appendix E: Supplemental Data and Analysis, trait variation across taxonomic scales
Supplemental Material for Chapter 3

Table S1: Sample sizes for 16 common conifers from the PNW database used for within-species trait analyses.

Species	nplots	nsamples
Abies.amabilis	9	25
Abies.concolor	33	89
Abies.grandis	30	101
Abies.procera	8	22
Juniperus.occidentalis	11	68
Picea.sitchensis	10	27
Pinus.contorta	19	40
Pinus.jeffreyi	17	45
Pinus.ponderosa	54	267
Pseudotsuga.menziesii	113	311
Tsuga.heterophylla	33	82

Table S2: Total sample sizes by trait for trait variation by taxonomic level analysis.

	Within-species			Within-genus			Within-family (species means)		
	N spp	Mean reps	Median reps	N gen	Mean reps	Median Reps	N fam	Mean reps	Median Reps
LL	30	28.7	6.5	61	3.5	2	65	7	3
LMA	38	35.3	8.5	73	10.1	7	73	18.9	9
N	38	32.9	8.5	73	8.6	6	73	16.4	9

	Within-family (species means)			Within-family (genus means)			Between families	
	N fam	Mean reps	Median Reps	N fam	Genera in Family	Median Reps	Families	Familes w/ at least 3 species
LL	65	7	3	43	6	4	115	79
LMA	73	18.9	9	44	12.4	8	180	96
N	73	16.4	9	44	11.5	7	164	92

Table S3: Details of the PCA on climate normal from sites in the PNW dataset. Mean annual temperature, precipitation, and climate moisture index (potential evapotranspiration – precipitation) were calculated from the PRISM 4km gridded climate normals (Daly *et al.*, 2002). Max vapor pressure deficit and soil moisture content variables were calculated for each stand using the Variable Infiltration Capacity Model run with XX meteorological data (cite).

	PC1 ('wetness')	**PC2** ('warmth')
Variance explained	71.7%	18.0%
Variable Loadings		
Mean Annual Temperature	0.081	0.943
Mean Annual Precipitation	0.465	0.137
Mean annual climate moisture index	0.474	0.055
Max annual Vapor Pressure Deficit	-0.401	0.258
Mean soil moisture content – surface soil layer	0.439	0.009
Mean soil moisture content – total soil column	0.446	-0.149

Table S4: Likelihood ratio test results testing the significance of taxonomic scale for standardized major axis regression slopes and correlation coefficients of trait-trait relationships. Columns show different weighting methods.

		unweighted	sample size	V1 variance	V2 variance
Nmass v LL	SMA slope	0.31	0.087	0.61	0.31
	Correlation	**0.018**	**<0.0001**	**0.005**	**<0.0001**
Nmass v LMA	SMA slope	0.736	0.96	0.9	0.44
	Correlation	**0.027**	**<0.0001**	0.19	**0.0008**
LL v LMA	SMA slope	**0.044**	**<0.0001**	**0.002**	**0.031**
	Correlation	**0.007**	**<0.0001**	**<0.0001**	**0.002**
LMA v Narea	SMA slope	**0.02992**	**<0.0001**	0.4077	**0.001735**
	Correlation	0.8787	0.2666	0.306	0.1208

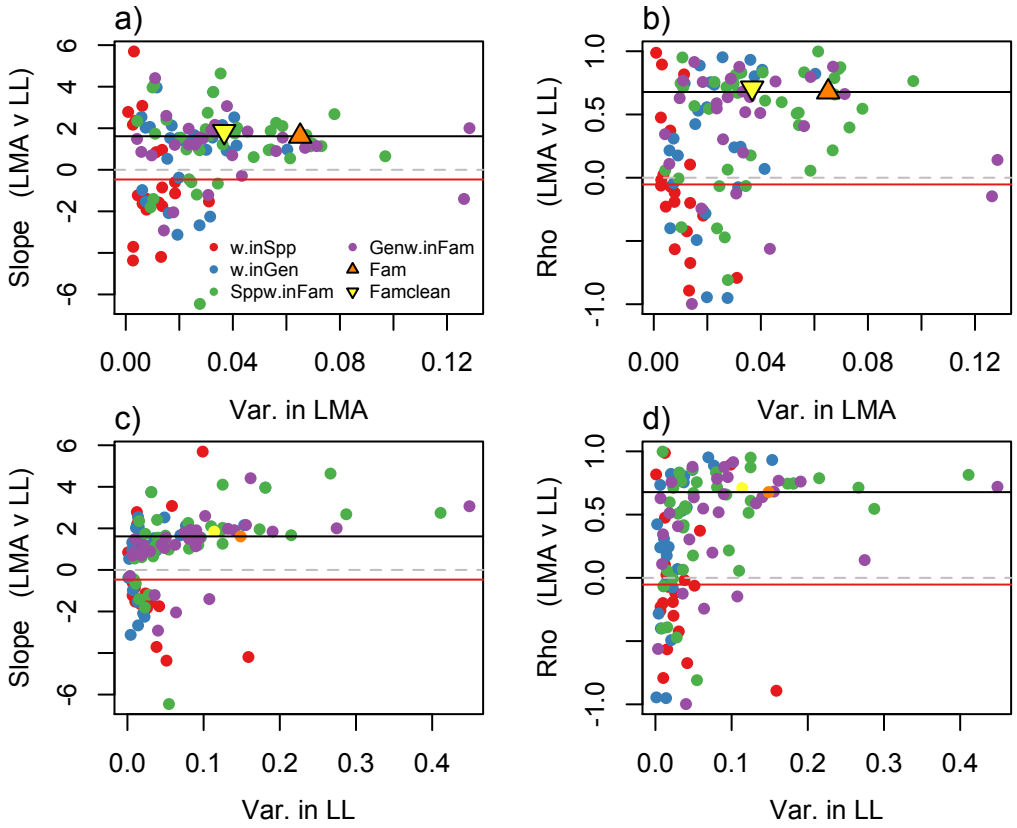

Figure S2: Funnel plots showing the slope of SMA regression lines (a,c) correlation coefficients (b,d) of all individual within-taxon trait relationships between $\log_{10}$(LMA) and $\log_{10}$(leaf lifespan) as a function of the within-taxon variance in LMA (a,b) and sample size (c,d). The black horizontal lines indicate the slope or correlation across families, while the red horizontal lines indicate the mean within-species slope or correlation. Trait correlations between congeneric species (blue points) and between confamilial species or genera (green and purple points, respectively) largely converge on the between-family trait relationships at higher LMA variances and particularly at higher sample sizes. However, within-species LMA-leaf lifespan relationships do not converge on a positive relationship at higher LMA variances, and instead converge on a slight negative relationship at larger sample sizes.

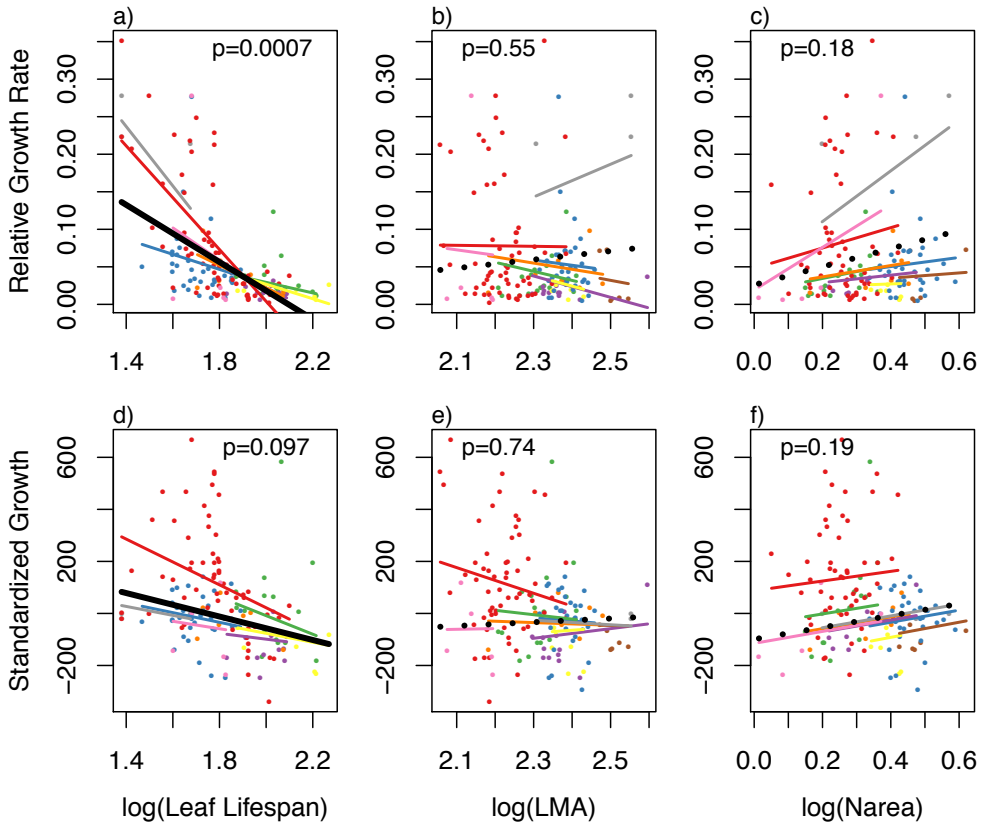

Figure S3: The relationship between stand Relative Growth Rate (a-c) or raw biomass standardized growth (b-d) and stand mean $\log_{10}$ transformed leaf lifespan (a,d), LMA (b,e) and N_{area} (c,f). Colored lines show relationships for each of eight dominant conifer species that made up at least 50% of the basal area of at least three plots. Black lines show the mean relationship across species, significant or marginally significant mean relationships are solid lines (p values from Likelihood Ratio Tests shown in plots).

Methods: The PNW dataset provides a unique opportunity to test the presumed link between plant functional traits and at least one fitness component, growth, in long live tree species. The PNW dataset was largely the result of projects characterizing primary productivity in Pacific Northwest forests. Because most of the sampled sites in the dataset are dominated by a single species (one species makes up >50% of the basal area of over 80% of the sampled sites), these productivity estimates can be used to estimate stand growth rates that can be related to stand average foliar trait values for mono-dominant stands.

First, we calculated stand relative growth rate ($RGR = \ln(biomass_{t2}) - \ln(biomass_{t1})/ \Delta t$, here in gC * $(gC*m^{-2}*yr)^{-1}$), which presumes an exponential growth function. Because relative growth rate tends to decrease with plant age, particularly in trees (cite?), we also calculated biomass standardized growth that does not presume an exponential growth function by subtracting from the observed growth the mean growth expected from a general additive model of biomass gain as a function of stand biomass fit to the data from all sites using the *gam* function from the *mgcv* package in R (Woods 2011). Sites with positive biomass standardized growth grew faster than expected based on their standing biomass, while stands with negative biomass standardized growth grew slower than expected.

Then, we related stand growth to the mean trait value of the dominant species for the 151 plots that were dominated by a well sampled species (i.e. one species sampled in at least two other plots made up >50% of the plot basal area), and that had productivity and trait data. We used linear mixed effects models to relate Relative Growth Rate or biomass standardized growth rate to mean log LMA, log leaf lifespan or log N_{area} with a random slope and intercept per species. We tested the significance of the fixed effect (i.e. the mean growth vs. trait slope across all species) using likelihood ratio tests. Relative Growth Rate was somewhat log-normally distributed, but statistical results were qualitatively identical with raw RGR and log-RGR values, so only the results from the raw RGR analysis are presented.

As with the trait-environment relationships, trait relationships with stand growth rate were subtle at best (Figure S3). Log leaf lifespan was the only trait that had a consistent and significant or near significant relationship with stand growth across species (LRT p=0.0007 for growth as RGR, p=0.098 for biomass standardized growth). Relative growth rate consistently increased at sites with shorter leaf lifespans across all species (marginal R^2 of fixed effect = 0.26, conditional R^2 including random variations between species = 0.45). While the general trends were consistent with expectations for N_{area} (RGR increases with higher stand average N_{area}), neither log LMA nor log N_{area} were significantly related to either formulation of stand growth.

Chapter 5: Conclusion

Ecology in the Anthropocene faces an extreme challenge: transitioning from a fundamentally descriptive science into a predictive science in time to provide management-relevant understanding of how ecosystem structure and function will be altered by global environmental change (Clark *et al.*, 2001; Moorcroft, 2006; Evans, 2011; Evans *et al.*, 2013; Grimm & Berger, 2016; Houlahan *et al.*, 2016; Torossian *et al.*, 2016; Urban *et al.*, 2016). While reductionist biology has experienced astounding breakthroughs in the past half century, the system science of ecology continues to labor to define the rules that govern species interactions, population dynamics, and ecosystem functions. The only universal rule seems to be that nothing is universal, and the most common ecological result by far is "it's complicated." While the task of the ecologist may feel a bit like trying to recreate Newtonian physics from quantum observations (Doak *et al.*, 2008; Beckage *et al.*, 2011; Blonder *et al.*, 2017), establishing fundamental ecological principles is the key to predictive ecology. This dissertation helps work towards a predictive ecology by empirically testing a potentially powerful ecological theory, detailing an example of the predictive power of functional traits, and examining some of the foundational assumptions of trait-based plant ecology. In so doing, it attempts to contribute to the theory that guides eventual model development and application and to improve the tools (i.e. functional traits) with which eventual predictive models will likely be built.

The first chapter of this dissertation furthers the development of predictive ecology by testing the power of a long held ecological theory to predict the mechanisms of tree range constraints. The Stress Trade-off Hypothesis is elegant and intuitive, positing that organismal fitness is more constrained by environmental stress in harsh environments and by species interactions in benign environments (MacArthur, 1972; Brown, 1995; Loehle, 1998). It also has

considerable predictive potential, because it implies that most organisms inhabiting a gradient of abiotic stress will face an abiotic range constraint at their harsh range boundary and a biotic constraint at their benign boundary (Loehle, 1998; Koehler *et al.*, 2012; Savage & Cavender-Bares, 2013). It is perhaps not surprising that the story is not quite so simple when this theory is applied to explain real-world tree elevation ranges (Chapter 1 of this dissertation). The challenges of defining abiotic 'harshness', difficulties of measuring range constraints with tree rings, and the disturbance-related ecology of many western tree species together decrease the predictive power of the STH at local scales. However, it is encouraging that, despite local complexities, a broad scale pattern emerged. While the exact mechanism of any particular local range constraint is difficult to predict, across all species and sites, climatic and competitive growth constraints did trade off. This chapter finds support for a basic ecological theory, but highlights the importance of spatial scale for the validity of the Stress Trade-off Hypothesis. This emergence of patterns at larger spatial scales is indicative of complex systems whose behavior can be 'coarse-grained' to develop probabilistic estimates of future system behavior (Beckage *et al.*, 2011). Such behavior is not novel in spatial ecology (Schneider 2001), and has to some extent been predicted by the range shift literature (e.g. Araújo & Peterson, 2012). Nonetheless, our results provide some of the first plant-based evidence for generalizable patterns of range constraint mechanisms, and yield useful insights about where, when and at what spatial scale tools such as climate envelope models may be useful for predicting range shifts (see Chapter 1: Discussion).

The second chapter provides an example of how spatial variation in plant functional traits and physiological rates can provide powerful inferences about complex tree drought tolerances, yielding at least qualitative predictions of how the low elevation range boundaries of two tree

species will respond to a drying climate. A combination of morphological, hydraulic, and plant water potential measurements revealed how ponderosa pine avoids drought stress by limiting water use, and how trembling aspen tolerates drought stress by maintaining transpiration but growing stress resilient tissues. These strategies imply a long-term limitation on carbon fixation at the dry range margin of ponderosa pine, and increased cost of growth and susceptibility to extreme events at aspen's dry range margin. From knowledge of these range constraint mechanisms, we can then predict that range contractions due to decreased water availability will probably be gradual in ponderosa due to long-term suppression of growth. Meanwhile, range contractions will likely be sporadic in aspen due to mortality during extreme droughts. This type of prediction highlights the powerful potential of functional traits to simplify complex ecologies and physiologies. But it also hints at some limitations of functional ecology, in that any one or two of the physiological traits that we measured on their own would have provided an incomplete picture of either species' drought resilience. More-over, without a priori knowledge that drought was the dominant low-elevation range constraint for these species, measuring traits related to other biotic or abiotic stresses would likely have yielded few inferences. While this point may seem obvious to plant physiologists, it provides a cautionary tale for community ecologists, and lines up strongly with community ecological results such as the relatively poor univariate strength of functional traits to predict co-existence in annual plants (Kraft *et al.*, 2015), the poor link between functional traits and global sapling survival and growth rates (Paine *et al.*, 2015), or the inability of a small number of niche axes to explain coexistence in eastern hardwood forests (Clark *et al.*, 2010).

Two undergraduate research projects that spun out of this research also underscore this point. A. Baird found that the ubiquitous functional trait leaf mass per area (LMA) was only

weakly linked to either assimilation rate or water use efficiency in a greenhouse drought and shade study in trembling aspen (Baird *et al.* 2017). Instead, orthogonal light-related and water-related leaf anatomical changes drove physiological changes, and LMA was a poor 'functional' predictor of these responses. V. Reynolds characterized the drought resistance of four species from the Australian genus *Brachychiton* and found that traits and rates such as LMA, maximum unstressed assimilation rate, and unstressed water use efficiency were exceedingly poor predictors of the species aridity niche (where each species grew on an aridity gradient). Only by measuring multiple traits and rates in well watered versus drought stressed conditions was she able to show that dry-adapted *Brachychiton* species rely on physiological plasticity and drought avoidance as their key drought resistance strategy (Reynolds et al. *in revision, Tree Phys.*).

Chapter 3 continues to focus on testing and developing the foundations for predictive ecology by further exploring the strengths and limitations of the trait-based approach of Chapter 2. In this chapter, I used one of the most extensive datasets of within-species foliar trait variation gathered to date to test four foundational hypotheses of trait-based ecology. 'Trait-based' approaches have been heralded as the future of predictive ecology in both the plant and the animal literature (e.g. Pavlick *et al.*, 2012; Scheiter *et al.*, 2013; Grimm & Berger, 2016; Peaucelle *et al.*, 2016; Urban *et al.*, 2016). However, the 'functional trait' is only functional in-so-far as 1) our assumptions about the appropriate scale for trait measurement are true, 2) the trait can reduce the complexity of biological diversity by serving as a proxy for universal axes of trait co-variation indicative of ecological, evolutionary or physiological 'strategies', 3) the trait responds in a predictable way to environmental gradients. Chapter 2 illustrated the potential power of within-species trait variation to quantify complex physiologies. Chapter 3 builds on this example to turn the data-intensive but potentially rewarding tool of within-species trait variation

to test these foundational assumptions of functional ecology. I found that trait variation below the species level (within-population and between population trait variation) is small compared to between-species variation for some leaf economics traits, but that leaf nitrogen content per unit area is highly variable within an individual species. This suggests that species trait means are reasonable units of measure for some critical traits, but may fail to capture critical axes of diversity for some traits. I also found that the central relationships between leaf lifespan or leaf mass per area and mass-based leaf nitrogen content that are the backbone of the Leaf Economics Spectrum remain relatively stable across taxonomic scales. However, this stability hides fascinating taxonomic scale-dependence in the relationships between leaf lifespan and LMA, and leaf lifespan/LMA and area-based leaf nitrogen content. Moreover, with the exception of leaf lifespan, the assumed functionality of these leaf traits was called into question by the limited predictability of their within-species variation across environmental gradients. This chapter highlights the need for a mechanistic understanding of trait variation and covariation that can scale across space, time and taxonomic organization. As demonstrated in Chapter 2, within-species patterns of trait variation and covariation have the potential to yield this mechanistic understanding. However, the poor trait-environment links documented in Chapter 3 and the multiple traits required to understand the physiological complexity of tree drought strategies in Chapter 2 together suggest that the dominant axes of plant functional variation are more complicated and nuanced than global patterns such as the Leaf Economics Spectrum might imply.

In this dissertation, as with much of ecology, complexity abounds. However, this work has yielded some encouraging findings for the long-term development of a predictive ecology. The findings of Chapter 1 illuminated an emergent trade-off between climatic and competitive

growth constraints at broad spatial scales, and illuminated key local scale processes that warrant future study. The analysis of Chapter 2 demonstrates that functional traits can be used to understand organismal abiotic stress tolerance in a way that yields qualitative yet useful predictions about species responses to climate change. The results of Chapter 3 reveal that leaf lifespan is a relatively predictable trait that correlates with growth, and that the variable relationships between leaf lifespan and other foliar traits at different taxonomic scales may provide the cornerstone for a taxonomy-free understanding of trait covariation. While our current ecological understanding is still far from predicting species responses to climate change, the results of this dissertation provide nuance to existing biogeographic and functional trait theory, highlighting the causes of current weaknesses and suggesting critical avenues for future progress.

Works cited:

Araújo MB, Peterson AT (2012) Uses and misuses of bioclimatic envelope modeling. *Ecology*, **93**, 1527–1539.

Baird AS, Anderegg LD, Lacey ME, Hillerislambers J, Van Volkenburgh E (2017) Comparative leaf growth strategies in response to low-water and low-light availability: variation in leaf physiology underlies variation in leaf mass per area in *Populus tremuloides*. *Tree Physiology*, 1–11.

Beckage B, Gross LJ, Kauffman S (2011) The limits to prediction in ecological systems. *Ecosphere*, **2**, art125.

Blonder B, Moulton DE, Blois J et al. (2017) Predictability in community dynamics (ed Storch D). *Ecology letters*, **20**, 293–306.

Brown JH (1995) *Macroecology*. The University of Chicago Press. Chicago, IL, USA.

Clark JS, Bell D, Chu C et al. (2010) High-dimensional coexistence based on individual variation: a synthesis of evidence. *Ecological Monographs*, **80**, 569–608.

Clark JS, Carpenter SR, Barber M, Collins S (2001) Ecological forecasts: an emerging imperative. *Science.* **293**, 657-659.

Doak DF, Estes JA, Halpern BS, Jacob U (2008) Understanding and predicting ecological dynamics: are major surprises inevitable. *Ecology*.

Evans MR (2011) Modelling ecological systems in a changing world. *Philosophical transactions of the Royal Society of London. Series B, Biological sciences*, **367**, 181–190.

Evans MR, Bithell M, Cornell SJ et al. (2013) Predictive systems ecology. *Proceedings of the Royal Society B: Biological Sciences*, **280**, 20131452–20131452.

Grimm V, Berger U (2016) Ecological Modelling. *Ecological Modelling*, **326**, 177–187.

Houlahan JE, McKinney ST, Anderson TM, McGill BJ (2016) The priority of prediction in

ecological understanding. *Oikos*, **126**, 1–7.
Koehler K, Center A, Cavender-Bares J (2012) Evidence for a freezing tolerance-growth rate trade-off in the live oaks (Quercus series Virentes) across the tropical-temperate divide. *New Phytologist*, **193**, 730–744.
Kraft NJB, Godoy O, Levine JM (2015) Plant functional traits and the multidimensional nature of species coexistence. *Proceedings of the National Academy of Sciences of the United States of America*, **112**, 797–802.
Loehle C (1998) Height growth rate tradeoffs determine northern and southern range limits for trees. *Journal of Biogeography*, **25**, 735–742.
MacArthur D (1972) *Geographical Ecology: Patterns in the Distribution of Species*. Harper & Row, New York.
Moorcroft PR (2006) How close are we to a predictive science of the biosphere? *Trends in Ecology & Evolution*, **21**, 400–407.
Paine CET, Amissah L, Auge H et al. (2015) Globally, functional traits are weak predictors of juvenile tree growth, and we do not know why (ed Gibson D). *Journal of Ecology*.
Pavlick R, Drewry DT, Bohn K (2013) The Jena Diversity-Dynamic Global Vegetation Model (JeDi-DGVM): a diverse approach to representing terrestrial biogeography and biogeochemistry based on plant functional trade-offs. *Biogeosciences*. **10**, 4137-4177.
Peaucelle M, Bellassen V, Ciais P, Peñuelas J, Viovy N (2016) A new approach to optimal discretization of plant functional types in a process-based ecosystem model with forest management: a case study for temperate conifers. *Global ecology and biogeography*, **26**, 486–499.
Savage JA, Cavender-Bares J (2013) Phenological cues drive an apparent trade-off between freezing tolerance and growth in the family Salicaceae. *Ecology*, **94**, 1708–1717.
Scheiter S, Langan L, Higgins SI (2013) Next-generation dynamic global vegetation models: learning from community ecology. *New Phytologist*, **198**, 957–969.
Schneider DC (2001) The Rise of the Concept of Scale in Ecology. BioScience, 51, 545.
Torossian JL, Kordas RL, Helmuth B (2016) *Cross-Scale Approaches to Forecasting Biogeographic Responses to Climate Change*, 1st edn, Vol. 55. Elsevier Ltd., 63 p.
Urban MC, Bocedi G, Hendry AP et al. (2016) Improving the forecast for biodiversity under climate change. *Science*, **353**, aad8466–aad8466.